EXPERIMENTAL AND STATISTICAL EVALUATION OF THE PERFORMANCE OF CHITOSAN AS A COAGULANT IN THE TREATMENT OF SUGAR REFINERY EFFLUENTS

Submitted in fulfillment of the requirements of the degree of Master of Engineering: Chemical Engineering in the Faculty of Engineering and the Built Environment at the Durban University of Technology

RITHA-LORETTE LUTI PAMBI

August, 2015

Supervisor: Prof. Paul Musonge

DECLARATION

I hereby declare that this dissertation is a record of my original work and research for the obtention of my Master of Engineering qualification in chemical engineering with the Durban University of Technology. The content of this document has not been previously published or written by another person for the award of any other degree at Durban University of Technology (DUT) or any other educational institution. Furthermore, I declare that the content of this dissertation does not violate any copyright as every indication to the work of others has been indicated and acknowledged by means of a comprehensive list of references.

This document must not be reproduced, copied or sold without the consent of the author and the authorities of the Durban University of Technology.

Ritha L.L. Pambi

Signature: .....Date……

Supervisor:
Prof. P. Musonge.

Signature: .....Date……

DEDICATIONS

I dedicate this dissertation to my “crew”:

My father Salomon “Max” Pambi: My hero, my superman. I love you more than words can describe.

My mother Adeline “Mandolina” Obey: Our gift from Heaven, the strongest woman I have ever met. I will forever cherish and emulate your values.

My grandfathers, Nelson Pambi Mazida and Charles Obey Nkwitani, gone but never forgotten.

With all my love, I also dedicate this work to Elysée Tubar, Robert Obey, Jimmy Pambi, Gacy Pambi, Christelle Pambi, Eric Jordan Pambi, Françoise Obey, Jeanne Pambi, Charles Obey, Jerry and Myriam Dungu, Rita Pambi, Jeannette Isuku, Verocious and Daniel Oliphant, Raquelle Bhengu, as well as my extended family and my dearest friends; and lastly, to my creator, God through my Lord and Saviour Jesus-Christ.

ACKNOWLEDGEMENT

Firstly, I would like to thank the Almighty God who made all this possible in my life. My sincere gratitude goes to Dr. Sudesh Rathilal. I thank you sir for giving me the opportunity to start my Masters with the department of Chemical Engineering. I want to thank Dr. Maggy Chetty. I appreciate that you saw the potential in me.

To my supervisor, Prof. Paul Musonge, thank you for your guidance and your genuine heart. I appreciate all your encouragement and all the support you have given me during my studies.

My heartfelt gratitude goes to Prof. Sibusiso Moyo for her encouragement and for imparting some of her strength and determination on me.

Furthermore, I thank all the laboratory staff and my fellow postgraduates in the Department of Chemical Engineering for their encouragement, and for bringing rays of sunshine and warmth to my studies.

I also wish to acknowledge Jean-Claude and Simphiwe Munyaka, Martha Chollom, Jaffa Bux, and my family for their support throughout my studies.

In addition, I would like to express my deep gratitude to the management of Tongaat-Huletts sugar refinery and to all the staff of their quality control laboratory for giving me the opportunity to perform my experimental work on their premises. Special thanks to Zyven Rambakus, Nonhlanhla Nkomo, Kenneth Macinga, Israel Thumba, Nomusa Maduna and Pearl Shavhani.

ABSTRACT

The implementation of new water regulations from the local government has been a motivation for most industries to treat the effluent before disposal or reuse within the plant, in order to save costs and avoid sanctions. Tongaat-Huletts sugar refinery has therefore invested in this collaborative research with the Durban University of Technology in order to investigate new technologies for wastewater treatment and water recovery using an organic coagulant called chitosan.

Chitosan is a natural non-toxic polymer extracted from the exoskeleton of crustaceans. Chitosan has gained extensive attention as a coagulant in the treatment of wastewaters from various industries. However, no attention has been given to the coagulation of effluents from the sugar industry using this polymer. In this work, chitosan coagulant (CCo) was prepared by dissolution of known amounts of chitosan powder in aqueous acid at 50℃. The solution was diluted to desired concentrations using distilled water at room temperature.

The removal of impurities using chitosan was investigated for two effluent streams from the sugar refinery, namely the final effluent (FE) and the resin effluent (RE) by applying the one-factor-at-a-time (OFAT) method. The optimum chitosan loading was found to be 138 mg/l for the RE and 7.41 mg/l for the FE, beyond which the efficiency of the coagulant decreased. The coagulation of FE removed 97% of the total suspended solids (TSS), 61% colour and 35% chemical oxygen demand (COD). The treatment of RE resulted in the removal of 68% TSS, 30% colour and 15% COD due to its high content of impurities. Therefore, RE was not considered for statistical studies.

The Box-Behnken (BBD) design, which is a statistical response surface methodology (RSM) model was used to study the simultaneous effect of pH, coagulant loading and settling time on the removal of the COD, TSS and colour, with the help of an overlay plot for the FE. The optimum values from the overlay plot were 92% for TSS, 83% for colour and 29% for COD.

The model equations generated by the BBD for individual responses involved all the manipulated variables contrary to the OFAT which only considered one manipulated parameter per response. Moreover, the BBD allowed the simultaneous analysis of all the parameters and the identification of interactions which occur when the effect of one factor is dependent on the level of another. The most important interaction for the removal of TSS was the combination of the variation in pH and coagulant dosage. The COD removal was mostly affected by the interaction between the coagulant loading and the settling time. The colour removal increased with the simultaneous increase of the pH and the settling time.

A comparative study between the wastewaters from the sugar industry, the brewery industry and milk processing industry revealed that the performance of the chitosan was also affected by the amount of total dissolved solids (TDS) in the wastewater. A model was developed relating the TSS, COD and TDS from all these wastewaters, and was used to predict the TSS removal for the effluent from the olive oil mills and the wastewater from the winery.

Chitosan can be considered as a good alternative to inorganic and synthetic coagulants for the pre-treatment of the FE due to its ability to efficiently remove the levels of TSS and colour. Furthermore, the production of chitosan from crustacean shells is a good method of reducing pollution from the fishery industry. Chitosan can be produced locally at low cost due to both the abundance of crustacean shells in the coastal regions of South Africa and the simplicity of its preparation process.

It is recommended that a mathematical model be developed to accurately predict the influence of chitosan on all types of effluent. Such a model will provide an indication of the performance of the chitosan and guide experimenters. It is further recommended that the effect of the use of organic coagulants on the destabilization of dissolved solids in wastewater be given greater attention.

TABLE OF CONTENTS

LIST OF FIGURES

Chapter 1

Chapter 2

Chapter 3

Chapter 4

Chapter 5

Appendix A

Appendix B

LIST OF TABLES

Chapter 2

Chapter 3

Chapter 4

Chapter 5

Chapter 6

Appendix A

Appendix B

Appendix C

LIST OF ABBREVIATIONS

ANOVA: Analysis of variance

AP: Adequate Precision statistic

BBD: Box-Behnken design

CCo: Chitosan coagulant

COD: Chemical Oxygen Demand

CV: Coefficient of variation

df: Degrees of freedom

DOE: Design of experiments

DWA: South African Department of Water Affairs

DPW: South African department of public works

EPA: United States Environmental Protection Agency

ESR: Effluents from the sugar refinery

FE: Final effluent

LOF: Lack-of-fit

MC: Medium concentration

MS: Mean square

OM: Organic matters

RE: Resin effluent

RSM: Response surface methodology

TSS: Total suspended solids

TDS: Total dissolved solids

OFAT: One-factor-at-the-time

PRESS: Predicted residual sum of squares

SADC: Southern African Development Community

SD: Standard deviation

SE: Standard error

CHAPTER 1: INTRODUCTION

1.1. AN INSIGHT INTO THE SOUTH AFRICAN WATER CRISIS

South Africa is faced with issues such as variable climatic conditions, industrial pollution and socio-economic difficulties. Figure 1.1 shows that South Africa, Zimbabwe, Botswana and Namibia are the most water-stressed countries of the SADC region. The average rainfall in South Africa (497 mm) is below the global average (860 mm). The rainy season in South Africa lasts for three months on the average, thus affecting the surface flow of rivers (Hattingh et al., 2015).

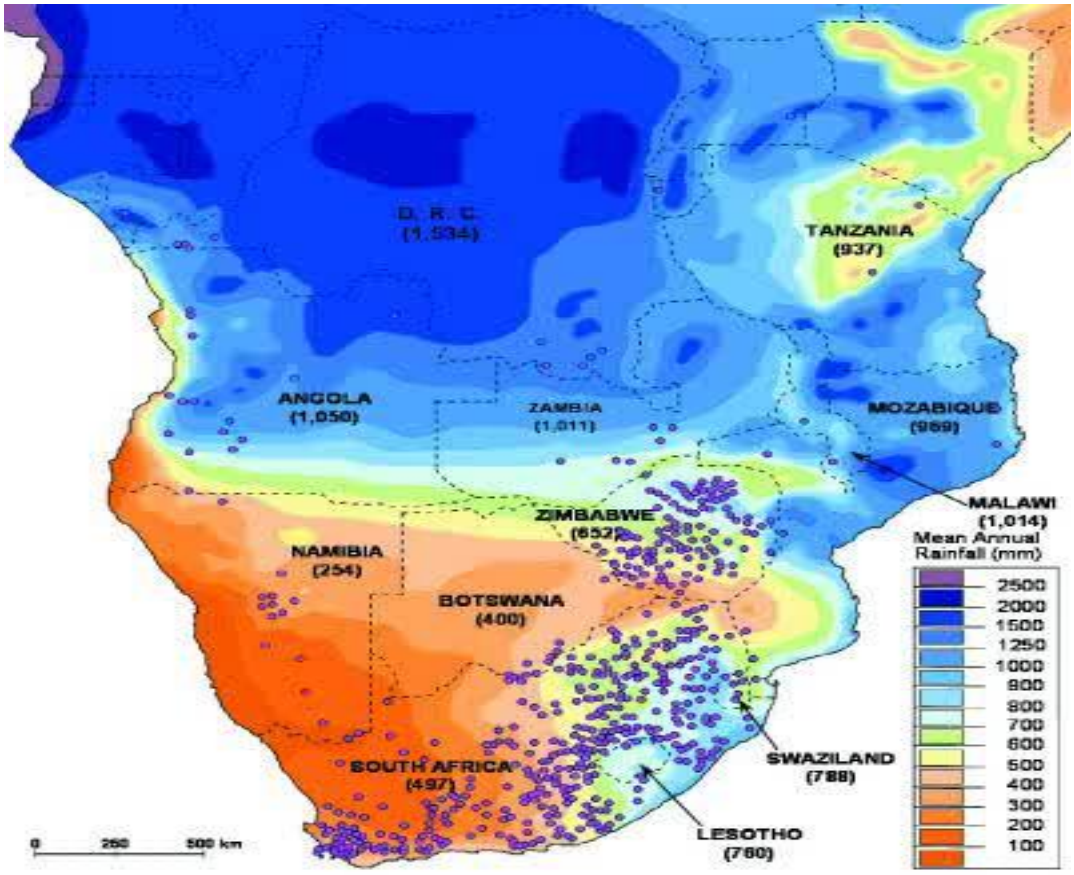

Figure 1.1: Mean annual rain fall for the SADC region. (Hattingh et al., 2015)

Pollution of common water sources such as the Orange, the Okavango and the Incomati rivers has brought conflicts between some SADC nations. This is mainly due

to the fact that water flowing from the highly industrialized areas of the SADC carries pollutants and limits access to clean water for regions downstream. Hence, the need to treat these waters at the source of pollution before flowing into other countries (Gleick, 1998; Ashton, 2000; Ashton, 2007; Hattingh et al., 2015).

In South Africa, water sources are being polluted due to heavy industrial activities, the multiplication of informal settlements as well as the debilitated condition of the infrastructures in some municipalities among other reasons. In 2008, there were reports of high levels of the potentially deadly Escherichia-coli (E-coli) bacteria in the water tested from the Western Cape Province municipal supplies. High levels of E-coli in water have also been reported in impoverished districts of the Eastern Cape Province like uKhahlamba. Water tankers had to be sent out to the community to supply potable water to the residents in these two provinces, and residents were recommended to boil the tap water before use (Integrated Regional Information Networks, 2013; Hattingh et al., 2015).

On the 14th of February 2011, an article published by *Times LIVE* on the inaugural South African Water and Energy Forum held in Johannesburg, indicated that South Africa could be facing critical water shortages by 2020, unless immediate action is taken. The experts also indicated the potential causes of the crisis, such as the possibility of the water demand outweighing supply, the deterioration of municipal infrastructures, and the looting of water supplies along the Vaal River by some farmers (Masondo, 2011).

Chemical and toxic spills also pose a threat to communities and to the environment. A media release from the South African Department of Water Affairs (DWA) on the 17th of February 2012 reported the spillage of high concentrations of Cyanide from a synthetic rubber manufacturing company into the nearby Karbochem Spruit, a tributary to Ngagane River leading to the death of cattle drinking from the river. This further highlights the necessity of proper water monitoring and water treatment (DWA, 2012).

Industries such as mines, breweries, sugar processing plants and textiles manufacturers are the greatest contributors of the South African water crisis because they consume

large amounts of clean water and also discharge large quantities polluted wastewater (e.g.: acid mine drainage, coloured effluent, wastewater of high organic content).

The presence of coloured effluent from textile industries into the Sterkspruit River has been observed in the Hammarsdale area of KwaZulu-Natal (Mutambanengwe et al., 2008), affecting the aesthetic appearance of the river as a direct effect.

Coloured effluents are also released from the sugar industries and molasses-based distilleries. These effluents contain melanoidin, a natural brown polymer of high molecular mass found in molasses and other organic material such as coffee beans, sugar cane, malts, etc., which is very recalcitrant to most conventional treatment methods (Satyawali and Balakrishnan, 2008; Tokumura et al., 2008). Sugar mills with ethanol distilleries generally release an average of 156 litres of stillage and 250 kg of bagasse per 1000 kilograms of cane to obtain 12 litres of alcohol and 94 kilograms of sugar (Gunkel et al., 2007). Breweries release approximately 3 to 14 litres of effluent per litre of alcohol produced (Pant and Adholeya, 2007; Kowsalya et al., 2010). If released into nature untreated, these effluents can have many negative effects on the communities and the environment.

Industries in South Africa are faced with environmental issues due to the pollution caused by impurities in their effluents. They are also confronted with new government regulations and sanctions on effluent disposal. Therefore, there has been an increasing emphasis on water treatment and reuse in most industries. Some companies save cost by treating the effluents in order to decrease the level of pollutants before disposal, thus avoiding fines and sanctions. Others save costs by purifying the water for reuse within the plant

1.2. THE SUGAR INDUSTRY AND THE ENVIRONMENT

The sugar industry contributes significantly to the economic growth of South Africa by creating jobs in the agricultural and industrial sectors. There are approximately 38200 registered sugar cane growers located mainly in the KwaZulu-Natal, Eastern Cape and Mpumalanga with 14 sugar mills creating an estimate of 79 000 jobs in direct

employment and 350 000 in indirect employment (SASA, 2014) . However, there are many environmental and health issues associated with effluents from the sugar refinery (ESR). This is due to the composition of the organic impurities in this wastewater which affects the physico-chemical properties of the aquatic life forms in the receiving streams. The ESR has a high content of organic matters (OM) which are the major problems for conventional treatment methods.

The main OM are dissolved sugar, molasses, phenolics and bagasse. These contaminants are non-toxic, but they are used as nutrients by microorganisms and increase the oxygen demand of receiving streams. The colour of this effluent and the high total suspended solids (TSS) content also poses a problem by decreasing the amount of sunlight that penetrates into the rivers, therefore, interfering with the photosynthetic cycle which is vital for the aquatic flora. The sugar industry wastewater is commonly used in agriculture for irrigation so as to reduce the water demand in farms. However, studies have shown that the use of the effluent from the sugar industry in agriculture causes damage to crops, reduce crop yield and weakens soil health (Wadley and Buckley, 1991; Purchase, 1996; Roussy et al., 2005; Pant and Adholeya, 2007; Ayyasamy et al., 2008; Doke et al., 2011). Therefore, proper treatment is required to reduce the amount of the impurities in this wastewater.

1.3. THE SEAFOOD INDUSTRY AND LAND POLLUTION

The seafood industry discards a large amount of shells and other wastes per year. Archer et al. (2001) stated that in the UK, for a total fish and shellfish resource of 851 984 tonnes, an estimated of 42% ends up as products for human consumption and the remainder (492 020 tonnes) is classed as waste.

The South African seafood industry is also very competitive on the international scale. This industry is worth approximately R4 billion a year, of which an estimated R625 millions is from lobster export. According to Oelofse (2014), South Africa produces on average 224 000 tonnes of seafood per annum for local consumption, and 33% of this is discarded as waste. Empty shells from crustaceans washed out of the ocean are

also found on the coastal regions, such as KZN, Eastern Cape and Western Cape. These waste crustacean shells pose a problem due to the fact that they degrade at very slow rates, and in some countries these waste are disposed of on landfills posing a problem of land space (Archer et al., 2001; Karaan and Rossouw, 2004; Heinecken and Smith, 2007).

Seafood shells contain a non-toxic, biodegradable polymer known as chitin. The chitin extracted from the shellfish and crabs is often converted into chitosan which has more economic value than chitin due to its wider range of application. Chitosan is capturing the attention of scholars mostly as an adsorbent in water treatment for the removal of impurities such as heavy metals and colour among many others (Archer et al., 2001; Azlan et al., 2009; Aranaz et al., 2009). This polymer is very versatile and has a wide range of applications in many sectors and it needs to be studied further and optimized for continuous industrial uses.

1.4. PROBLEM STATEMENT

Conventional technologies for treatment of industrial effluents include biological treatment, ozonation, electrochemical processes, nanofiltration (membrane technology) and activated carbon adsorption (Siew-Teng Ong et al., 2010). Most of these methods are not efficient for the effluents from the sugar industry due to their high content of OM, suspended solids and colour.

Furthermore, companies are facing heavier and more severe sanctions for failing to comply with the established standards. Effluent treatment is now a common practice in many industries in order to conform to the specifications for re-use within the plant or for release into the environment, and to reduce the cost of effluent treatment from the municipalities.

Hence it is important to find alternative ways of removing the pollutants in coloured wastewater efficiently and conveniently. The treatment of wastewater using biodegradable polymers such as chitosan is being widely studied. Moreover, chitosan

has many properties such as non-toxicity and it can be used to immobilize enzyme and other material into beads, membranes and films. It can also be used as coagulant and as a coagulant aid in the treatment of wastewater (Chi and Cheng, 2006; Gunkel et al., 2007; Crini and Badot, 2008; Lukum and Djafar, 2012). However, the use of chitosan as a coagulant for the treatment of ESR has not been widely documented. Thus, it is important to establish if this well-praised polymer can provide satisfactory results for the treatment of the effluents from the sugar industry.

1.5. OBJECTIVES

The main objective of this work was to investigate the possibility of using chitosan as a coagulant for the treatment of ESR for colour, chemical oxygen demand (COD) and TSS reductions. This was part of a collaboration between Tongaat-Huletts and the Durban University of Technology, thus the main focus on sugar effluents.

The specific objectives of this work were:

1. To evaluate the performance of the coagulant in terms of the concentration of chitosan, the initial pH of the wastewater and the influence of the concentration of the impurities using the traditional jar-test method.
2. To identify the factors that influence the performance of chitosan and the variables that can be optimized to enhance the performance of chitosan.
3. Compare results obtained from the ESR with those obtained from similar industries using chitosan as a coagulant.
4. To evaluate the efficiency using statistical design of experiment and compare the outcomes of the RSM method with the results from the traditional jar-test method (OFAT).

1.6. APPROACH

In this study, the effluents from Tongaat-Huletts refinery were treated with chitosan prepared by dissolution in aqueous acid. All experimental runs were conducted in Tongaat-Huletts quality control laboratory.

This study was done in two stages. The first stage was implemented using the one-factor-at-a-time (OFAT) method. This is also referred to as the traditional jar-test method in this document.

The second stage involved the statistical and optimization studies done using response surface methodology (RSM). The Box-Behnken (BBD) design was selected for this study. At this stage, experiments were conducted according to the Box-Behnken matrix and analyzed using statistics in order to generate model equations required to optimize the process.

1.7. STRUCTURE OF THE DISSERTATION

This work is presented as follows:

CHAPTER 1: Introduction

This section introduces the reader to the problems that motivate this study. Issues such as water scarcity and industrial pollution in South Africa are gaining the attention of many scholars and a few of those issues are mentioned in this section. The challenges encountered by industries in terms of waste minimization, wastewater treatment and water reclamation are also briefly discussed in this section.

CHAPTER 2: Literature review

This section is a survey of existing works and findings on the coagulation process and the coagulant selected for this project. It also provides knowledge on the problem solving strategies and short-comings encountered in the sugar refinery industry. The most common methods of experimental designs and data collection were studied in order to have an understanding of the optimization methods used by other experimenters.

CHAPTER 3: Methodology

The methodology section provides details of the means and approaches taken in order to achieve the research aims and objectives. The techniques and strategies used for the design of experiments (DOE), data collection, and analysis of results are detailed.

CHAPTER 4: Application of the OFAT methodology in the treatment of effluents from the sugar industry using chitosan

This section provides the detail of the experimental findings and the interpretation of the results for the preliminary experiments. This was done to find optimum ranges for the optimization experiments and compare the findings from the ESR with similar research outputs.

CHAPTER 5: Statistical and optimization studies

This section provides the results of the statistical and optimization studies whereby experiments are done following a particular DOE known as the Box-Behnken design.

CHAPTER 6: Comparison between OFAT and RSM

In this section, the traditional OFAT is compared to the statistical RSM in order to establish the advantages and the disadvantages of the various experimental designs.

CHAPTER 7: Conclusions and recommendations

This section summarizes the research findings according to the objectives set and demonstrates whether the researcher has met the targets set at the commencement of this work. It also provides recommendations and directions for future studies in the light of the results obtained and short-comings encountered.

CHAPTER 2: LITERATURE REVIEW

2.1. INTRODUCTION

This chapter introduces the reader to the existing research findings on the topic currently investigated. It also explores similar studies in order to provide knowledge on the problem solving strategies and short-comings encountered by other researchers.

Coagulation is a process used to remove the turbidity in water. The turbidity is caused by suspended solids, colloid particles and dissolved matters. These particles can be inorganic (e.g. sand) or organic (e.g. bacteria) and have slow settling times due to small diameters which enable them to pass through most conventional filters (Table 2.1). The presence of these particles poses aesthetic and health issues by causing cloudiness in the water and sheltering microorganisms.

Table 2.1: Particles classification

Type of particle	Diameter (nm)	Settling time*	Example
Suspended solids	>1000	0.3 seconds to 35 hours	Silt (10 000nm): 33 minutes to settle Gravel (10^7 nm) : 0.3 sec to settle
Colloids	1-1000	35 hours-63 years	Clay (100 nm) : 230 days to settle
Dissolved solids	< 1	>63 years	Nutrients, Calcium

**Settling time applicable for particles with a density of 2 650 kg/m^3 (Tzoupanos and Zouboulis, 2008; Safferman, 2010)*

Coagulation using organic and inorganic substances has been used in water purification since ancient times in Africa, Asia and other parts of the world. Ancient Egyptians discovered the principles of coagulation approximately in 2000 BC, using plant seeds and beans as natural coagulants for water purification. The use of beans, seeds and other plant materials such as copra (Cocos nucifera), Moringa oleifera seeds,

Strychnos potatorum seeds have also been reported in ancient Sudan and in ancient India. Water purification using inorganic coagulants such as alum has been practiced in Europe by the Romans and some of these coagulants are still being used in modern water treatment plants (EPA, 2000; Bina et al., 2009).

The performance of conventional inorganic and synthetic coagulants such as aluminium sulphate (alum), polyaluminium chloride (PAC) and acrylamide has been established widely in literature. However, there have been health concerns about the use of these inorganic coagulants. Residues of coagulants containing aluminium and iron have been linked as a possible cause of neurological diseases such as Alzheimer disease, Parkinson disease and clinical neurotoxicity in humans. Derivatives of synthetic organic polymers are reported to have strong carcinogenic and neurotoxic properties (Pant and Adholeya, 2007; Safferman, 2010; Miller, 2013). Thus, there is an increasing interest on the performance of non-toxic and biodegradable coagulants.

The sections below provide an insight into the fundamentals and the steps of the coagulation process. It also takes into account the type of wastewater being treated, the experimental design applied in order to gain a clear understanding of the topic being studied.

2.1.1. Coagulation theory

Coagulation is the process of destabilization of the repulsive potential of colloids and dissolved particles in water which occurs in consecutive steps that neutralizes the forces stabilizing those particles, resulting in the formation of micro-particles (microflocs), followed by particle collision leading to the growth of floc size (Gao et al., 2002; Matilainen et al., 2010).

The coagulation process in industrial water treatment plants, generally occurs in four steps:

(1) First step: Charge destabilization

In general the colloidal particles in water carry a negative charge. In order for the destabilization step to occur, the coagulants and coagulant-aids must carry a charge opposite to the charge of the impurities in the water being treated. This destabilization

of the impurities potential allows the colloids to agglomerate into microscopic particles known as microflocs. This step is achieved by one or a combination of the mechanisms below (Tzoupanos and Zouboulis, 2008; Vijayaraghavan et al., 2011):

(a) Sweep flocculation which occurs by overdosing the coagulant, consists of the surrounding and enclosing of the impurities by the coagulant.
(b) Adsorption with charge neutralization occurs when the impurities are adsorbed onto the sites of a coagulant of opposite ionic charge, which is followed by the neutralization of the ionic charge.
(c) Adsorption with interparticle bridging occurs when the impurities adhere into the polymer chains of the coagulant.
(d) Compression of the electrical double layer mostly occurs with the use of salts as coagulants.

The mechanisms (a) and (d) are more common with inorganic coagulants while (b) and (c) occurs mostly with organic coagulants.
The efficiency of this step depends on the amount of coagulant added and on the mixing. Sufficient amount of coagulant is required to ensure that the neutralization step is carried to completion. Flash mixing is important to achieve the optimum blending of the coagulant and the water and promote adequate particle collision.

(2) Second Step: Flocculation
Flocculation occurs under slow mixing and it is the step where the microflocs collide and agglomerate into larger particles called macroflocs. Coagulant-aids can be added at this stage to help increase the size, the weight and the strength of the flocs and facilitate settling.
The efficiency of this step depends on the degree of completion of the previous step and on the mixing speed. The mixing energy and speed have to be decreased as the flocs sizes increase to prevent the flocs from tearing apart. This is important since it is difficult to recombine the torn flocs to the optimum size and weight.

(3) Third Step: Sedimentation

This step is used to settle out the flocs and separate them from the clarified water. This often takes place in clarifiers or settling ponds where the clear water is collected from the top, and the flocs slurry is removed from the bottom. The success of this stage depends on the previous steps and on the settling rate of the flocs formed. The settling of the flocs can take several hours.

(4) Fourth Step: Filtration

This is done to polish the quality of the final water and remove particles that failed to settle during the sedimentation stage.

The efficiency of the coagulation process is affected by the pH, coagulant dosage, the efficiency of the flash mixing, the temperature of the wastewater, and the characteristics of the impurities in the water (Freese et al., 2003).

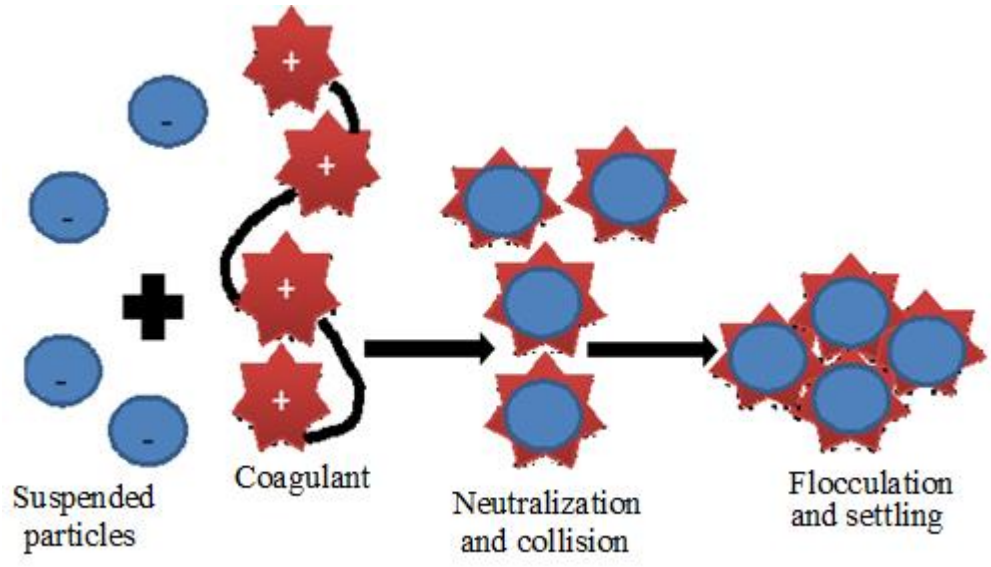

Figure 2.1: Coagulation/flocculation steps

The pH range for optimum coagulation and the coagulant dosage vary with the type of coagulant used. Flash mixing is the determining step of the coagulation process. Poor mixing will result in inadequate blending of the coagulant and the water. Over-mixing does not affect the coagulant efficiency, but slows the process, consumes energy and

is not suitable for large scale processes. The optimum time range for flash mixing is 1-5 minutes (Nozaic et al., 2001; Freese et al., 2003).

The temperature of the water affects the floc formation, thus affecting the time required for slow-mixing. According to Freese et al. (2003), the floc formation is slow and the slow-mixing time is longer at low temperature. They stated that optimum temperature range for effective flocculation lies between 20 and 40℃. The range of slow-mixing time used in literature varies from 8-40 minutes. This step is followed by the settling of particles which may take several hours or less depending on the process (Freese et al., 2003; Bina et al. 2009; Lopus et al., 2009). Coagulant and coagulant aids are compounds used to accelerate the settling rate of the impurities in the water through chemical and physical reactions. They can be organic or inorganic. Inorganic coagulants are widely used for water treatment and can be classified into two types: (a) Ferric salts (e.g. ferric suphate, ferric chloride) and (b) Aluminum salts (e.g. Aluminum sulphate, aluminum chloride).

Organic coagulants are classified as nonionic, cationic and anionic macromolecular polymers, and can be either of natural origins or synthetic. The term polyelectrolytes refers to polymers that are either positively or negatively charged. Natural organic coagulants are water soluble polysaccharides and proteins derived from plant or animals. They are used when there is a need for sludge production due to the fact that they generally produce large amount of flocs. Because of their low toxicity, they are used to avoid the health concerns of inorganic coagulants. The most widely used animal-based polyelectrolyte is chitosan.

2.1.2. Wastewater treatment using coagulation

Coagulation is common in modern water treatment plants. Thus, a lot of studies have been undertaken on improving this process and on finding better alternatives in terms of costs and toxicity. Inorganic coagulants have been used for decades and are widely documented in the literature. Polymers have been used for large scale operations at Umgeni Water, South Africa, yielding satisfactory results in terms of water quality and

costs. Blends of organic-inorganic compounds have been reported to provide good results (Nozaic et al., 2001; Miller, 2013).

Coagulants are used for different types of wastewaters. Amuda et al. (2006) studied the purification of wastewater from brewery industries. Results showed that a combination of an inorganic salt with a nonionic polyelectrolyte provided above 90% removal of the COD and TSS. Dwyer et al. (2009) reported the removal of colour and dissolved organic nitrogen related to melanoidins in sewage water using alum.

Liang et al. (2009) investigated the removal of melanoidins using Ferric Chloride in terms of COD and colour decrease with molasses wastewater. They reported that the use of this particular coagulant was able to reduce colour, COD and the turbidity of the effluent better than biological treatments.

Zhang et al. (2006) used a natural organic coagulant to treat sewage wastewater, seawater and high turbidity water. The coagulation of storm water and river waters using various coagulants has been widely documented. Coagulation has been proven efficient for the removal of inorganic particulates as well as organic matters from wastewater (Annadurai et al., 2004; Sansalone and Kim, 2008; Lopus et al., 2009).

Dissolved air flotation tanks (DAF) and clarifiers are most common units used for industrial coagulation. Whereas jar-tests are small laboratory scale experiments used to determine the optimum conditions for the coagulation process.

2.2. CONVENTIONAL TREATMENT METHODS FOR SUGAR EFFLUENTS

Table 2.2 shows the ranges of the impurities contained in the ESR from various sources relative to the limits of the South African Department of Water Affairs (DWA).

The sugar industry produces a large quantity of wastewater due to water intake and the fact that the industry operates on water surplus from sugar canes which is constituted of 70% water among other components. Therefore, this industry releases a large amount of wastewater into the environment.

Table 2.2: Characterization of the effluents from the sugar refinery

Parameters	Ranges	DWA Guidelines
COD	150-86020	75
TSS (mg/l)	615-146000	25
TDS	700-2458	-
pH	4.35-11	5.5-9.5
Colour	Light to dark brown	None

(Wadley and Buckley, 1991; Purchase, 1996; Ayyasamy et al., 2008; Li et al., 2010; Doke et al., 2011; Samuel and Muthukkaruppan, 2011; DPW, 2012)

These effluents carry suspended particles and OM that impart colour and increase the COD. Chemicals such as Sodium Chloride (NaCl), phosphorus are used in the sugar refineries and are eventually found in the effluent streams.

Organic molecules such as melanoidins are highly resistant to biodegradation and they pose a problem to the environment due to their high COD (Satyawali and Balakrishnan, 2008; Tokumura et al., 2008). The presence of melanoidins in wastewater increases the COD, makes the receiving stream septic and the material is very difficult to remove when treated using conventional methods. Thus, there is a need to develop new treatment methods.

2.2.1. Biological treatment

Biological treatment is the most common method used for the purification of wastewater from the sugar industry. Aerobic and anaerobic treatments using microorganisms are the most common methods used in the purification of effluents containing sugar residues.

During aerobic digestion, microorganisms decompose organic pollutants in the presence of oxygen, whereas anaerobic treatment occurs in the absence of oxygen. Both methods are pH and temperature sensitive. In addition, they require proper selection of microorganisms and nutrients, have high retention time, produce by-products that can be detrimental to the industry and have low efficiency for wastewater of low COD content. These methods are not very efficient for wastewater that contain high amount of melanoidin because of the antioxidant properties of this biopolymer which makes it toxic to bacteria and thus, hinder biodegradation (Ramjeawon, 2000; Pant and Adholeya, 2007).

Liang et al.(2009) reported that biological treatment of melanoidins water failed to remove the colour and the solid particles in the effluents. A pretreatment stage is required to remove solids and other debris from the water. There are other biological treatment used for the removal of COD, BOD, and colour using enzymes, and microorganisms immobilized on different matrices. However, the final water from biological treatment needs to undergo further treatments downstream in order to meet acceptable standards and remove the microorganisms.

2.2.2. Other treatment methods

Wastewaters purified using biological methods often need to be further treated by one or a combination of the following methods:

(a) Filtration: The separation of impurities using nanofilters, ultrafilters, reverse osmosis and membranes are widely practiced in water treatment.
(b) Chemical and biological treatment: these are done to disinfect and further clarify the final water.
(c) Physico-chemical and electrochemical treatments: ion-exchange, electrolysis, electro-dialysis, coagulation and electrocoagulation.

The impurities in the sugar wastewater often cause the filters to foul. Some of the chemicals used in these methods pose health issues, such as aluminium in the coagulation of wastewater. The cost of some of these treatment techniques is a problem, especially since some anodes used in electrochemical procedures are made of precious or expensive metals (Liang et al., 2009; Zhao et al., 2010; Filloux et al., 2012; Robles-González et al., 2012).

2.3. CHITOSAN

2.3.1. Introduction

Chitosan is a polymer made of variable amounts of β-(1–4) linked 2-acetamido-2-deoxy-β-D-glucopyranose and 2-amino-2-deoxy-β-D-glycopyranose prepared by deacetylation of chitin (Barreiro-Iglesias et al., 2005; Crini and Badot, 2008; Azlan et al., 2009; Aranaz et al., 2009; Dash et al., 2011; Setthamongkol and Salaenoi, 2012).

Chitin has not found many applications compared to chitosan due to its poor solubility and lower adsorption capacities among other properties. Aranaz et al. (2009) provided details of the two major preparation methods of chitosan, namely heterogeneous and homogeneous. Both methods utilize concentrated alkali solutions and require long processing time. A simplified diagram of the preparation of chitosan from crustacean shells and other organisms is depicted in Figure 2.2.

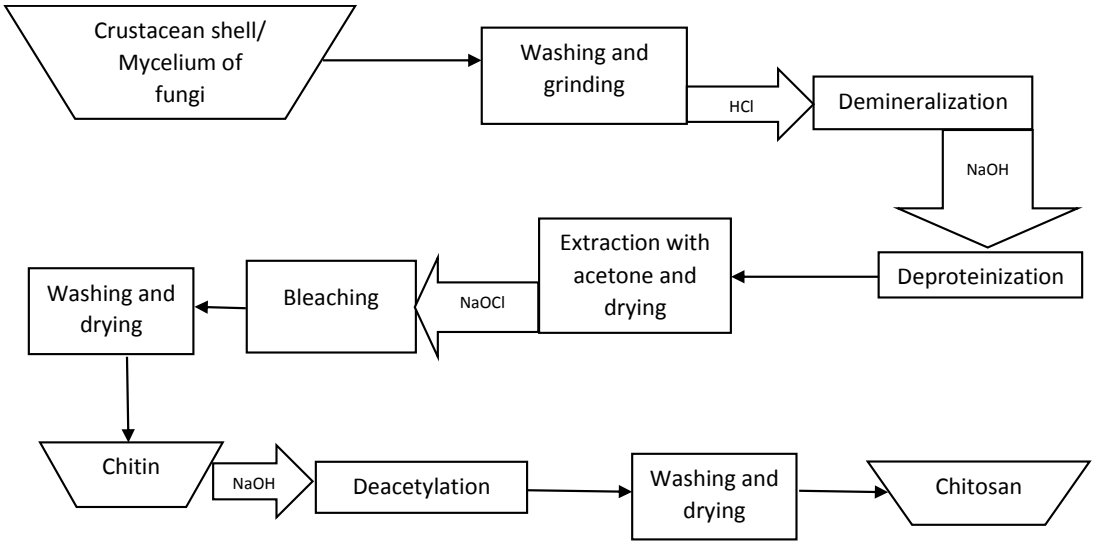

Figure 2.2: Preparation of chitosan

Chitosan can be characterized in terms of its quality, intrinsic properties such as purity, molecular weight, viscosity, and degree of deacetylation and physical forms (Dash et al., 2011; Khan et al., 2002).

Chitosan has many applications in various industries. It is used in the medical industry and in the bioprocessing industry for wound healing, tissue engineering, drug delivery systems, cell immobilization, gene delivery and enzyme immobilization.

In the food industry, it is used as dietary ingredient, food preservative and emulsifying agent. It is also used in the water treatment for the removal of heavy metals, toxic materials and other bio-recalcitrant wastes such as phenols and dyes. Other uses of chitosan are in the paper industry, photographic industry, agricultural industry, in the textile and cosmetic industries (Cestari et al., 2008; Crini and Badot, 2008; Gyananath and Balhal, 2012; Setthamongkol and Salaenoi, 2012).

This wide range of applications is due to the versatile properties of chitosan and its oligomers, some of which can be found in Table 2.3. These properties are often attributed to the cationic nature of chitosan (Crini and Badot, 2008).

2.3.2. Some applications of chitosan in water treatment

Chitosan can be prepared on its own or along with semiconductors, adsorbents, enzyme and other materials (Zainal et al., 2009; Cao et al., 2013). Sadighi and Faramarzi (2013) removed Congo Red by immobilizing an enzyme of chitosan and glass beads and found that it provided a high colour removal.

Chitosan beads have been used for metal adsorption, colour removal as well in biotreatment (Chiou et al., 2004; Osifo et al., 2008; Wan Ngah et al., 2008). Azlan et al. (2009) used crosslinked chitosan beads to adsorb acid dyes and found that chitosan was a promising composite for effective colour removal under adequate optimization and modifications.

Table 2.3: Properties of chitosan

Physical and chemical properties	Linear aminopolysaccharide with high nitrogen content
	Rigid D-glucosamine structure; high crystallinity; hydrophilicity
	Capacity to form hydrogen bonds intermolecularly; high viscosity
	Weak base; the deprotonated amino group acts a powerful nucleophile (pKa 6.3)
	Insoluble in water and organic solvents; soluble in dilute aqueous acidic solutions
	Numerous reactive groups for chemical activation and crosslinking
	Forms salts with organic and inorganic acids
	Chelating and complexing properties
	Ionic conductivity
Polyelectrolytes (at acidic pH)	Cationic biopolymer with high charge density (one positive charge per glucosamine residue)
	Flocculating agent; interacts with negatively charged molecules
	Entrapment and adsorption properties; filtration and separation
	Materials for isolation of biomolecules
Biological properties	Biocompatibility:
	*Non-toxic
	*Biodegradable
	*Adsorbable
	Bioactivity:
	*Antimicrobial activity (fungi, bacteria, viruses)
	*Antiacid, antiulcer, and antitumoral properties
	*Blood anticoagulants
	*Hypolipidemic activity
	Bioadhesivity

(Crini and Badot, 2008; Aranaz et al., 2009)

2.4. WASTEWATER TREATMENT USING CHITOSAN AS A COAGULANT

Lukum and Djafar (2012) used chitosan to coagulate Pb(II) from a sugar factory effluent. They investigated the effect of pH and the influence of chitosan loading on the Pb(II) removal. Their results demonstrated that chitosan was able to effectively remove Pb(II) at the pH value of 9 and a mass load of 10 g of chitosan per 100 ml of sample.

Chi and Cheng (2006) studied the coagulation of milk processing plant wastewater using chitosan and found the optimum pH value for the experiment was close to neutral (pH = 7) and they recommended the chitosan dosage range to be between 20-30mg/l. Chitosan effectively decreased the COD and the TSS content of the wastewater by over 50%.

Bina et al. (2009) investigated the effectiveness of chitosan as a coagulant-aid for the treatment of turbid water caused by the suspension of kaolin by using chitosan in conjunction with alum. They prepared the chitosan solution by diluting 100 mg of chitosan powder into 10 ml of 0.1 M HCl, the mixture was then diluted by adding distilled water to obtain a solution containing 1 mg of chitosan per litre of solution. Chitosan solution was added as a coagulant aid one minute after the samples were mixed with alum. They found that chitosan effectively reduced the turbidity, hardness, Escherichia-coli and total organic carbon (TOC) of the water studied. The amount of alum used was reduced by 50% to 87.5% when chitosan was used as a coagulant aid. Jadhav and Mahajan (2013) used a similar procedure as Bina et al. (2009) for the preparation of the materials used in their experiments to flocculate clay. They also reported a considerable reduction in alum dosage (75%) with the use of chitosan as a coagulant aid along with alum.

Both authors prepared a fresh solution of chitosan for each set of experiments due to reports that chitosan properties are altered when kept in acid over a prolonged period of time. The optimum pH range was found to be between 7 and 7.5 for Bina et al. (2009) and 6.5 to 8.5 for the studies conducted by Jadhav and Mahajan (2013). In the case of Bina et al. (2009) studies, the optimum range of chitosan dosage was found to be between 0.5 mg/l to 10 mg/l whereas Jadhav and Mahajan (2013) found the

optimum range of chitosan dosage to be between 0.5 mg/l to 2.5 mg/l. The efficiency of chitosan as a coagulant has been reported to be greatly affected by the initial turbidity of the samples. Bina et al. (2009), Jadhav and Mahajan (2013) reported higher removal efficiency at higher initial turbidity.

Roussy et al. (2005) studied the influence of chitosan, prepared in acetic acid, on the coagulation and the flocculation of bentonite suspensions. They found that the flocculation was more effective at the pH of 5, high molecular weight chitosan yielded better coagulation capacity compared to low molecular samples except when the molecular weight exceeded 100 000 g/mol. They used a chitosan dosing as low as 0.02 mg/l to reduce the bentonite content of water of 5 g/l by over 95%.

Chitosan has also been used for the treatment of coloured wastewater. Szygula et al. (2009) used chitosan prepared in acetic acid for the removal of acid blue 92. They reported that the discolouration of the dye solution using chitosan was 99% efficient under optimum conditions. They also pointed out that efficiency of the system was considerably affected by the pH of the solution. The chitosan dosage required increased with the increase in pH value.

Their studied also indicated that the behaviour of the chitosan in the solution as a coagulant was influenced by the experimental conditions, namely pH, the type of wastewater, the nature of the colloids and the initial concentration of the solution. Therefore, the coagulation occurred either by chain association through hydrogen bridging, or by hydrophobic interactions through charge neutralization. Their optimum pH value was found to be 5 and the chitosan dosing ranged from 50 mg/l to 120 mg/l. The ranges above are very useful to provide a basis for the preliminary experiments.

2.5. DESIGN OF EXPERIMENTS

Design of experiments (DOE) can be defined as the systematic planning of information gathering with the use of experimental and statistical methods to identify the optimum factors and levels for a particular problem either of industrial scale or for research purposes.

The main aims of DOE include the screening of variables, the optimization of the process and the development of a robust system from the experimental outcomes. There are three fundamentals to this design method, namely, randomization, blocking and replication. Randomization involves running experimental trials at irregular order in order to avoid biased conclusion and to guard against the influences of unknown variables. Blocking refers to the process whereby experimental unit are arranged in groups based on their similarities. Replication is the repetition of experimental runs including the repetition of the set-up of each run.

Other principles include comparison and othogonality. Orthogonality is a type of comparison represented by vectors. In DOE orthogonality is most commonly applied with factorial designs. The particularity of the orthogonal comparison is the fact that individual sets of orthogonal runs are not related to each other, providing an independent distribution of the information provided by each run.

2.5.1. OFAT Design

The most commonly used DOE is the one-factor-at-a-time design which vary only one variable at a time while keeping others constant. This design method can be used for the screening stage as well as the optimization stage of an experiment. The objective of OFAT is to provide information about individual variables and to optimize the process as the experiment proceeds (Qu and Wu, 2005).

The OFAT design carries a number of advantages reported in literature. Qu and Wu (2005) reported that OFAT design provided a faster identification of the influence of a given factor on the system, and allows more flexibility than orthogonal fractional factorial designs (OFFD). They also reported that the OFAT design requires less run than the OFFD and is therefore more economical. The OFAT design also allows the

rapid identification of maxima, minima as well as curvatures in an experiment (Friedman and Savage, 1947; Czitrom, 1999).

McDaniel and Ankenman (2000) stated that OFAT exploration can detect significant effects and they demonstrated that a combination of the OFAT design with the Box-Behnken design provided better results than the use of factorial designs.

The use of OFAT is being discouraged and many authors prefer the factorial design due to the following reasons (Czitrom, 1999; Montgomery, 2005; Wahid and Nadir, 2013):

- The OFAT designs do not show interactions between the variables.
- The prediction of the response in the factor space is improved in factorial designs.
- The lack of randomization can lead to biased conclusions.

However, the OFAT design is less complex and requires less training for the readers to understand the experimental outcomes (McDaniel and Ankenman, 2000; Qu and Wu, 2005).

2.5.2. Factorial designs

The factorial design consists of performing experiments with all possible combinations of the levels of the variables for each trial. This design provides an understanding of the effects and takes into account the interactions between the factors (Fig. 2.3).

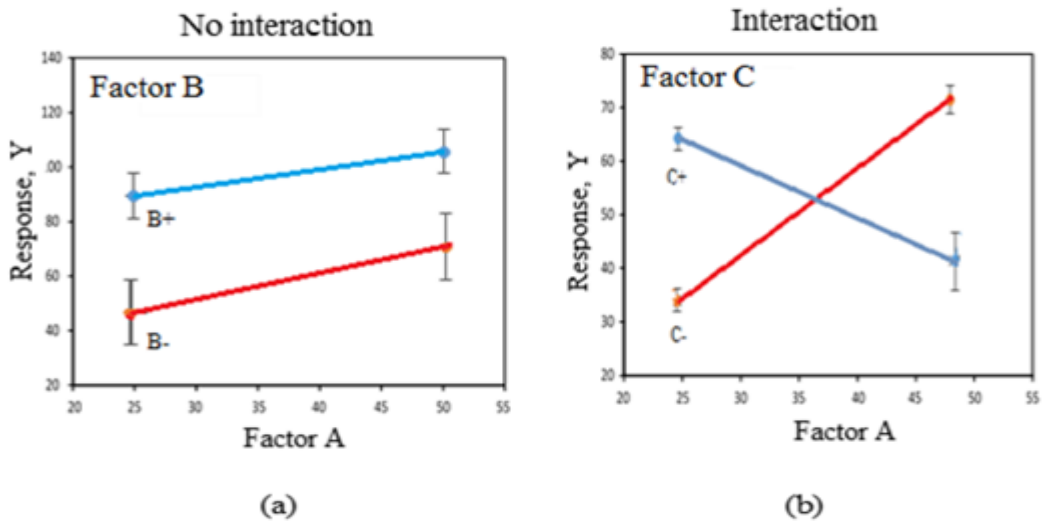

Figure 2.3: (a) Factorial design without interactions (b) Factorial design with interaction.

Interaction occurs when the effect of one factor is dependent on the level of another. Fig. 2.3a shows that the response Y increases with an increase in each levels of factor B (B-) as the minimum and B+ as the maximum) and an increase in factor A. Factors A and B do not interact.

The plot in Fig. 2.3b indicate that the minimum level of factor C (C-) provides a higher value of the response as factor A increased. Whereas the high level of C (C+) had a contrary effect. There is interaction between factors A and C.

A factorial design of *n* number of factors and L levels (represented as L^n) where all the possible combinations of the levels of all variables are taken into account is referred to as a full factorial design (FD). The most basic FD is the two-level factorial design (2^n FD). The 2^n FD provides good information on the effects and the interactions but operates on the assumption of linearity, thus failing to identify the curvatures that might be present in the experiments.

The FD is not suitable for a high number of variables because the number of runs required for the experiment increases with high number of factors, making this method uneconomical as illustrated in Table 2.4. Therefore, designs which carefully select a fraction of the FD are used. They are referred to as fractional factorial design (FFD), represented as $F^{(n-p)}$, where n is the number of runs and p represents the fraction used (e.g. for a fraction of ½ , p = 1; ¼ , p = 2; $1/_8$, p = 4).

Table 2.4: Number of runs for a two-level full factorial design.

Two-level factorial design 2^n	
# of factors (n)	# of runs required
2	4
4	16
8	256
10	1024
20	1048576
30	1073741824

The FFD are used for the following reasons:

- Screening of the variables to identify the important factors
- The number of experimental runs required for FD exceeds the resources available (time, cost, etc.)
- When the investigation focuses mainly on low-order interactions and main effects, under the assumption that only a small number of effects are significant.

The analysis of experimental data is done through the analysis of the effects and interactions as well as the analysis of variance (ANOVA). These can be done manually through the use of formulae widely documented in literature or with the use of computer software packages such as JMP, BMDP, Mintab, GLIM, Design Expert, Analytica, SPSS etc., which provide faster results and are more convenient to use than the manual method.

In factorial designs and RSM, the terms are codified to normalize the variables before regression analysis. This is done to eliminate the effect of different units and ranges in the experimental domain and allows parameters of different magnitude to be investigated more evenly in a range between -1 to +1. The equation used for coding is:

$$X = \frac{x - \left(\frac{x'' + x'}{2} \right)}{\left(\frac{x'' - x'}{2} \right)} \quad (2.1)$$

Where X is the coded factor/variable, x is the natural variable, x'' and x' represent the maximum and the minimum of the values of the natural variable respectively (Baş and Boyaci, 2007).

The optimization of the process can be carried out using factorial designs; however they have limits that are remediated through the use of response surface methodology (RSM). Some of the setbacks of factorial design (FD and FFD) are listed below (Ferreira et al., 2007; Bezerra et al., 2008; Wahid and Nadir, 2013):

- Lack of visualisation: The factorial designs on their own do not provide a 3D visual pattern of the behaviour of variables being investigated which is compensated in the response surface methodology.
- Factorial designs with two-levels do not show curvatures and are not efficient for second degree polynomial.
- The three-level factorial design is inefficient in response surface methodology applications when the number of factors exceeds 3 (See Table 2.5).

The following section describes the theory of response surface methodology as an optimization tool.

2.6. RESPONSE SURFACE METHODOLOGY MODELS

Response surface methodology (RSM) uses a set of mathematical and statistical procedures to describe the relationship between a set of data described by a polynomial equation that relates to the experimental data, in order to concurrently optimize the responses. The RSM application proceeds according to the following steps (Baş and Boyaci, 2007; Bezerra et al., 2008):

1. The screening of variables with the use of DOE.
2. The choice of an experimental design that will be used to generate the polynomial equation.
3. The statistical analysis of the data and the generation of a polynomial model.
4. The verification of the model fitness and the investigation of optimum conditions.

2.6.1. Two-level factorial design

2^n designs generate linear functions of the response (Y) which can be used in RSM.

$$Y = \beta_0 + \sum_{i=1}^{n} \beta_i X_i + \varepsilon \qquad (2.2)$$

Where β_0 represents the constant term and β_i represent the coefficient of the linear parameters respectively. X_i represents the factor and ε is the residual from the treatments.

This design does not accommodate second degree polynomial equations due to the fact that it does not represent curvatures. However, the 2^n can be modified by the addition of centre-points that generate three-level designs that are suitable for higher degree polynomial in RSM.
The most common types of designs with centre-points are the central composite design (CCD), the Doehlert design (DD) and the Box-Behnken design (BBD) (Baş and Boyaci, 2007; Bezerra et al., 2008).

2.6.2. Three-level full factorial design

The three-level full factorial (3^n) overcomes the limitations of the 2^n. The set back of this type of designs is the fact that it loses its efficiency as the number of variable increases and requires more runs, and it is limited to the treatment of two variables.

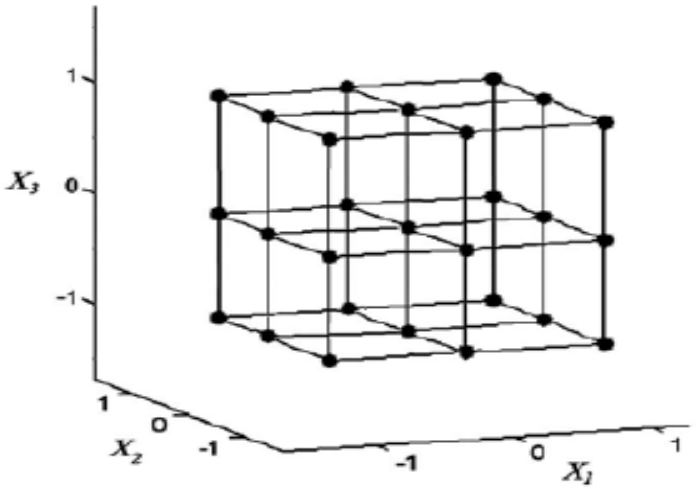

Figure 2.4: Surface plot for 3-factors FD(Jambrak, 2011).

The three-level FFD has a lower efficiency than the CCD, the BBD and the DD due to the fact that it requires a higher number of experiments needed per factor used (Montgomery, 2005; Ferreira et al., 2007; Bezerra et al., 2008). The surface plot for 3^n is shown in Fig. 2.4.

2.6.3. Central composite design

This is a factorial design with the addition of points at the centre and at a distance α from the centre forming a star design (Fig. 2.5), where all factors are investigated at five levels (-α, -1, 0, +1, + α).

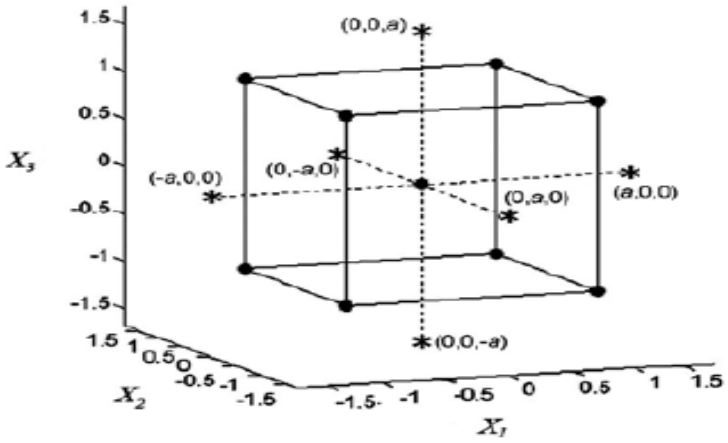

Figure 2.5: Surface plot for 3-factors CCD (Jambrak, 2011).

In Figure 2.5, X_1, X_2 and X_3 represents the manipulated factors.

The distance α can be calculated for a given number of factors using the formula below:

$$\alpha = 2^{\left(\frac{k-p}{4}\right)} \tag{2.3}$$

The number of experiments required (N) can be computed as follows:

$$N = k^2 + 2k + C \tag{2.4}$$

Where k is the number of variables and C represents the replicate number of centre-points.

The CCD is the most widely used DOE. There are three main variations of the CCD used for quadratic designs:

- The central composite circumscribed design (CCC)
- The central composite face-centred design (CCF)
- The central composite inscribed design (CCI)

These variations are briefly discussed in Table 2.6.

2.6.4. The Doehlert design

The DD is the most economical, requiring the least number of runs as shown in Table 2.5, and yielding high efficiencies compared the other designs. The design domain varies with the number of variables. The domain for:

- $k = 2$ is circular
- $k = 3$ is spherical
- $k > 3$ is hyperspherical

The number of experiments required (N) can be computed as follows:

$$N = k^2 + k + C \tag{2.5}$$

The surface plot for DD of three factors requires 13 runs as shown in Fig. 2.6.

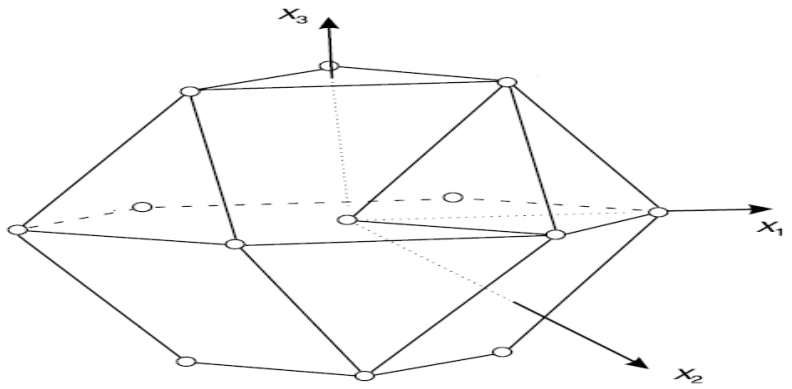

Figure 2.6: Surface plot for 3-factors Doehlert design
(Adapted from Sautour et al. 2001)

Table 2.5: Comparison between three-level designs

	Minimum number of experiments needed (*N*)			
# Factor (*k*)	Three-level FFD	CCD	DD	BBD
3	27	15	13	13
4	81	25	21	25
5	243	43	31	41
6	729	77	43	61
7	2187	143	57	85
8	6561	273	73	113

Ferreira et al., 2007

2.6.5. The Box-Behnken design

In the BBD, points are situated at the same distance from the central point as shown in Figure 2.6, and all factors must be adjusted at three levels (-1, 0, +1) (Bezerra et al., 2008).

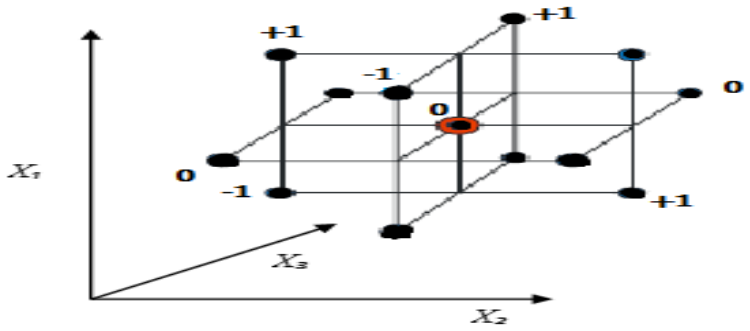

Figure 2.7: Surface plot for 3-factors Box-Behnken design

(Adapted from Statease Inc, 2014)

The number of experiments required (N) can be computed as follows:

$$N = 2k(k-1) + C \tag{2.6}$$

Table 2.6: Comparison between various DOE styles

DOE style		Details
Three-level full factorial		Three levels are required for each variable. Requires high number of experimental runs compared to the other DOE types below.
CCD	CCI	Five levels are required for each variable. Only uses points specified in the experimental constraints. Gives poor predictions compared to the CCF and the CCC.
	CCF	Three levels are required for each variable. Provide better predictions than the CCI.
	CCC	Five levels are required for each variable. This design requires points outside of the constraints of the original factorial design. Provides better predictions than the CCI and the CCF.
BBD		Three levels are required for each variable. Similar to CCI in terms of the quality of the prediction when the number of factors exceeds 3. Requires fewer runs than the CCD for 3<n<4.
DD		Five levels are required for each variable. The experimental domain expanded by moving the design towards a different domain or by the addition of other parameters. Requires lower runs than all the DOE above. Provides good predictions.

(NIST/SEMATECH. 2012; Ferreira et al., 2007; Bezerra et al., 2008; Sautour et al. 2001)

2.7. MODEL ANALYSES

The critical points in the RSM plot can be represented by maximum, minimum or saddle patterns (Fig. 2.8) and are obtained from the following quadratic polynomial equation (Bezerra et al., 2008):

$$Y = \beta_0 + \sum_{i=1}^{n} \beta_i X_i + \sum_{i=1}^{n} \beta_{ii} X_{ii}^2 + \sum_{i<j}^{n} \beta_{ij} X_i X_j + \varepsilon \qquad (2.7)$$

β_{ii} represents the coefficient of the quadratic parameter and β_{ij} represents the coefficient for the interaction parameters.

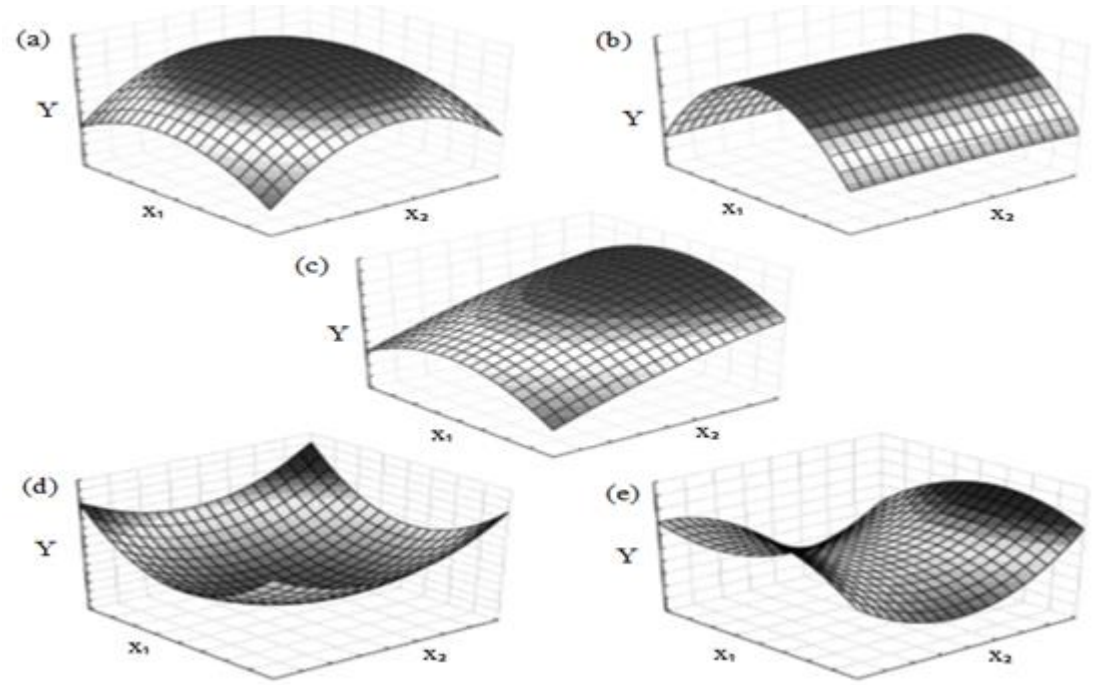

Figure 2.8: RSM profiles (a) maximum, (b) maximum plateau, (c) maximum outside the experimental region, (d) minimum, and (e) saddle surfaces (Bezerra et al., 2008).

The RSM profiles are generated using specialised software packages and show the behaviour of a combination of factors relative to the response. Figure 2.8 shows different RSM profiles which correspond to the behaviour of the experimental data. In order to gauge the efficiency of the model, these graphs alone are not sufficient. There

are many steps that need to be followed, which include statistical and graphical analyses of the model. These steps are discussed in the following sections.

2.7.1. Evaluation of a chosen design

In order to obtain good results from a particular design, the latter needs to satisfy certain conditions. When a software such as Design Expert is used, the designer must ensure that the correct model order is selected. The linear model (Eq. 2.2) is the lower order and is applicable to factorial design with no curvatures. The two-factor interaction (2FI) model (Eq. 2.8) should be used when the experimenter is sure that there are interactions between the factors and that there are no terms of higher order than 1, this is determined during screening experiments.

$$Y = \beta_0 + \sum_{i=1}^{n} \beta_i X_i + \sum_{i<j}^{n} \beta_{ij} X_i X_j + \varepsilon \tag{2.8}$$

The quadratic model (Eq. 2.7) includes terms raised to the power 2. Higher order polynomials can be used but they require more experimental points in order to avoid aliases. A model is aliased when the effect of one or more variables in the equation is linearly dependent on others.

Another element to consider is the variance inflation factor (*VIF*) for each term in the model. The *VIF* measures how much the variance of the model is inflated by the lack of orthogonality in the design. Orthogonality means that the factors are randomly independent on each other. If the factor is orthogonal to all the other factors in the model, the *VIF* is 1.0 and the correlation coefficient (Ri^2) is equal to 0.

$$VIF = \frac{1}{1 - Ri^2} \tag{2.9}$$

A high value of the Ri^2 indicates that the terms are correlated to each other and will lead to poor models (Statease Inc, 2014). It is important that the selected manipulated variable have no correlation with one another. Each term must be independent. For example when investigating the cost of electricity (response) variables such as demand

and population growth are correlated, whereas variables such as turbine size and cable cost are independent (or orthogonal to each other).

The standard error (SE) is the estimated standard deviation multiplier for the coefficient estimate. In a well-designed experiment the standard errors should be approximately the same within the type of coefficient. In this step a 3D graph of the SE is plotted. The profile of the graph should be flat centred in the middle of the design space and the contour should appear either as a circle or as a square of uniform precision. The initial evaluation step is described extensively in the handbook for experimenters published by Statease (Statease Inc, 2014).

2.7.2. Analysis of the fitted model

The fit test includes the sequential model sum of squares, the lack-of-fit (LOF) test, the model summary statistics and the analysis of variance (ANOVA). The ANOVA provides a comparison between the variations caused by the experimental runs and the variations caused by the measurement errors (Table 2.7).

Table 2.7: ANOVA of the significance of a model (Adapted from Bezerra et al. 2008)

Variation	SS	df	Mean square (MS)	F-value
Regression	SS_R	$v-1 = df_R$	$MS_R = SS_R/df_R$	MS_R/MS_E
Residuals	SS_E	$t-v = df_E$	$MS_E = SS_E / df_E$	
Lack of fit	SS_L	$L-v = df_L$	$MS_L = SS_L / df_L$	MS_L/ MS_P
Pure error	SS_P	$t-L = df_P$	$MS_P = SS_P / df_P$	
Total	SS_T	$t-1 = df_T$		

t represents the number of trials; *L* is the total number of levels in the design and *v* is number of variables in the model. The degrees of freedom (df) is the number of values that can vary without violating the constraints of a design. The sum of square (SS) is a measure of variability, and can be used to estimate the variance of the mean value of a statistical analysis when scaled for the df. The sum of square for the deviations in all the trials is known as the total sum of square (SS_T). It is computed by adding the sum

of square caused by the residual (SS_E) and the sum of square caused by the regression (SS_R).

$$SS_T = SS_E + SS_R \tag{2.10}$$

In general, an experiment is repeated for accuracy and confidence in the results. However this leads to errors and deviations. For an experiment that involves repeatability, the SS_R is found by adding the sum of square due to the lack-of-fit (SS_L) and the sum of square due to the pure error (SS_P):

$$SS_R = SS_L + SS_P \tag{2.11}$$

The sequential model sum of square (SS_{seq}) is used when the regression model involves additional predictor variables. The SS_{seq} selects the highest order polynomial where the additional terms are significant and the model is not aliased (Baş and Boyaci, 2007; Bezerra et al., 2008; Montgomery, 2009; Trinh and Kang, 2011).

The Fischer test (F-test) of a model evaluates the significance of the model by calculating the ratio of the mean square of regression (MS_R) to the mean square of residuals (MS_E). A small F-value for the model is not desired since it indicates that the variance is caused by random unexplained disturbances referred to as noise. The p-value (p > F) provides an indication of the significance of a model in relation with the F-value. It can be defined as the probability that a variable did not affect the response for a given F-value. If the p > F for the model is less than 0.05 a model is said to be significant, meaning that there is 5% chance that the F-value is due to noise. If the p > F is above 0.1, the model is insignificant (Montgomery, 2005; Trinh and Kang, 2011).

The lack-of-fit test (LOF) determines the inability of a model to fit experimental data that are not represented in the experimental domain. This is commonly done by calculating its F-value. A small F-value for the LOF is desired, since the experimenter wants the model to fit. If the p > F is greater than 0.05 the LOF for the model is insignificant and the model is able to fit any data that are not specified in the experimental domain (Trinh and Kang, 2011). A good LOF does not guarantee the adequacy of a model, the coefficient of determination (R^2) must be considered given

the fact that it measures the overall performance of a model and its value should be close to 1 (Baş and Boyaci, 2007).

$$R^2 = 1 - \left(\frac{SS_E}{SS_T} \right) \tag{2.12}$$

The adjusted R^2 ($\check{R}^2$) is computed by arranging the number of terms in a regression relative to the number of design points and it is usually equal to or lower than the R^2. It has the particularity of being less subjected to variation than the R^2 when a new term is added to the regression (Myers et al., 2009).

$$\check{R}^2 = 1 - \left(\frac{SS_E / df_E}{SS_T / df_T} \right) \tag{2.13}$$

$$PRESS = \sum_{i=1}^{n} \left(\frac{e_i}{1 - h_{ii}} \right)^2 \tag{2.14}$$

Where e_i represents the residual and h_{ii} is the leverage (Montgomery, 1997)

$$\acute{R}^2 = 1 - \left(\frac{PRESS}{SS_T} \right) \tag{2.15}$$

The predicted residual sum of squares (PRESS) measures how well a particular model fits individual design points and it is used to compute the predicted R^2 ($\acute{R}^2$) which indicates the level of change in the data using the model. During the selection of a model, the aim is to maximize the $\check{R}^2$ and the $\acute{R}^2$. For a perfect fit, the difference between the $\check{R}^2$ and the $\acute{R}^2$ must be less than 0.2 and model transformations should be considered if this criterion is not met.

Other parameters in the analysis of a model include the standard deviation (SD) expressed as:

$$SD = \sqrt{MS_E} \tag{2.16}$$

The coefficient of variation (CV) measures the unexplained changes in the data:

$$CV = \left(\frac{SD}{\bar{Y}} \right) \times 100 \tag{2.17}$$

Where $\bar{Y}$ is the mean of the response variable.

The adequate precision statistic (*AP*) determines the performance of the model in predicting the responses. A value of *AP* greater than four means that the model will give good predictions.

$$AP = \tilde{Y}_{max} - \tilde{Y}_{min} \tag{2.18}$$

Where $\tilde{Y}_{max}$ and $\tilde{Y}_{min}$ represent the maximum predicted response and the minimum predicted response respectively (Anderson and Whitcomb, 2000; Montgomery, 2009; Myers et al., 2009).

2.7.3. Model diagnostics

Diagnostic plots provides a confirmation that the ANOVA assumptions are correctly met by analysing the residuals versus various other elements that will be discussed in this section.

$$\text{Residual} = e_i = Y_i - \tilde{Y}_i \tag{2.19}$$

Where Y_i is the actual response and $\tilde{Y}_i$ is the response predicted by the model.

The residuals are classified as externally studentized (ESRes) or internally studentized (ISRes). A residual is said to be studentized when it is divided by the estimate of its standard deviation (SD).

The ISRes (*r*) compares the value of a residual to the residual variance in order to measure the number of SD that separates the actual from predicted values.

$$\text{ISRes} = r = \frac{e_i}{s\sqrt{(1 - h_{ii})}} \tag{2.20}$$

Where *s* is the standard deviation.

ESRes (t) makes a comparison between the residual and the residual variance, excluding the first case of SD (s_{-1}). It represents the number of SD between the predicted value and the actual response (Montgomery, 2009; Statease Inc, 2014).

$$\text{ESRes} = t = \frac{e_i}{s_{-1}\sqrt{1-h_{ii}}} \tag{2.21}$$

1. Normal plot of residuals

The normal plot of residual is used to validate the equal variance and normality assumption. Normality indicates whether or not a set of data is normally distributed by plotting the data against the theoretical normal distribution in order to form an approximate straight line (Chambers et al., 1983; Montgomery, 2009).

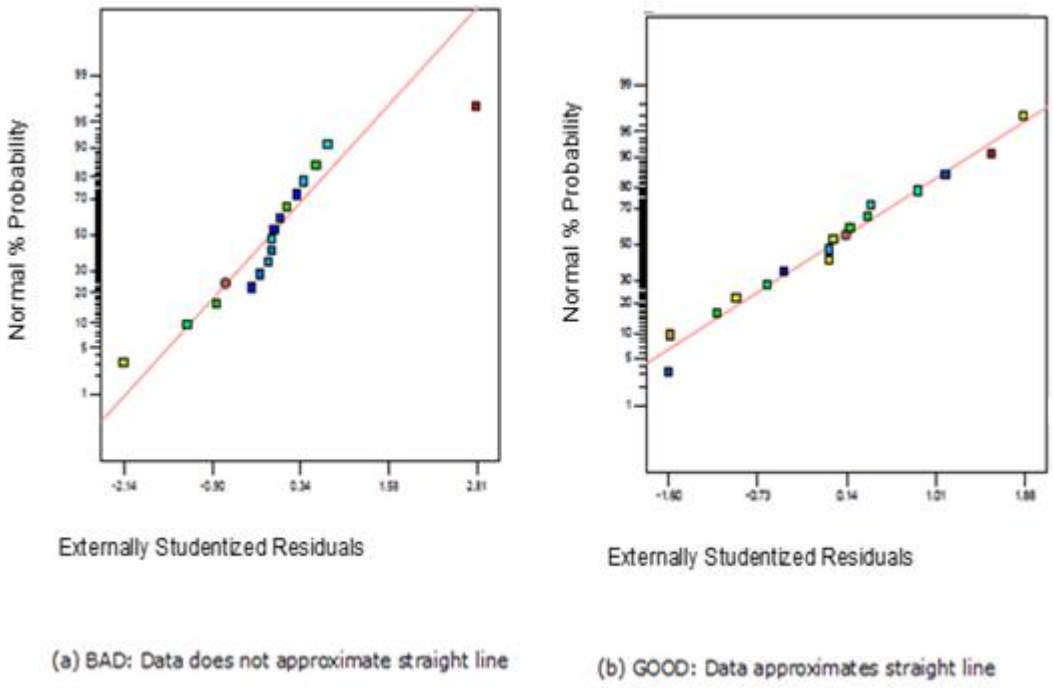

Figure 2.9: Normal plot of residual (a) Data is not normally distributed (b) Data is normally distributed (Adapted from Statease Inc, 2014).

It can be seen from Figure 2.9a that there is a point (red on the right) that is far from the other residual data points. That point is called an outlier and are caused by mistakes

in calculation or experimental errors. Outliers can be examined manually using the following formula for standardised residuals (d_i) (Montgomery, 2009):

$$d_i = \frac{e_i}{\sqrt{MS_E}} \tag{2.22}$$

Statistical programs such as Design Expert, compute the outliers automatically as they generate the normal plots.

2. Residuals plots

Residual plots are used to verify that all the assumptions of a particular DOE are satisfied and the model is correct. For a well-fitted model, residual plots data are scattered randomly, producing a structureless pattern. There are two types of residuals plots that need to be analysed in order to check a particular model:

- Residuals vs. predicted values from the model (Fig. 2.10)
- Residuals vs. experimental runs (Fig. 2.11).

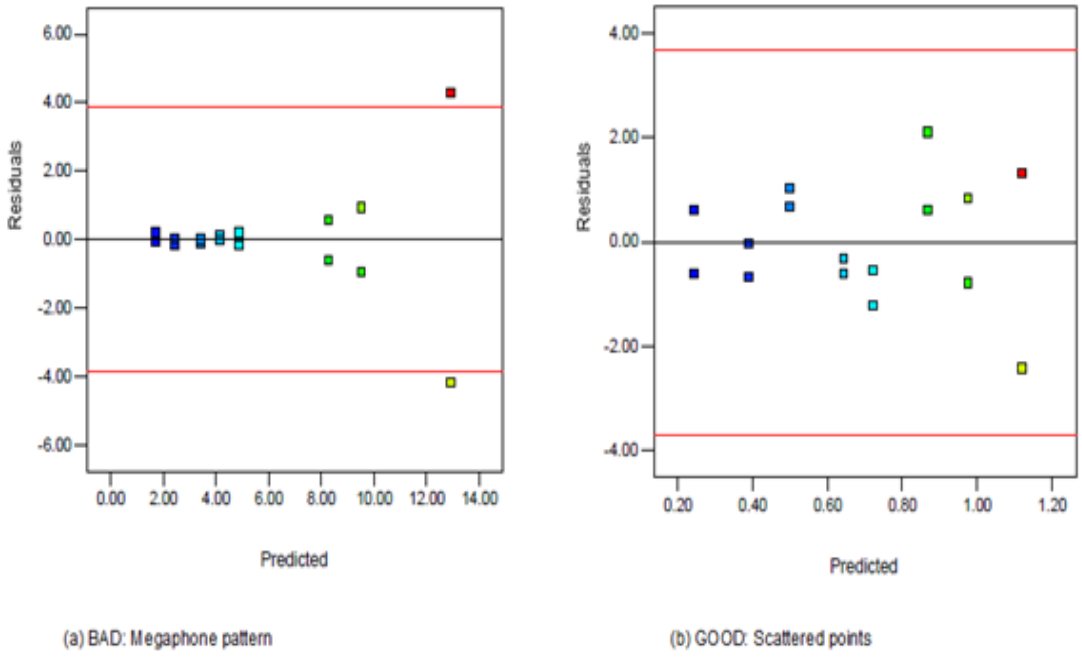

Figure 2.10: Residuals vs. predicted values (a) Model is bad: Megaphone shape (b) Model is good: Randomly scattered (Adapted from Statease Inc, 2014).

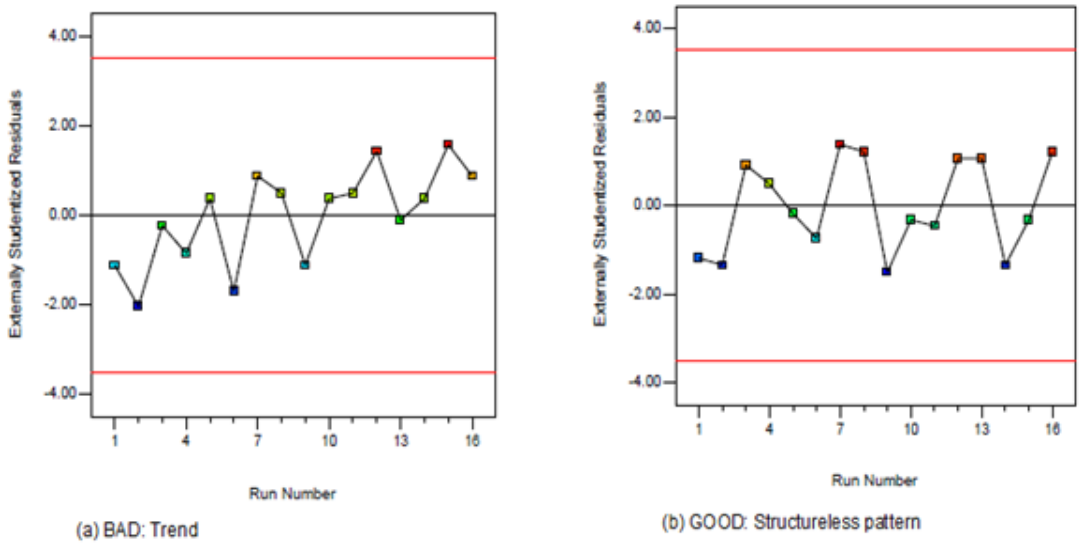

Figure 2.11: Residuals vs. runs (a) Model is bad: Data points form a trend (b) Model is good: data are structureless (Adapted from Statease Inc, 2014).

3. Predicted vs. actual

The predicted vs. actual plot provides an indication of the fitness of a particular model. In order to affirm that a model fits the experimental data using this plot, the data points must be distributed randomly along a 45 degree line in the manner shown in Figure 2.12b (Statease Inc, 2014).

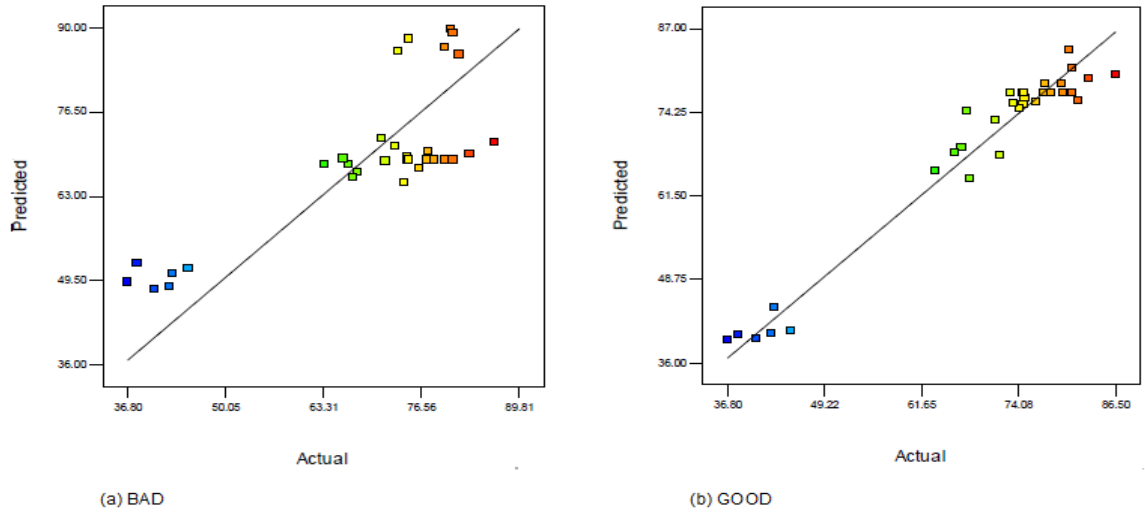

Figure 2.12: Predicted vs. actual (a) Poor prediction (b) Good prediction (Adapted from Statease Inc, 2014).

2.7.4. Box-Cox plot for power transforms

When the diagnostics plots exhibit an abnormal behaviour, a useful way to fix the model is by selecting the appropriate power transformation. The most common method for the selection of a power transformation is by trial and error, whereby the experimenter tries different power transformations and selects the one that gives satisfactory plot of residuals versus predicted values (Montgomery, 2009). The experimental data are transformed using a transformation parameter to generate the response Y^*.

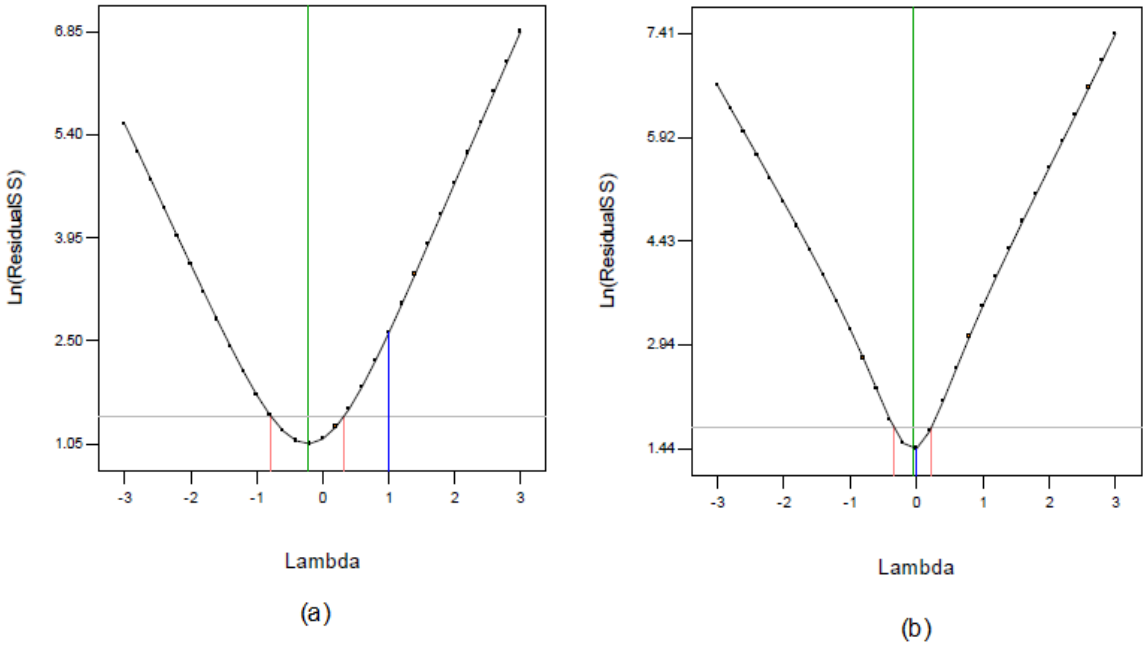

Figure 2.13: Box-Cox plots for power transformation for model (a) Without transformation (b) After transformation (Adapted from Statease Inc, 2014).

Power transformations in statistics are used to:

- Approximate the distribution of the response variables to the normal distribution.
- Stabilize the residual variance and the response variance.
- Ameliorate the fit of the model regression to the experimental data.
- Most statistical tools use the Box-Cox transformation method expressed as:

$$Y^{*} = Y^{\lambda} \tag{2.23}$$

Where λ (lambda) is the transformation parameter, *Y* is the response before the transformation.

Most statistical packages plot Box-Cox transformation as the natural logarithm of the residual versus λ, and provide an indication of the best value of λ that needs to be used in order to fix the variance in the response. In Figure 2.13, the vertical line which goes from the top to the bottom of the plot represents the best λ value. The red parallel lines on both sides of the best λ line indicate a 95% confidence interval associated with the best lambda value. The blue line touching the curve shows the actual transformation (Statease Inc, 2014)

The effect of Box-Cox transformations will not be discussed in this work since their influence on the RSM 3D plots is negligible. However, analyses of transformed data can be found in Appendix B.

2.7.5. Optimization

Chemical engineering is mostly about optimizing processes through new designs and other methods. RSM provides models that can be used to predict optimal conditions of a particular system. Using Design Expert software, the optimization can be done graphically or numerically, where the experimenter sets goals or criteria of the conditions desired for a given process.

2.8. SUMMARY

Coagulation is a process that has been used for centuries for the purification of water. The process takes place in stages whereby the charges of the impurities are neutralized by forming bonds with the coagulant which leads to flocculation and settling. There are many types of coagulants used to speed up the settling of particles in water. They can be categorised as natural coagulants and synthetic coagulants. Chitosan is a cationic biopolymer that can be used as a natural organic coagulant. Water treatment with chitosan is classified as an emerging treatment method, its efficiency for the

treatment of industrial wastewater is being widely investigated. However, few make mention of its efficiency in treating wastewater from the sugar industry. Further in this work, the treatment of sugar refinery effluents using chitosan as a coagulant is addressed.

The OFAT method is the most used design of experiment. However, there are new methods that have emerged, which offer many advantages and more flexibility than the traditional OFAT. The Box-Behnken design was selected for this study because of its simplicity and the reliability of its predictions when the number of factors is lower than 4.

CHAPTER 3: METHODOLOGY

3.1. INTRODUCTION

Two streams of effluents from Tongaat-Huletts were considered in this study to test the efficiency of Chitosan as a coagulant for the ESR namely the final effluent (FE) and the resin effluent (RE). The FE carries dissolved sugar, solids, chemicals (e.g. soda ash, sulphates, manganese, etc.) and ash from the boilers and from the plant general activities. The COD of this stream exceeds the limit specified by the standards of the refinery. It has a milky to a greyish colour and it is sent out to the local municipality for purification. The RE is the wastewater produced from the discolouration of brown sugar syrup to yield white sugar using resin ion-exchanged. It has a high COD and a thick brown colour. Although the RE constitutes only 7% of the overall effluent from the refinery, it is more expensive to treat due to the presence of melanoidin, a natural brown polymer of high molecular mass found in sugar cane and other organic material such as molasses, coffee beans, malts, etc., which is very recalcitrant to conventional treatment methods. Thus, the RE is disposed of in authorized landfills through a waste management company. A simplified flow diagram of the effluents system is represented in Figure 3.1. Table 3.1 shows the level of impurities in both streams in terms of percentage based on Tongaat-Huletts specified limits (Average values from January 2009 to March 2014).

Table 3.1: Characterisation of the sugar effluents.

Parameters	FE	RE	Specified limits	DWA guidelines
COD (mg/l)	16837	53688	<1000	75
TSS (mg/l)	309	7350	<1000	25
Colour	Milky to grey	Dark brown	Not specified	None
pH	8.5	10.02	>6.5	5.5-9.5
Temperature (℃)	25-34	34-40	25-35	25-33

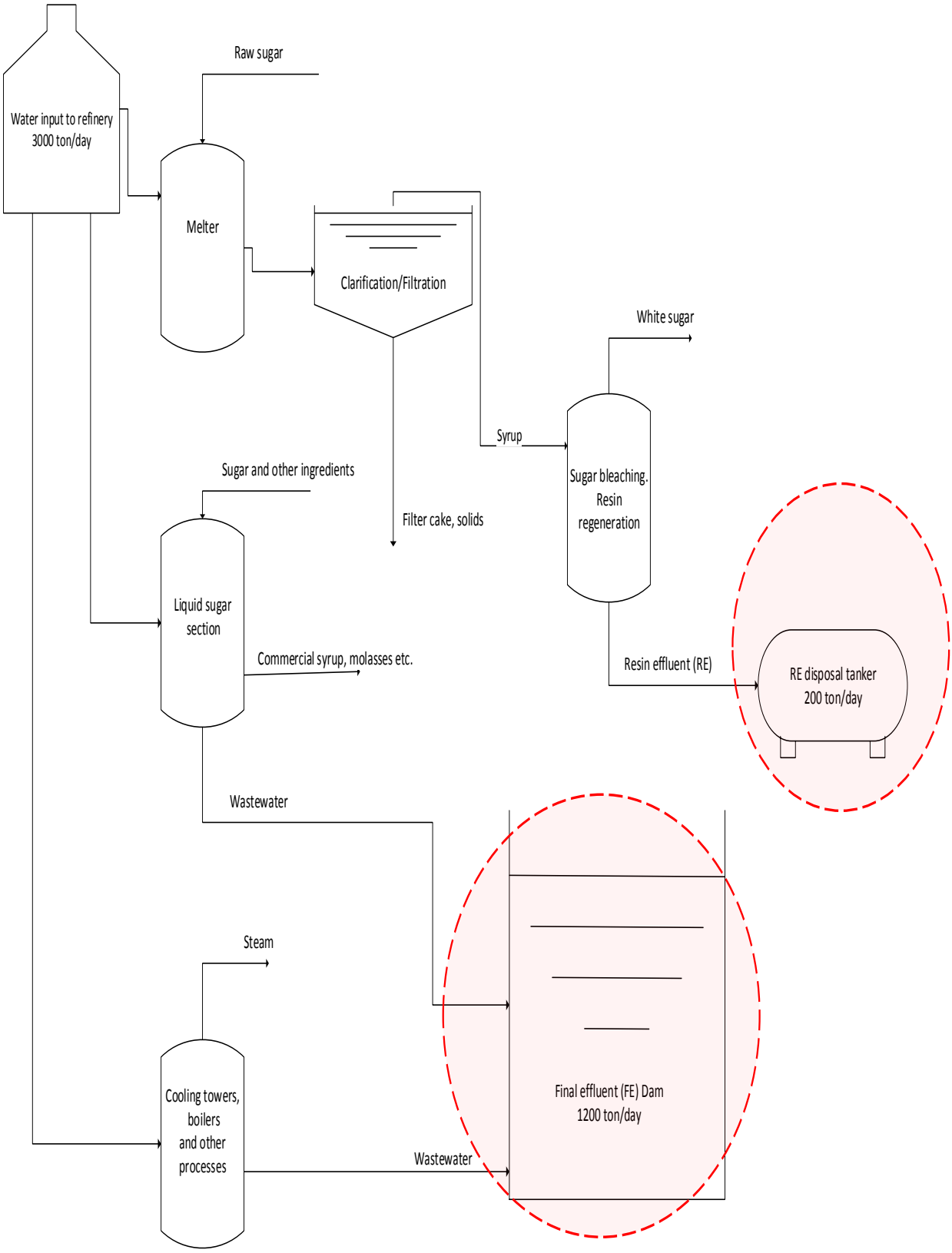

Figure 3.1: Simplified effluent system from the sugar refinery.

3.2. MATERIALS AND EXPERIMENTAL PROCEDURES

3.2.1. Preparation of the coagulant

The chitosan coagulant (CCo) was prepared using a method adapted from literature (Bina et al., 2009; Divakaran and Sivasankara Pillai, 2001; Jadhav and Mahajan, 2013).

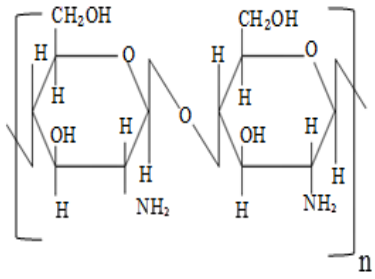

Figure 3.2: Chemical structure of chitosan.

The high molecular weight chitosan powder was purchased from Sigma Aldrich South Africa, with a degree of deacetylation greater than 75% (Fig. 3.2). Figure 3.2 is a pictorial representation of the description of the chitosan as discussed in section 2.3.

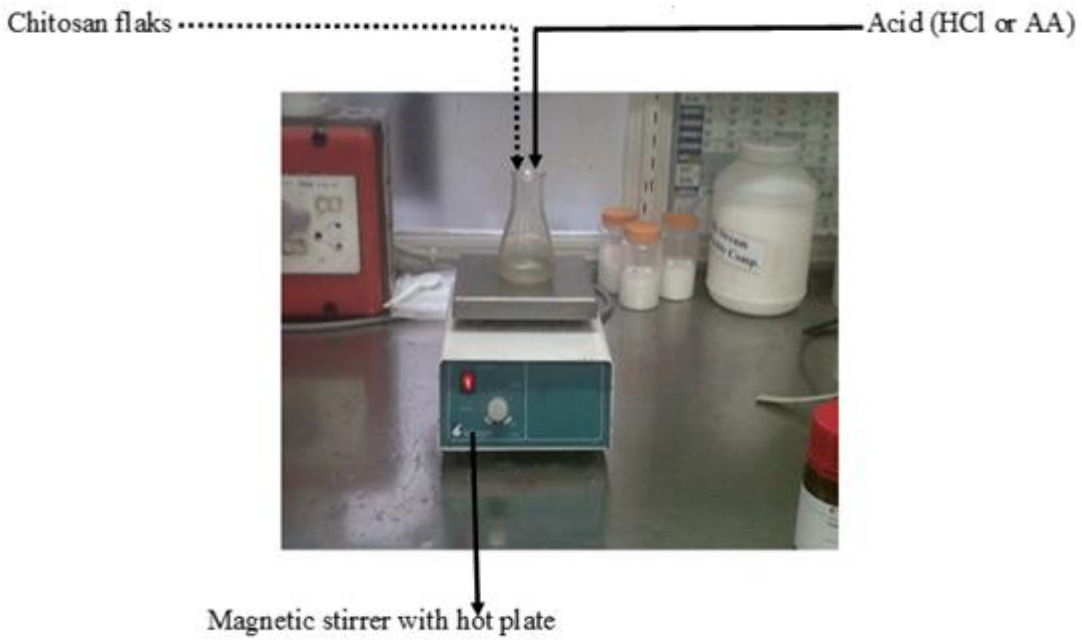

Figure 3.3: Coagulant preparation.

A chitosan mass of 100 mg was dissolved in an aqueous solution containing known volumes of 0.1 M hydrochloric acid (HCl) in a glass beaker. The mixture was stirred for an hour using a magnetic stirrer equipped with a hot plate at 50℃ (Fig. 3.3), then it was diluted by adding distilled water to obtain a 1000 ppm bulk colourless solution. This method was repeated using 100 mg of chitosan in an aqueous solution containing known volumes of 30% acetic acid (AA). Fresh CCo was prepared for each batch of experiments.

The AA was purchased from ACE (associated chemical entreprises) with 98% purity and was diluted to the desired concentrations using distilled water. HCl was obtained from Laboratory & Analytical Supplies Co. (Pty) Ltd with a molarity of 0.1 M. A comparative study in the preliminary experiments was used to determine which of the two acids is best suited for the sugar refinery effluents.

3.2.2. Collection of the effluents

The effluents were collected from Huletts-Tongaat sugar refinery in Durban, South Africa for each batch of experiments. The samples were characterized (see Table 3.1) for COD, TSS, pH and colour in accordance with the procedures of the refinery's quality laboratory which are in line with the South African National Standards (SANS), the International Organization for Standardization (ISO) and the American Public Health Association (APHA et al., 1999; SANS 241:1, 2011; ISO 9001:2008).

The samples were diluted with distilled water to obtain samples of high, medium and low concentrations for the experiments, a method adapted from Jadhav and Mahajan (2013). The pH of the samples was adjusted by adding small amounts of HCl or sodium hydroxide (NaOH).

3.2.3. Experimental procedure and analysis

All the experiments were performed using a non-programmable Voss flocculator (6 paddles) from the refinery's quality control laboratory (QC lab) using 300 ml glass beakers (Fig. 3.4). The jar-test procedure was adapted from Freese et al. (2003) and

Bina et al. (2009). The CCo was introduced into the wastewater using a pipette under flash mixing (100 rpm) for 3 minutes. The mixing speed was then reduced to 40 rpm for 15 minutes to promote bridging and flocculation, and the solution was left to settle for 2 hours unless indicated otherwise. The supernatant water was drawn out with a syringe and analysed using a Hach DR3900 UV-vis photospectrometer for COD and TSS. Colour was measured using a Unicam LA 055 at a wavelength of 490 nm and a Hach pH-meter was used to measure the pH of the solutions.

Figure 3.4: Experimental set-up.

The removal efficiency was calculated from the following expression:

$$\% \text{ Removal} = \left(\frac{C_0 - C_i}{C_0} \right) \times 100 \tag{3.1}$$

Where C_0 and C_i, respectively, represent the initial values of the response variables (TSS, COD and colour) and their values after the coagulation process.

The relationship between the coagulant loading in terms of its volume and the coagulant concentration based on the volume of the sample was calculated using the following equation:

$$C_1 V_1 = C_2 V_2 \tag{3.2}$$

Where C_1 and V_1, respectively, represent the concentration and the volume of the coagulant introduced into the wastewater sample. The total volume of the sample after the addition of the coagulant is represented as V_2 and C_2 represents the concentration of the coagulant in the sample.

3.3. EXPERIMENTAL SET-UP

3.3.1. List of equipment

The list of the major equipment used for the preparation of the coagulant and the analysis of the data is given below:

- A magnetic stirrer with hot plate from FMH instruments (Model STR/MH)
- Magnet follower
- Thermometer
- Pipettes
- Glassware (conical flasks, beakers)
- Hach DRB 200 COD Digester
- Hach DR 3900 UV-Vis photospectrometer
- Voss FL0/1 Jar-test apparatus
- Unilab LA 055 photospectrometer
- Computer software package (Design expert version 9.0)

3.3.2. Overview of the preliminary experiments

The preliminary experiments provided the foundation of the studies. It aimed at identifying the optimum ranges of the experimental parameters, the significant factors and important responses as well as the best operating conditions for the research work.

The following factors were defined during the preliminary work:

(1) The optimum acid for coagulant preparation

An organic acid (AA) and an inorganic acid (HCl) were used as solvent in the CCo preparation in order to determine the acid type that is most suitable for ESR. Both acids

were selected due to their low toxicity and the fact they are generally used as food additives.

(2) The upper and lower operating limits

Although the operating conditions of the coagulation of ESR using chitosan dissolved in acid are not widely documented, the literature studies assisted in providing the basis for this study in terms of the chitosan mass loading used, pH values and concentration of the impurities. The upper limit in this work was set by considering the financial constraints such as the cost of the chitosan and COD vials, as well as industrial practicability considering the fact that most industries will most likely prefer a coagulant that removes large amount of impurities at lower dosages.

(3) The significant factors and responses

Three main responses (COD, TSS and colour) were selected by investigating the historical data from Tongaat-Huletts and through communication with the optimization team, which assisted in identifying the problematic parameters in the effluents. Three manipulated variables (pH, chitosan dosage and effluent concentration) were selected for the preliminary study.

3.3.3. Experimental design and data analysis

The DOE was defined and explained in more details in Chapter 2. DOE provides a plan of action for efficient experimental work. A failure to adequately select a suitable DOE might impede the success of an experimental study. The results of the OFAT studies laid the foundation for the second phase of the DOE. The three-factor Box-Behnken design (BBD) was used in order to identify the curvatures with the addition of centre-points and was also used for optimization studies using response surface methodology. The commercial software tool Design Expert version 9.0 was used for the statistical analysis of the experimental data.

CHAPTER 4: APPLICATION OF THE OFAT METHODOLOGY IN THE TREATMENT OF EFFLUENTS FROM THE SUGAR INDUSTRY USING CHITOSAN

4.1. INTRODUCTION

The OFAT experimental method is the most familiar design of experiment which generally does not require special statistical knowledge to interpret the results obtained. In this chapter, the chitosan was used to coagulate the impurities in the RE and FE in order to establish its performance for both effluents and identify important variables that affect the efficiency of the coagulant (McDaniel and Ankenman, 2000; Qu and Wu, 2005; Friedman and Savage, 1947; Czitrom, 1999).

4.2. MECHANISM OF COAGULATION USING CHITOSAN

The mechanism of coagulation of suspended particles using chitosan occurs in three steps: (1) the cationic charge of the protonated chitosan destabilizes and neutralizes the anionic charge of the impurities, (2) bridging of the polymer with the suspended particles leading to flocs formation, (3) electrostatic patch (EPC), which is the coagulation induced by the contact between the neutralized patches that form when an anionic particle is neutralized by a cationic material as stated in step 1 (Guibal et al., 2006; Szugula et al., 2009; Cheng et al., 2010)

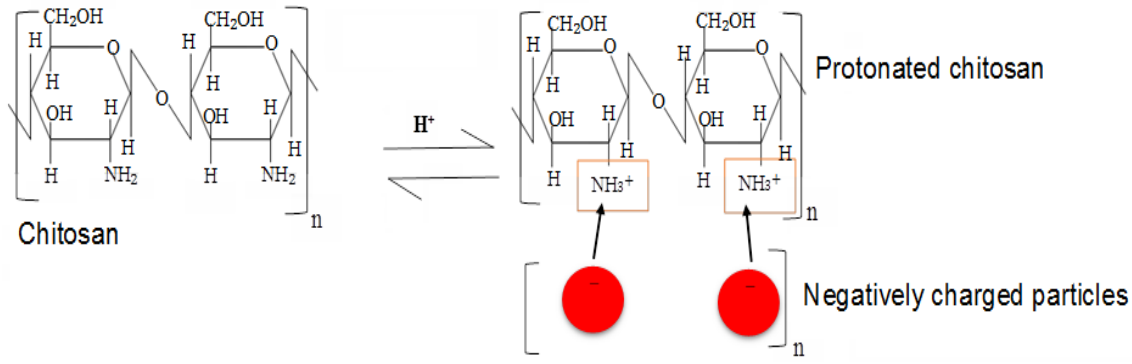

Figure 4.1: Mechanism of coagulation using chitosan *(Pambi and Musonge, 2015)*

Chitosan behaves as a coagulant and flocculant due to its long polymeric chain, the presence of NH_3^+ when dissolved in acid, the formation of bridges with the impurities, and the precipitation that occurs when the pH is above 6.5 (Fig. 4.1).

4.3. OFAT EXPERIMENTS

The RE and FE were both treated with chitosan in order to identify the best operating parameters that can be used later for optimization. The main reason for these preliminary runs were the lack of documented information on the performance of chitosan as a coagulant on effluents from the sugar industry.

4.3.1. Solvent selection

The performance of HCl which is an inorganic acid was compared to the performance of AA which is an organic acid for RE and FE as shown in Figure 4.2. A solution (50 ml distilled water) containing 1, 5, 10, 15 and 20 ml of HCl was used to dissolve the chitosan as mentioned in section 3.2.1, and compared with the chitosan prepared with AA under identical conditions. The effluents were used without pre-treatment, dilution or pH adjustment. The amount of chitosan used per litre of wastewater was 57 mg/l for RE and 38 mg/l for FE due to the fact that it had a lower impurity content than the RE.

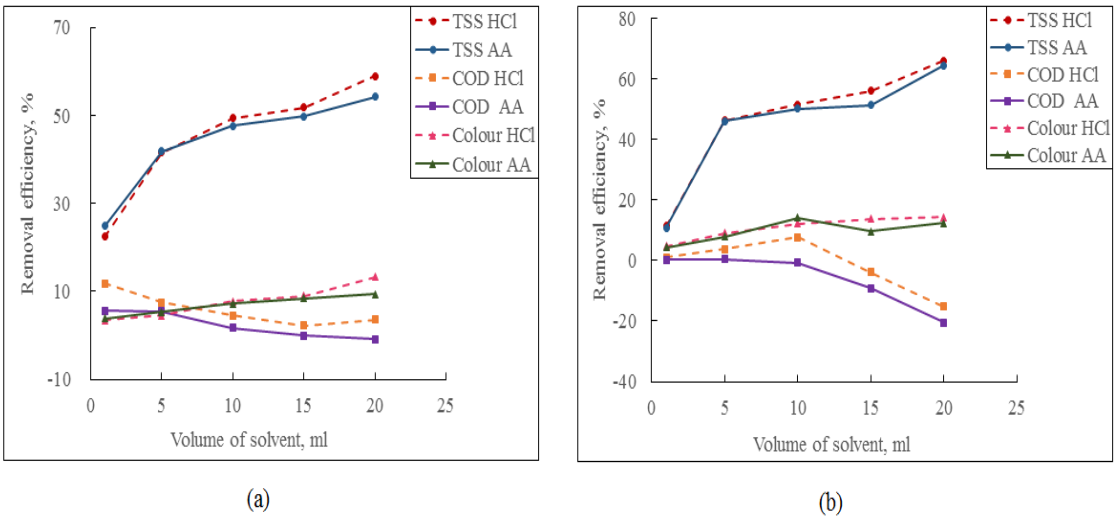

Figure 4.2: Comparison between HCl and acetic acid in terms of CCo effect on TSS, COD and colour removal for (a) RE and (b) FE.

The performance of the HCl was found to be better than that of AA in terms of TSS removal, effluent discolouration and COD reduction for both effluents. Figure 4.2 shows that increasing the volume of acid improved the removal of TSS and colour. This is due to the fact that HCl is an inorganic acid, whereas AA is an organic acid. The organic nature of AA added to the organic content of the sample thereby overshadowing the effect of the coagulant on the removal of COD.

The decrease in COD removal in Fig.4.2 with the increase in solvent volume can be explained by the fact that the acid used to dissolve the chitosan remains in the effluent and accounts for the COD especially when high volumes are used. Also, when the coagulant contains high concentrations of acid, it decreases the pH of the wastewater during the coagulation process, thus a large amount of chitosan remains dissolved in the water, adding to the amount of dissolved organic in the sample.

HCl was selected as the solvent for this study. This preliminary experiment indicated that the optimum volume of the solvent ranged from 10 ml to 20 ml; where 20 ml yielded the best results.

4.3.2. Effect of initial pH

Chitosan was prepared using 20 ml HCl and a loading of 57 mg/l CCo was used for RE and 7.41 mg/l was used for FE. The concentration of the FE was further decreased to improve the removal efficiency. A comparative experiment was conducted between samples at natural pH (without pH adjustment) and the samples where the pH was adjusted to acidic or basic using HCl or NaOH.

The natural pH varies from 7 to 13 for RE and 7 to 11 for FE. From Table 4.1 it can be noted that when the pH of water sample was adjusted toward the acidic range using HCl a high removal of TSS, COD and colour was observed.

Table 4.1: Effect of the pH on the coagulation using chitosan

Sample pH	RE						FE					
	% removal at natural pH			% removal at adjusted pH			% removal at natural pH			% removal at adjusted pH		
	TSS	Colour	COD	TSS	Colour	COD	TSS	Colour	COD	TSS	Colour	COD
4	N/A	N/A	N/A	77	19	14	N/A	N/A	N/A	97	88	11
5	N/A	N/A	N/A	68	10	14	N/A	N/A	N/A	98	86	11
6	N/A	N/A	N/A	50	9	8	N/A	N/A	N/A	98	85	10
7	63	16	5	37	6	0	97	87	9	97	86	9
8	60	13	4	0	0	0	97	85	9	95	85	5
9	57	12	2	0	0	0	N/A	N/A	N/A	87	76	-7
10	53	11	2	0	0	0	N/A	N/A	N/A	84	74	-12

N/A: No data available from the collected samples at this pH (Pambi and Musonge, 2015)

It was also observed (Table 4.1) that when experiments were conducted with samples at natural pH, the coagulant provided better results for TSS, COD and colour compared to the samples adjusted to the same pH value with sodium hydroxide (NaOH). Samples of RE that were adjusted to basic pH using NaOH yielded poor results. Adding NaOH on the FE led to precipitation which was more pronounced at pH above 10 without the assistance of chitosan. In Table 4.1, it can be seen that although most of the solids and colour were removed by that precipitation at pH 9 and 10, treatment of those samples with chitosan yielded poor results in terms of COD removal.

There are two possible explanations for the observations in Table 4.1:

(1) The resin effluent and the final effluent also contains lime carry-over from the carbonating station among other chemicals which may react with the NaOH or with both the NaOH and the chitosan and thus decrease the coagulation efficiency.

(2) The presence of NaOH precipitates the chitosan and impedes bridging (Osifo et al., 2008).

It can also be noted that the removal of COD for both effluents is very low. This is due to the fact that most of the COD in these effluents is caused by dissolved organics. This is discussed in detail later on in this in chapter.

The optimum range for the initial pH was found to be between 4 and 7 when the pH was adjusted towards the basic range using NaOH (Table 4.1).

4.3.3. Effect of the concentration of impurities

Test were conducted for effluents at high concentration (HC), medium concentration (MC), low concentration (LC) and very low concentration (VLC). The HC refers to the wastewater as collected from the effluent, therefore, it contains 100% ESR (Table 4.2).

Table 4.2: Effluent concentration

Level	ESR concentration (%)
HC	100
MC	50
LC	25
VLC	12.5

The ESR was then diluted using distilled water to make the other concentrations mentioned above. Table 4.2 indicates the ESR content of each level. The dosage of CCo used for the experiments depicted in Fig 4.3 was 57 mg/l for RE and 38 mg/l for FE.

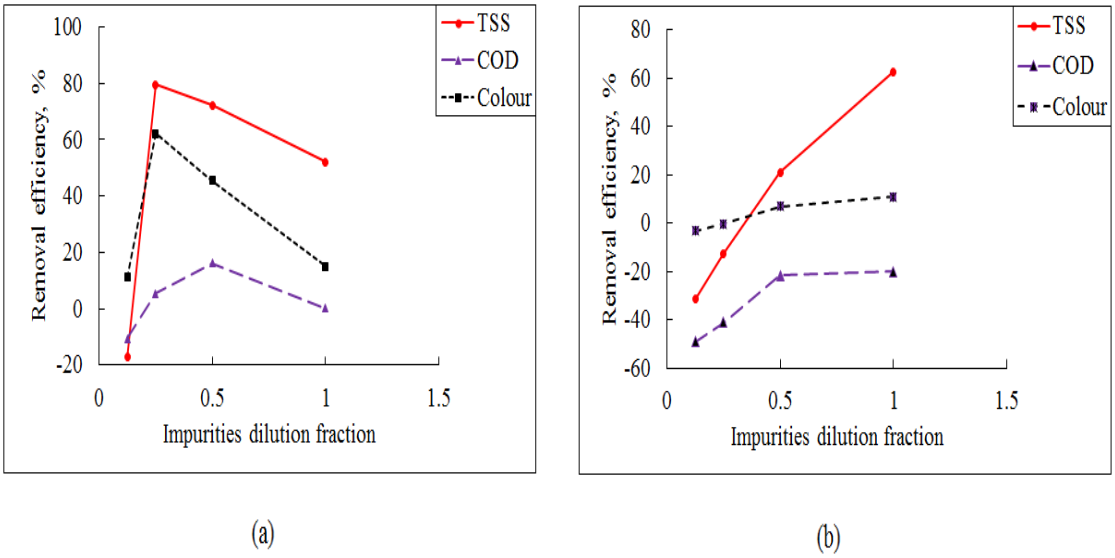

Figure 4.3: Effect concentration on TSS, COD and colour removal for (a) RE and (b) FE.

The experiments in this section were conducted immediately after the experiments in section 4.3.1, however its discussion and analysis is ore linked to section 4.3.3, for that reason, it is discussed here.

Results demonstrated that for the RE (Fig. 4.3a), the efficiency of the coagulant, in terms of TSS and colour removal increased as the impurities in the sample decrease. The reduction of COD was at its optimum at MC, but decreased afterward. Diluting the FE (Fig. 4.3b) yielded poor results for the removal of all the parameters (TSS, COD and colour).

At HC, the RE and FE carry a higher pollution, and require more chitosan in to neutralize the impurities for coagulation to occur. Figure 4.3a show that at HC and VLC, the amount of CCo used (57 mg/l) removed less quantities of impurities than at MC and LC. At HC, the pollution load was too high and the amount of CCo used was insufficient. At lower impurity concentrations there are few solids in the water and a larger amount of the coagulant remains suspended and/or dissolved in the water thus increasing the COD values due to the organic nature of chitosan. This explains the low removal efficiency at VLC for RE and the behaviour in fig.4.3 for FE. Zemmouri et al. (2011) reported in their studies that the efficiency of the chitosan coagulant was affected by the initial turbidity of the wastewater sample. They pointed that at low turbidity there is insufficient amount of particles to achieve adequate flocculation of the neutralized colloids. This further supports the findings above.

For the RE, optimum range was found to be at MC and LC, while the FE performed better between HC and MC. Operating below HC requires dilution with clean water. This was a major disadvantage as the aim in most industries is to purify the effluents without adding the cost of dilution water. The rest of the experiments were done for samples at HC. Data for RE experiments at MC can be seen in Appendix A.

4.3.4. Effect of coagulant loading

The influence of the chitosan loading in RE and FE was investigated. The optimum range was found to be between 138 mg/l and 192 mg/l for RE; while FE performed better between the loading of 4 mg/l to 15 mg/l. Figure 4.4 shows that the higher removal efficiencies for all three variables were achieved at the loading of 138 mg/l for RE (TSS: 68%, colour: 30% and COD: 15%) and 7.41 mg/l for FE (TSS: 97%, colour: 61% and COD: 35%), beyond which the performance of the CCo decreased.

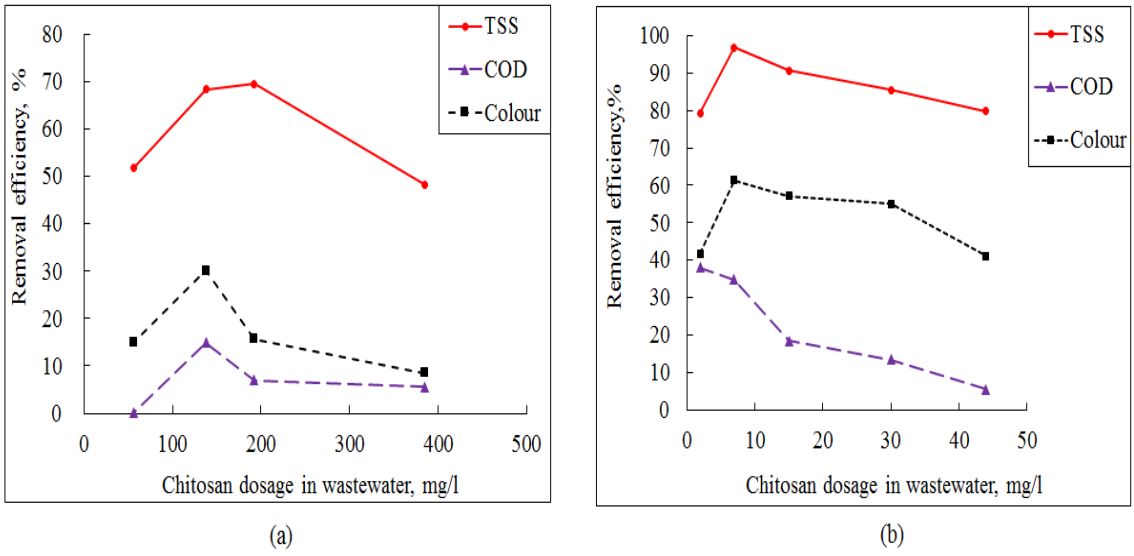

Figure 4.4: Effect of coagulant loading on TSS, COD and colour removal for (a) RE and (b) FE. *(Pambi and Musonge, 2015)*

This can be explained by the pH-dependent behaviour of chitosan. Under acidic conditions the chitosan is completely protonated (NH_2 to NH_3^+). The NH_3^+ neutralizes the negative charges of the impurities, entrapping them into the long polymeric chain (bridging) and forms flocs. As the flocs increase in size under slow mixing (40 rpm) they settle out.

Overdosing the coagulant destabilizes the neutralized flocs and impedes their settling. Excessive amount of chitosan increases the amount of NH_3^+ present in the RE and the neutralized flocs begin to repel each other and the protonated chitosan. The excess chitosan in this case forms gel-like film on the surface of the sample.

Chi and Cheng (2005) studied the effect of chitosan as a coagulant for wastewater from the milk processing industry. They reported that the impurity removal efficiency increased with an increase in chitosan dosage. They also stated that as the dosage increased continuously, the reversal of chitosan surface charge occurred, leading to a decrease of the removal of turbidity and COD.

Divakaran and Sivasankara Pillai (2001) reported that no advantage was obtained by increasing the dosage of chitosan after the optimum dosage was reached. A similar observation was made by Bina et al. (2009).

4.3.5. Cost and sludge handling

The coagulation of RE and FE using chitosan under optimum conditions resulted in the formation of large and dense flocs that settled easily. The treatment of 250 ml of RE under optimum conditions (20ml HCl as solvent, natural pH, HC and 138 mg/l loading) produced 20-30 ml of sludge, accounting for 8-12% of the total volume of the wastewater sample (Fig. 4.5). The FE at optimum conditions (20ml HCl as solvent, natural pH, HC and 7.41 mg/l loading) produced far less sludge than the RE (approximately 5-12 ml for 250 ml of sample treated).

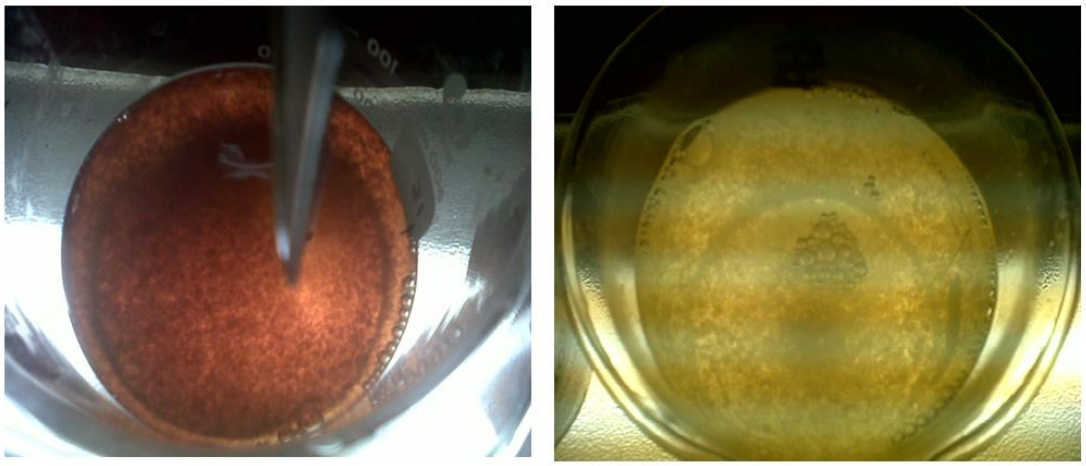

(a) (b)

Figure 4.5: Dense flocs forming on (a) RE and (b) FE.

The treatment of RE using chitosan was found to be unsustainable due to the following cost implications:

(a) The sludge contained chemicals that makes it unsuitable for use in agriculture or for any form of consumption and has to be disposed of. This adds costs in terms of sludge disposal.

Table 4.3: Water cost evaluation.

Cost	Fresh water	Disposal of RE	Treatment RE*	Treatment FE*
Rand/m^3	31.66	18.09	138	7.41

**Calculated for the market price of industrial chitosan in 2014 (R1000 per kg of chitosan) using the optimum coagulant loadings.*
Excluding Opex and Capex

(b) The treatment of RE using chitosan was found to more costly than using fresh water or disposing of the effluent through contractors (Table 4.3).

(c) Factors such as operating costs (Opex) and capital costs (Capex) for the implementation of a large scale treatment facility will add costs for the RE and are additional draw-backs to the use of the chitosan for this particular type of wastewater.

(d) Further treatments are required to completely remove the impurities such as COD, TDS and colour from the RE (Fig. 4.6a).

Chitosan was able to remove most of the suspended solids and decrease the cloudiness of the FE (Fig. 4.6b). Although the CCo failed to remove the COD which is the major concern of the refinery, its efficiency for TSS removal and potentiality for high colour removal makes it a good pre-treatment method for this effluent. Using effluents at natural pH saves costs on chemicals for pH adjustment.

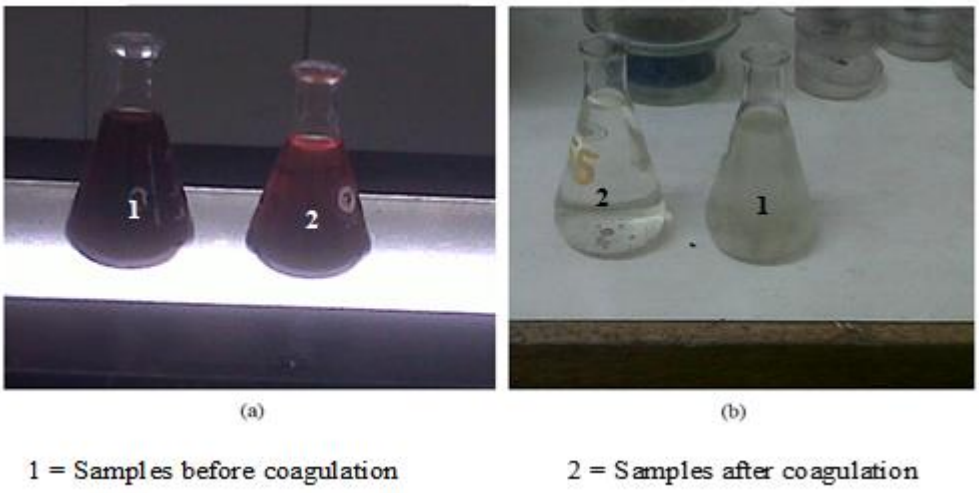

Figure 4.6: Effluent sample before and after coagulation (a) RE (b) FE.

The cost of sludge disposal, the need of the Opex and Capex of large scale operation made the treatment of the ESR using chitosan unattractive to this particular refinery. However, the health benefits of chitosan in the water treatment field and the fact that the production of chitosan from crustaceans shells is a good way of reducing pollution from the fishery industry, makes chitosan a good product to use for wastewater treatment as well as a good alternative to the inorganic coagulants.

4.4. INFLUENCE OF EFFLUENT TYPE ON THE PERFORMANCE OF CHITOSAN.

This section reviews the results from two published articles where chitosan was used to treat different kinds of effluents from different food and beverage industries namely, the wastewater from a milk processing plant (MPP) and the wastewater from a brewery processing plant (BPP); and compares it with experimental works conducted on the FE from the sugar refinery. The methodology for the FE is reported in chapter 3, whereas experimental methods for the MPP and the BPP can be found in the published articles by Cheng et al. (2005) and Chi and Cheng (2006) respectively. Two effluent streams from the MPP are considered in this study, the wastewater from cattle milk and wastewater from sheep milk.

The efficiency of chitosan in the removal of TSS and COD for the three industrial wastewaters is shown in Figure 4.7. It can be observed that the performance of the chitosan was influenced by the pH of the effluent. The optimum pH value of the BPP was found to be in the acidic region, whereas the MPP provided acceptable results for pH values of up to 9. In the case of FE, the performance of chitosan was higher at acidic pH and good results were obtain up to pH 7 (97%) above which the efficiency of the coagulant decreased. However, the performance of the chitosan for COD removal in the FE did not exceed 11% when the pH was adjusted (See Table 4.1).

This difference in optimum pH can be explained by the nature of the impurities in each of the effluents. Milk is composed of colloids in suspension in a water-based liquid, only 30% of the COD in the MPP from cattle milk is due to TDS. In the case of MPP from sheep milk it can be seen that the COD removal is lower compared to the MPP from cattle milk due to the fact that 96% of its COD is caused by dissolved particles. The use of the coagulant neutralizes the charge of the suspended particles in the MPP causing it to agglomerate into flocs and settle. Therefore, since most of the impurities in this effluent is caused by organic matters in suspension (such as lipids, proteins, etc.), the use of the chitosan was able to provide a high percentage removal for both TSS and COD compared to the FE and the BPP (Pambi and Musonge, 2014).

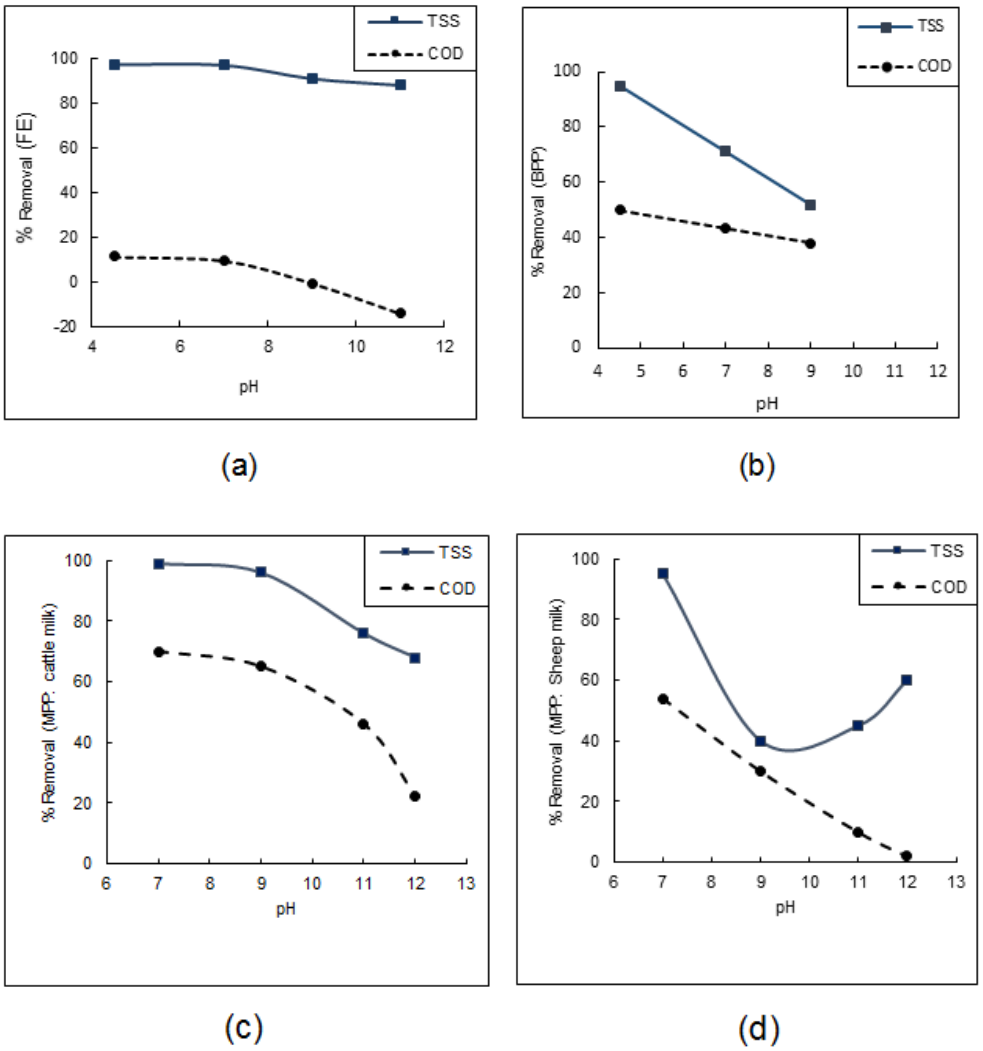

Figure 4.7: The influence of pH on the COD and TSS removal for (a) FE (b) BPP adapted from Cheng et al. 2005 (c) MPP from cattle milk adapted from Chi and Cheng 2006 (d) MPP from sheep milk adapted from Chi and Cheng 2006.

It can also be seen from Figure 4.8 that chitosan is not very efficient in removing dissolved organics from the wastewater. Islam and Guha (2013) reported that the coagulation process is generally less efficient for the removal of TDS than TSS.

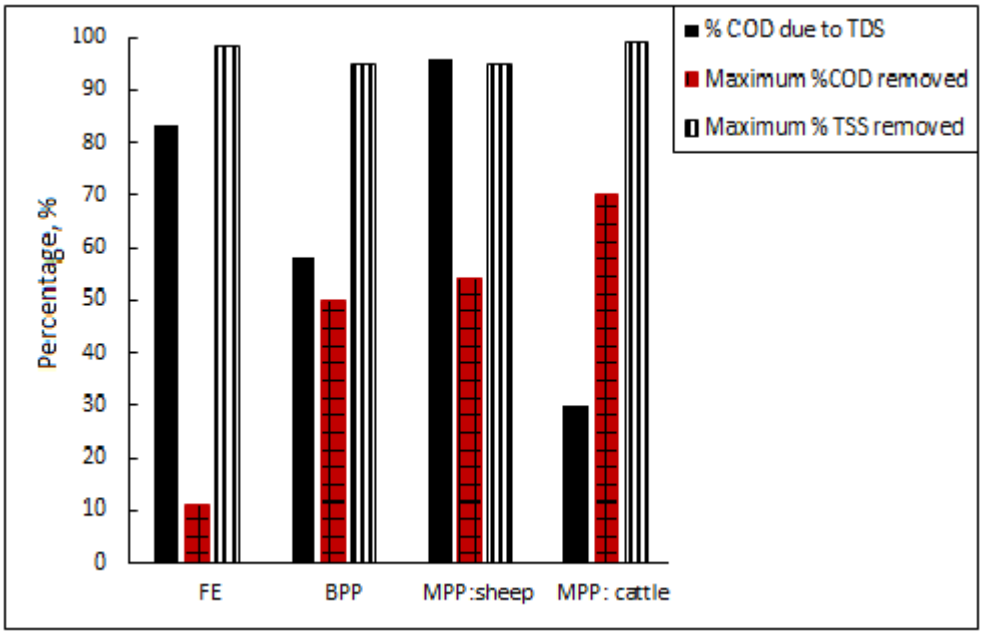

Figure 4.8: Relationship between COD due to TDS, and impurities removal *(Pambi and Musonge, 2014).*

In the case of the FE where approximately 80% of COD is caused by dissolved sugar and other organic matters, the maximum COD removed was only 11% which is insignificant compared to 50% for the BPP, 54% and 70% for MPP for sheep milk and cattle milk respectively. The impurities in the wastewater also have an effect on the amount of coagulant required. In general, the TSS (or turbidity) and the pH of a sample are the main variables that are taken into account when selecting the coagulant dosage range. However, it can be deduced from literature that the coagulant dosage is affected by a combination of factors such as the initial TSS of the effluent, the TDS, the chemical components in the effluent and the settling time (Pan et al., 1999; Divakaran and Sivasankara Pillai, 2001; Pambi and Musonge, 2014). Therefore, it is important to consider the interactions between the factors during a trial in order to affirm the performance of a coagulant and optimize its efficiency.

The coagulation process depends on the amount of particles in the wastewater. If the amount of colloids in the water is high, the coagulant forms larger flocs which settles readily, whereas at low turbidity there is insufficient amount of particles attaching

themselves to the polymer, therefore the formation of smaller and lighter flocs (Zemmouri et al., 2011). A higher dosage of coagulant is required for high turbidity water to ensure that all the particles are neutralized. The low dosage obtained for the FE (7.41 mg/l) can be explained by the fact that FE carried a low amount of TSS in comparison to the other effluents mentioned in this study.

Although the MPP carries more suspended solids than the BPP, it requires a lower dosage (15 mg/l for sheep milk and 25 mg/l for cattle milk) than the latter (120 mg/l for BPP) due to the nature of the impurities it carried. The removal of TSS was found to be more affected by the amount of suspended solids present in the effluent and the chitosan dosage used. This can be seen in Figure 4.8. For all these effluents under optimum conditions, the removal of TSS was above 90%.

A model was developed using Design expert 9.0, taking into account the ratio of initial TSS to the initial COD (X_A), the COD due to TDS (X_B) and the initial TSS value (X_C) for all four effluents (Table 4.4).

Table 4.4: Relationship between TSS, TDS, COD and coagulant efficiency.

	X_A $\left(\frac{COD}{TSS}\right)$	X_B $\left(\frac{COD_f}{COD_i}\right)\times 100$	X_C (TSS)	% TSS removed (Y_1)	% COD removed (Y_2)	Chitosan dosage, mg/l (Y_3)
FE	0.09	83	385	98	11	7.41
BPP	0.28	58	2100	95	50	120
MPP: Cattle	3.60	30	19485	99	70	25
MPP: Sheep	8.29	96	7410	95	54	15

X_A = Total COD (mg/l) divided by the TSS (mg/l); X_B represents the percentage COD due to TDS as a fraction of the COD after filtration (mg/l) to the total COD (mg/l) times 100; X_C is the TSS in mg/l. (Pambi and Musonge, 2014).

The relationship between X_A, X_B and X_C was deduced as follows:

$$Y_1 = 84.525 - 1.241X_A + 0.160X_B + 7.254\times10^{-4} X_C \quad (4.1)$$

$$Y_2 = 155.415 + 11.241X_A - 1.735X_B - 37.893\times10^{-4} X_C \quad (4.2)$$

$$Y_3 = 481.504 + 26.733X_A - 5.650X_B + 196.69\times10^{-4} X_C \quad (4.3)$$

The constraints for the model equations above can be expressed by considering the interaction between the values of X_A and X_B.

If X_A < 0.1 and X_B > 50, the removal of COD will be lower than 50%. Increasing the value of X_B above 80 reduced the COD removal efficiency below 15%. This constraints however, do not affect the TSS removal considerably.

If X_A >1 and X_B < 55, the dosage required as well as the removal of COD and TSS increased.

The dosage required decreased for value of X_A below 0.1 and increases as this value augments (for X_B > 50).

The model was tested against the findings from Rizzo et al. (2010) for wastewater from olive oil mills (OMW) and the wastewater from the winery (WW). The results are presented in Table 4.5. The article by Rizzo et al. (2010) did not present the values of the COD after filtration, so in this case an arbitrary value of X_B was used.

Table 4.5: Model validation.

	OMW			WW		
	X_A	X_B*	X_C	X_A	X_B*	X_C
	7.93	50	6700	2.07	50	750
Response	Actual		Predicted	Actual	Predicted	
Y_1 (TSS removed, %)	81		88	92	91	
Y_2 (COD removed, %)	32		132	72	89	
Y_3 (Dosage, mg/l)	400		279	20	240	

** The value for X_B was assumed to be 50% for both wastewater.*

From Table 4.5, it can be seen that Y_1 (Eq.4.1) is the only regression that provided a good fit for both OMW and WW. Y_2 predicted a value close to the actual response for the removal of COD for WW but failed to predict the response for OMW. The regression model Y_3 failed to fit for both effluents.

4.5. SUMMARY

The performance of chitosan was evaluated for the coagulation of the ESR using the OFAT method. The treatment of FE provided better results than RE, although the efficiency of chitosan in terms of COD removal was low for both effluents.

It was also noticed that the total dissolved solids (TDS) contributed to the poor COD removal in both effluent samples. Variables such as pH and coagulant concentration were found to have a great impact on the performance of the chitosan. Based on the results obtained in this section, the FE was selected for the statistical studies.

CHAPTER 5: STATISTICAL AND OPTIMIZATION STUDIES USING RSM

5.1. INTRODUCTION

The application of the BBD in the coagulation of the FE using chitosan is discussed in this section. This section combines laboratory experiments done according to the BBD matrix, with statistical analyses performed using Design Expert 9.0.

5.2. EVALUATION OF THE DESIGN

The BBD was used to generate the experimental matrix and the model equations for the optimization of the performance of chitosan for the FE. Three manipulated variables were varied at three levels: a high level, represented as (+1), a low level represented as (-1) a middle point (0).

The response variables represented as Y_1, Y_2 and Y_3 are the percentage removal of TSS, COD and colour respectively using CCo. The manipulated variables were selected based on the results from the OFAT experiments. Due to the fact that all experiments were done at HC, the settling time was used (see Table C-3, Appendix C).

The following variables were selected as manipulated variables for this study:

- Coagulant loading (X_1), here expressed as the volume of liquid CCo solution used in 250ml effluent sample.
- The initial pH of the FE (X_2)
- The settling time (X_3)

The values of these variables are shown in Table 5.1.

Table 5.1: Manipulated variable and BBD levels.

	-1	0	1
X_1: Coagulant loading (ml)	10	20	30
X_2: pH	4	7	10
X_3: Settling time (minutes)	30	60	90

The experiments were conducted in a random order instead of the standard order to avoid biases during the trials, and the analyses of the data were done at standard BBD run order as seen in Table 5.2 using the Design expert software.

Table 5.2: Experimental matrix

Standard runs	Randomized runs	X_1	X_2	X_3	Y_1 (TSS)	Y_2 (COD)	Y_3 (Colour)
1	6	-1	-1	0	88	32	72
2	5	+1	-1	0	80	21	72
3	10	-1	+1	0	89	21	80
4	11	+1	+1	0	91	14	82
5	1	-1	0	-1	87	26	69
6	3	+1	0	-1	79	11	71
7	9	-1	0	+1	96	26	87
8	13	+1	0	+1	89	23	80
9	2	0	-1	-1	80	13	69
10	4	0	+1	-1	88	13	76
11	8	0	-1	+1	92	25	72
12	17	0	+1	+1	99	18	90
13	15	0	0	0	93	28	84
14	16	0	0	0	92	28	85
15	12	0	0	0	93	30	87
16	7	0	0	0	92	29	83
17	14	0	0	0	93	31	86

The quadratic model (Eq. 2.7) was selected for this study. Before proceeding with the analyses of the responses, the design model had to be evaluate to ensure that it is the correct one for this particular experiment. The evaluation of a design was explained in detail in Chapter 2.

Table 5.3: Evaluation of the design model.

Term	SE	VIF	Ri^2
X_1	0.35	1.00	0.0000
X_2	0.35	1.00	0.0000
X_3	0.35	1.00	0.0000
X_1X_2	0.50	1.00	0.0000
X_1X_3	0.50	1.00	0.0000
X_2X_3	0.50	1.00	0.0000
X_1^2	0.49	1.01	0.0058
X_2^2	0.49	1.01	0.0058
X_3^2	0.49	1.01	0.0058

The results in Table 5.3 show that the model selected is suitable for the experimental data. The values of the VIF for the all the model terms can be rounded to 1. The relationship between the VIF and the Ri^2 is shown in equation 2.9. The values of the VIF and Ri^2 indicate that all the factors in this model are not correlated. The SE is the same for all the coefficients of the same type also showing that the model is suitable. The SE graph was plotted for the pH and the coagulant concentration at constant time and can be found in Appendix B, Figure B-1.

5.3. ANALYSIS FOR TSS

The fitness of the model for TSS removal was analysed using the software package Design Expert 9.0. The results of the ANOVA and LOF tests as generated from the experimental data are shown in Table 5.4.

Table 5.4 shows that the model has a large F-value and the p>F value is less than 0.05, meaning that the model is significant. The term X_3 has the highest F-value and the lowest p>F value, meaning that the settling time has the largest effect on the TSS removal, followed by the pH and the coagulant concentration. It can also be seen that there is 6.35% chance that the LOF is due to noise which is not a very significant value, as the LOF values greater than 0.05 (5%) are not significant, showing that the model can fit any data.

Table 5.4: ANOVA (TSS).

Variation	SS	df	MS	F-value	p-value p>F
Regression	487.90	9	54.21	31.70	< 0.0001
X_1	63.06	1	63.06	36.87	0.0005
X_2	92.07	1	92.07	53.84	0.0002
X_3	233.28	1	233.28	136.41	< 0.0001
X_1X_2	18.75	1	18.75	10.96	0.0129
X_1X_3	0.090	1	0.09	0.053	0.8251
X_2X_3	0.01	1	0.01	0.006	0.9412
X_1^2	59.76	1	59.76	34.95	0.0006
X_2^2	11.02	1	11.02	6.44	0.0388
X_3^2	4.06	1	4.06	2.38	0.1671
Residual	11.97	7	1.71		
LOF	9.69	3	3.23	5.67	0.0635
Pure Error	2.28	4	0.57		
Total	499.87	16			

The model equation for this response is expressed as:

$$Y_1=92.6-2.81X_1+3.39X_2+5.4X_3+2.16X_1X_2+0.15X_1X_3-0.05X_2X_3-3.77X_1^2-1.62X_2^2-0.98X_3^2 \quad (5.1)$$

The data in Table 5.4 is not the only way to identify significant factors. The coefficients in the model equations also indicate the significant variables. The pareto charts of the effects based on Eq. 5.1 can be seen in Appendix B, Figure B-18. Therefore, from Table 5.4 and Eq. 5.1 it can be seen that the removal of TSS is mostly affected by the settling time (X_3). The fact that the coefficient for X_3 in Eq. 5.1 carries a positive sign shows that the TSS removal increases when the sample is left to settle for longer.

It can also be seen that X_1X_2 is the most significant interaction term. This indicates that the removal of TSS is positively influenced by the combination of the variation in both pH and coagulant dosage. From Eq. 5.1 it can be seen that increasing the coagulant dosage can have a negative effect on the TSS removal. The term X_1X_3 in this equation means that the TSS removal is slightly boosted by the interaction between the chitosan dosage and the settling time. It can also be noticed that the TSS removal is negatively affected by the interaction between the pH and the settling time, even though these two factors individually increase the TSS removal, the negative sign of the term X_2X_3 means that the chitosan precipitates as settling time is prolonged, depending on the pH of the sample. However, in this equation, the effects of the interaction terms X_1X_3 and X_2X_3 are minimal.

The quadratic terms indicate the presence of curvatures. The negative signs in Eq. 5.1 reveal that the quadratic curves for X_1^2, X_2^2 and X_3^2 are concave. This means that removal of TSS increases with an increase in coagulant dosage, pH and settling time up to a maximum value beyond which the efficiency decreases with further increase of the three variables. The magnitude of the coefficients of the quadratic terms indicate the steepness of the curvature. Thus it can be seen from Table 5.4 and Eq. 5.1 that X_1^2 is steeper than X_2^2 and X_3^2.

Table 5.5: Model coefficients (TSS).

SD	CV (%)	R^2	$\check{R}^2$	$\acute{R}^2$	AP
1.31	1.46	0.9761	0.9453	0.6827	19.834

The low value of the CV shows that there are very few unexplained variations in the model. The value of the R^2 is close to 1, indicating a good fit. The $\acute{R}^2$ is not close to the $\check{R}^2$. It was mentioned in Chapter 2 that the difference between the $\check{R}^2$ and the $\acute{R}^2$ must be less than 0.2, if the difference is larger, transformation should be considered (See appendix B for transformations). AP greater than 4 is desired and shows that the model will give good predictions. In this case AP of approximately 20 is very good.

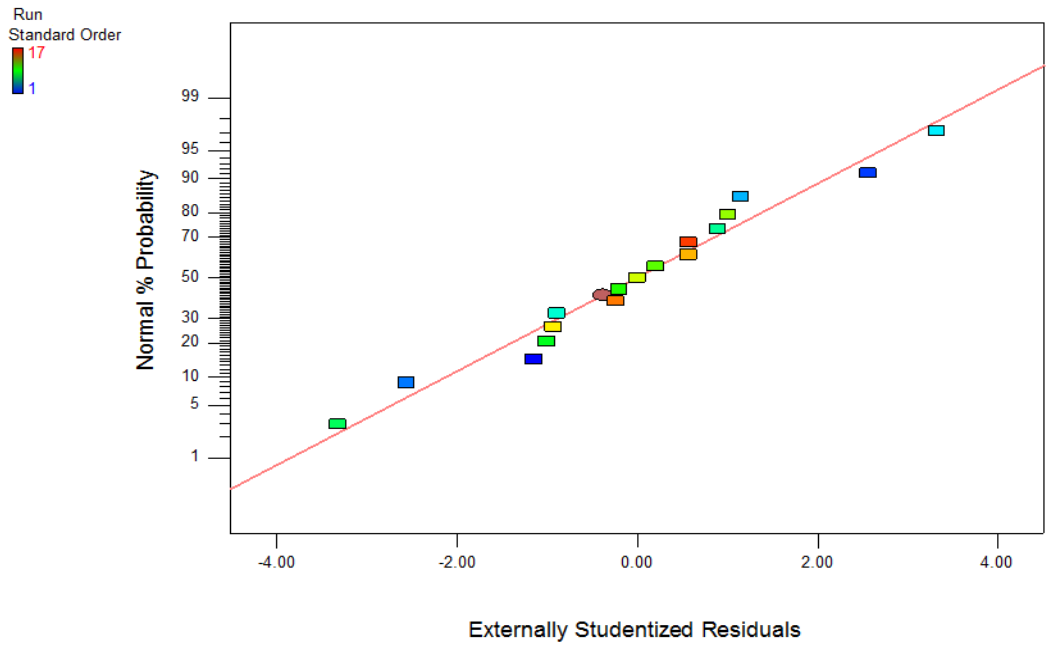

Figure 5.1: TSS - Normal plot of residuals.

The normal plot (Fig. 5.1) shows that the set of data used for this experiment is normally distributed because the pattern approximates a straight line and there are no outliers.

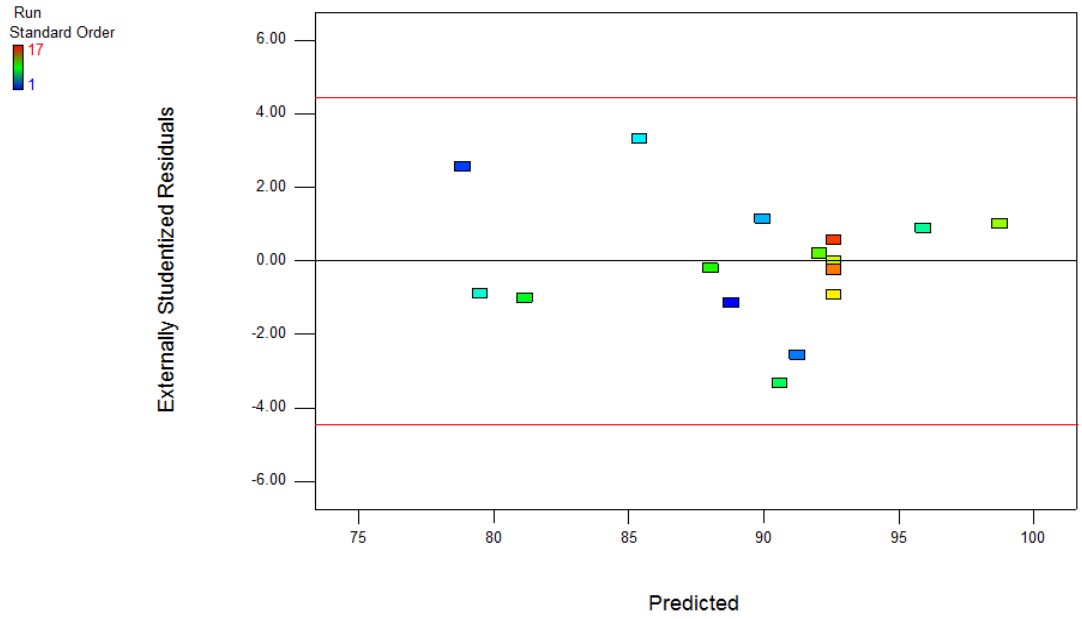

Figure 5.2: TSS - Residuals vs. predicted values.

From Fig. 5.2, it can be seen that the data points are scattered randomly without forming a pattern.

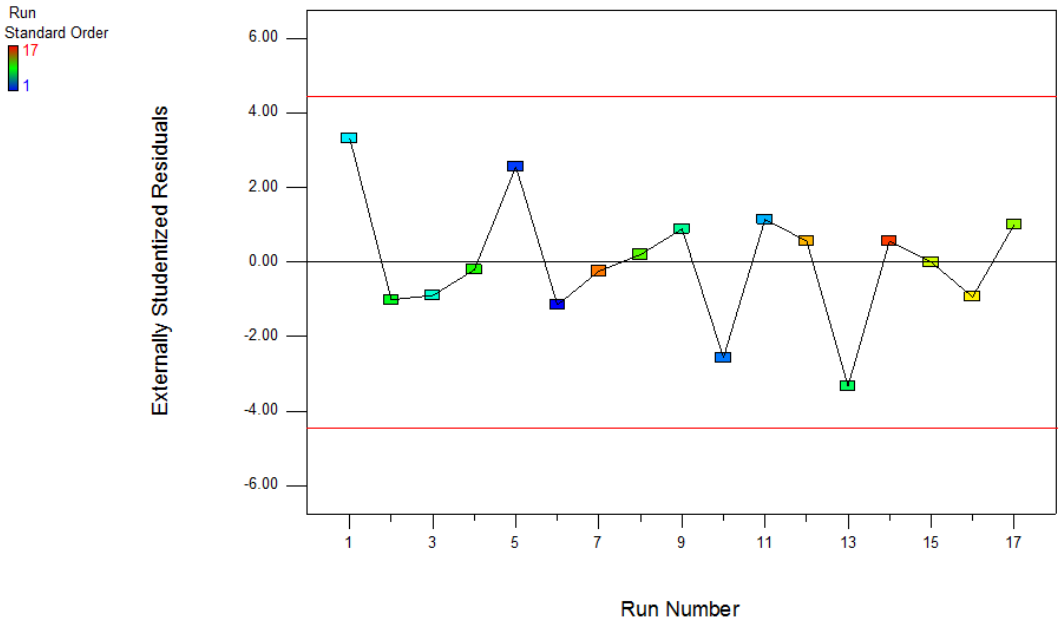

Figure 5.3: TSS - Residuals vs. run number.

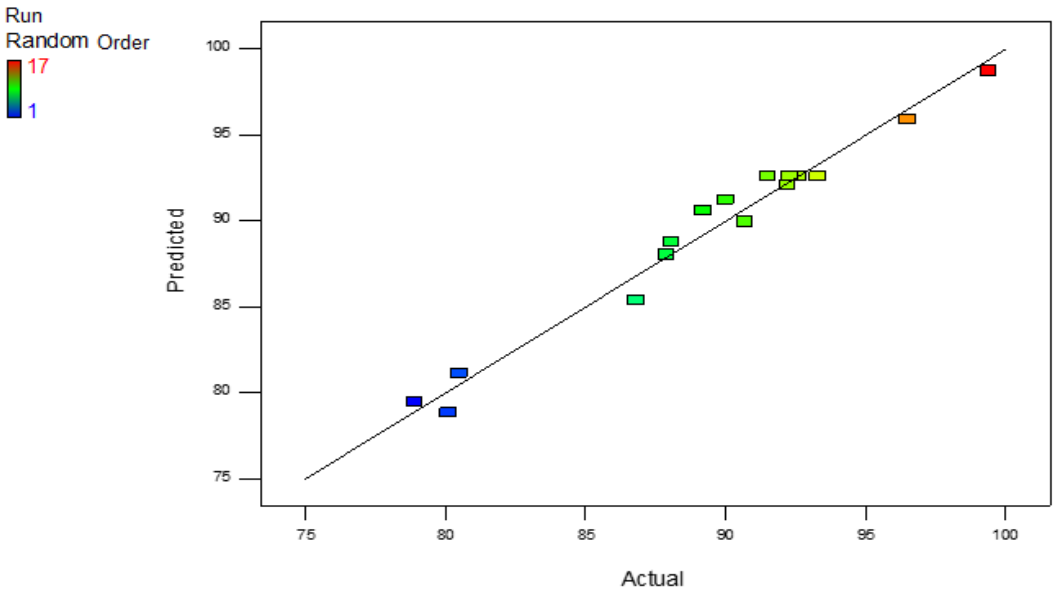

Figure 5.4: TSS - Predicted vs. actual.

The diagnostic plots from Fig. 5.3 to Fig. 5.4 are satisfactory, as described in chapter 2. Thus, we can conclude that the model is a good fit to the experimental data.

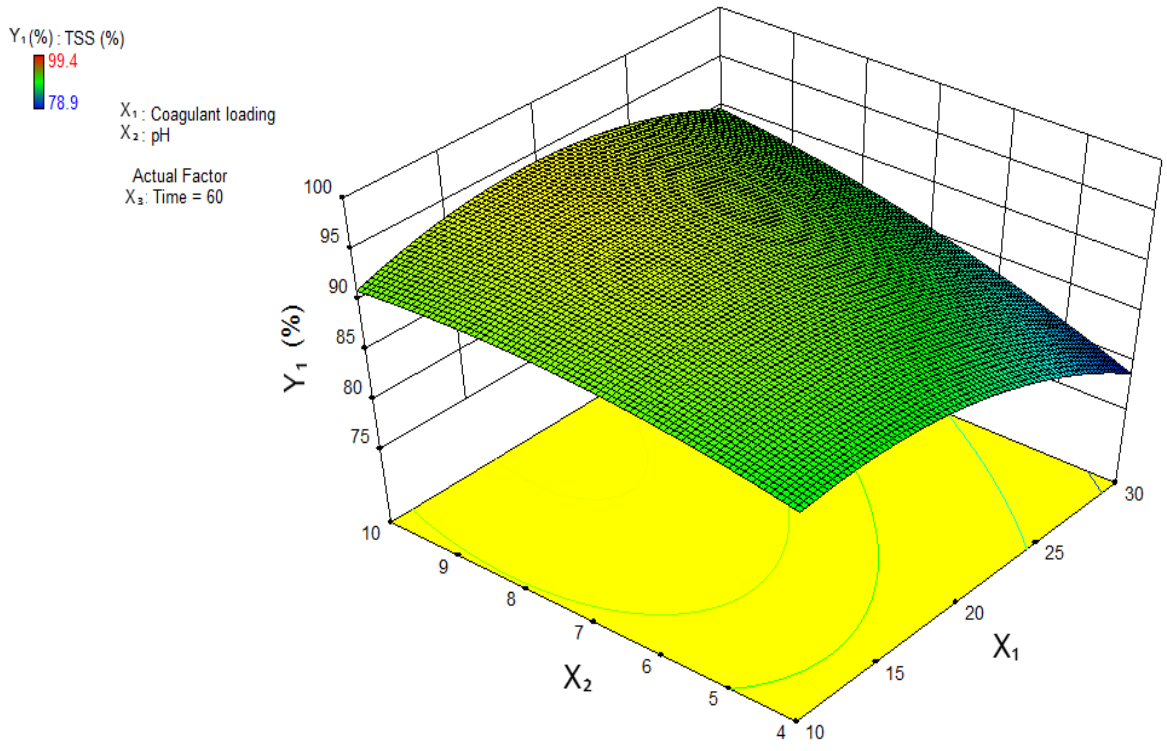

Figure 5.5: TSS - RSM plot for coagulant loading and pH.

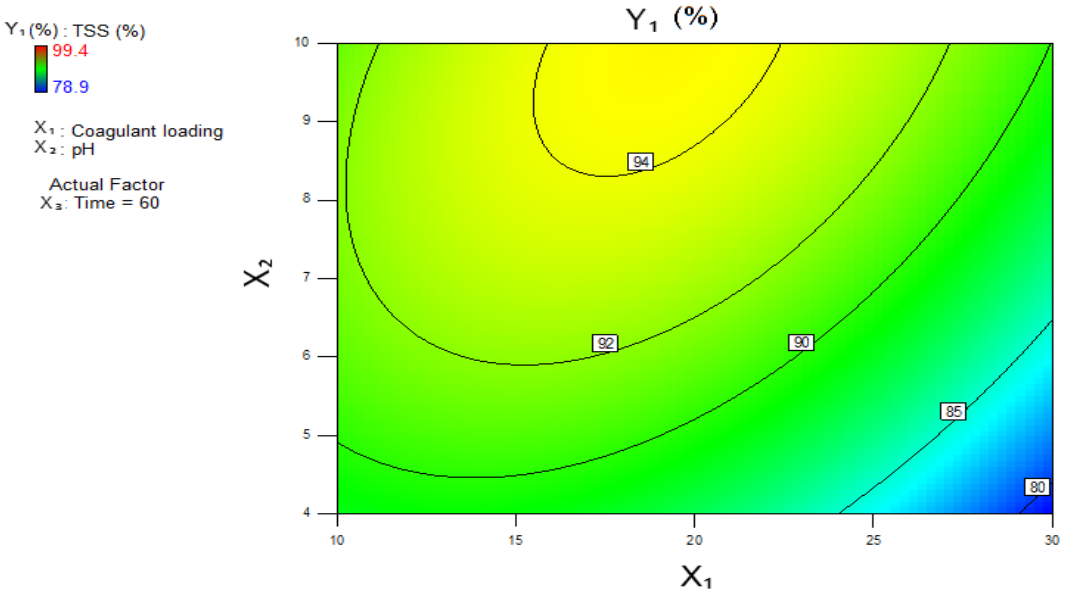

Figure 5.6: TSS - Contour plot for coagulant loading and pH.

The RSM plot only takes into account two manipulated variables and one response variable.

From Fig. 5.5 and Fig. 5.6, it can be seen that the optimum chitosan dosage was 20 ml which corresponds to 7.41 mg/l, beyond which the efficiency decreased. The optimum pH range was found to be between 8.5 and 10.

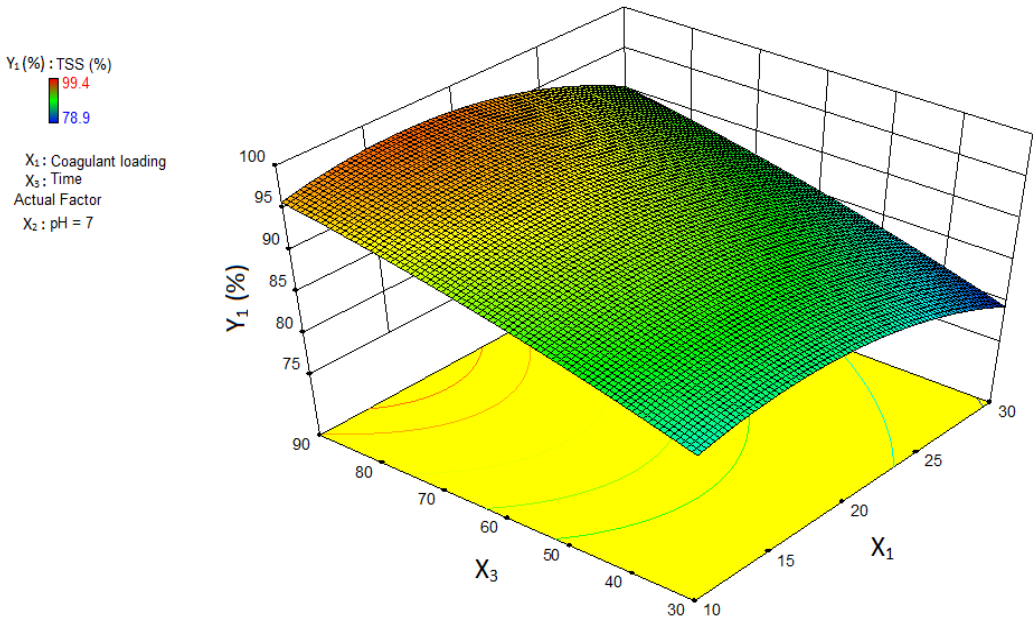

Figure 5.7: TSS - RSM plot for coagulant loading and time.

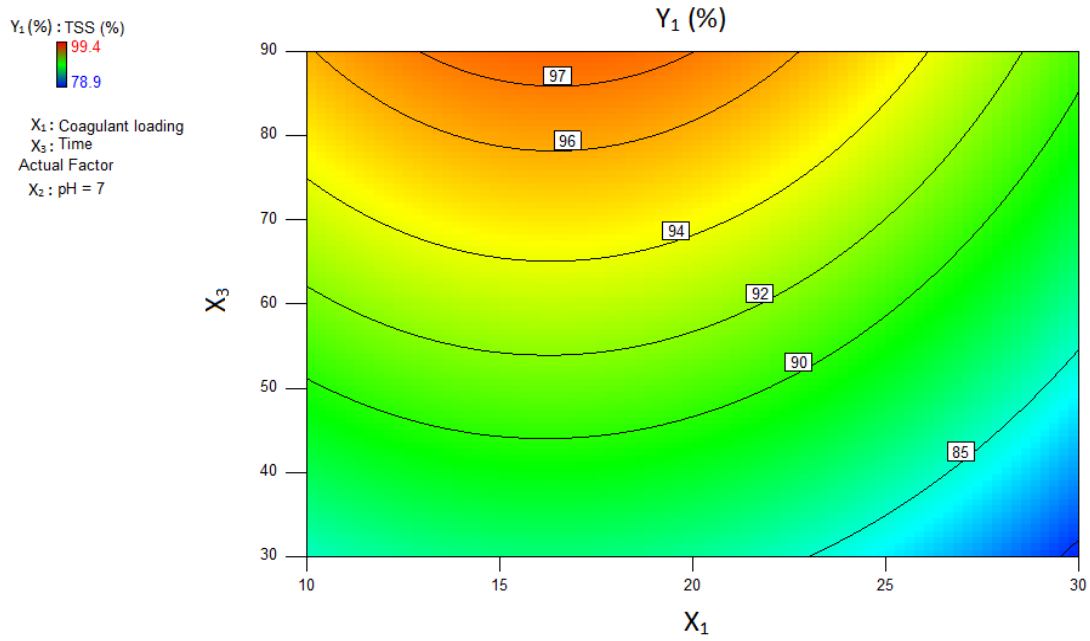

Figure 5.8: TSS - Contour plot for coagulant loading and time.

From Fig. 5.7 and Fig. 5.8 it can be seen that the removal of TSS increases with the increase in settling time, as mentioned earlier in the analysis of Eq. 5.1.

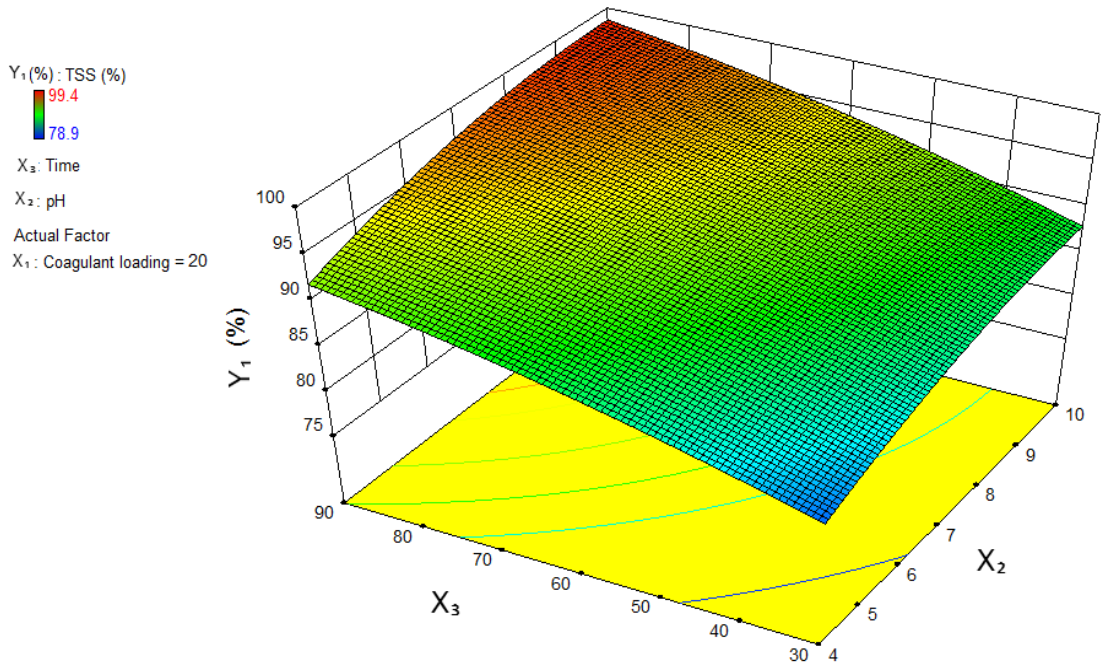

Figure 5.9: TSS - RSM plot for time and pH.

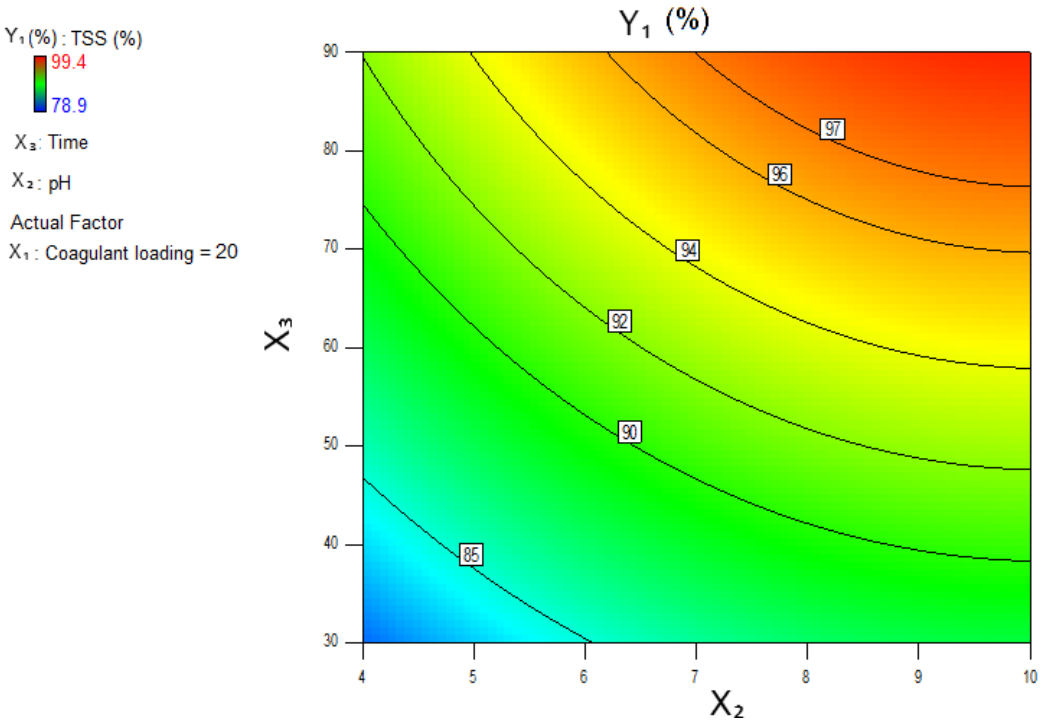

Figure 5.10: TSS - Contour plot for time and pH.

The plots in Fig. 5.9 and Fig. 5.10 confirm the pH ranges and stresses on the significance of the settling time. The maximum TSS removal efficiency was achieved at 90 minutes.

Based on the graphs above, it can be concluded that the optimum TSS removal was achieved at a pH of 10, CCo loading of 20 ml (7.41 mg/l) and a settling time of 90 minutes.

5.4. ANALYSIS FOR COD

The ANOVA and LOF test for the effect of chitosan on the COD removal is shown in Table 5.6. From the ANOVA table it can be seen that the regression is significant due to the large F-value and a p>F value less than 0.05.

The term X_1 has the highest F-value and the lowest p>F value, meaning that the coagulant dosage has the largest effect on the performance of the coagulant in terms of COD removal, followed by the settling time and the pH.

Table 5.6: ANOVA (COD).

Variation	SS	df	MS	F-value	p-value p>F
Regression	740.49	9	82.28	33.23	< 0.0001
X_1	162.90	1	162.90	65.79	< 0.0001
X_2	84.50	1	84.50	34.13	0.0006
X_3	101.53	1	101.53	41.00	0.0004
X_1X_2	5.29	1	5.29	2.14	0.1872
X_1X_3	31.92	1	31.92	12.89	0.0089
X_2X_3	12.25	1	12.25	4.95	0.0615
X_1^2	10.28	1	10.28	4.15	0.0810
X_2^2	133.82	1	133.82	54.04	0.0002
X_3^2	170.45	1	170.45	68.84	< 0.0001
Residual	17.33	7	2.48		
LOF	12.93	3	4.31	3.92	0.1101
Pure Error	4.40	4	1.10		
Total	757.82	16			

It can also be seen that there is 11.01% chance that the LOF is due to noise which is not a very significant value and the model can fit other experimental data. Thus, from the ANOVA, it can be concluded that the model is significant and it fits the experimental data.

The model equation for this response is expressed as:

$$Y_2=29.3-4.51X_1-3.25X_2+3.56X_3+1.15X_1X_2+2.83X_1X_3-1.75X_2X_3-1.56X_1^2-5.64X_2^2-6.36X_3^2 \quad (5.2)$$

From the sources above (Eq. 5.2 and Table 5.6) it can be concluded that the COD removal efficiency decreases with an increase in the coagulant dosage and pH, but

increases with an increase in the settling time. This can be explained as follows: (1) Increasing the CCo loading increase the amount of organic present in the water (2) At high pH the chitosan recombines and remain in suspension in the samples instead of settling down with the flocs (3) Most of the impurities will settle with time, therefore, the efficiency is positively affected by an increase in settling time.

The term X_1X_3 is the most significant interaction. The terms X_1X_2 and X_1X_3 positively influence the reduction of COD. This means that the removal of COD increase with coagulant loading depending on a particular pH range and on the settling time.
The negative signs of the quadratic coefficients reveal that the curves for X_1^2, X_2^2 and X_3^2 are concave.

Table 5.7: Model coefficients (COD).

SD	CV (%)	R^2	$\check{R}^2$	$\acute{R}^2$	AP
1.57	6.87	0.9771	0.9477	0.7179	17.017

There is 6.87% of unexplained variations in the model, which is acceptable. The value of the R^2 is close to 1, indicating a good fit. The $\acute{R}^2$ is not close to the $\check{R}^2$ (The difference between the two values is greater than 0.2), which can be overlooked if the diagnostic plots provide good fits. An AP of 17 shows that the model can give good predictions of the COD removal.

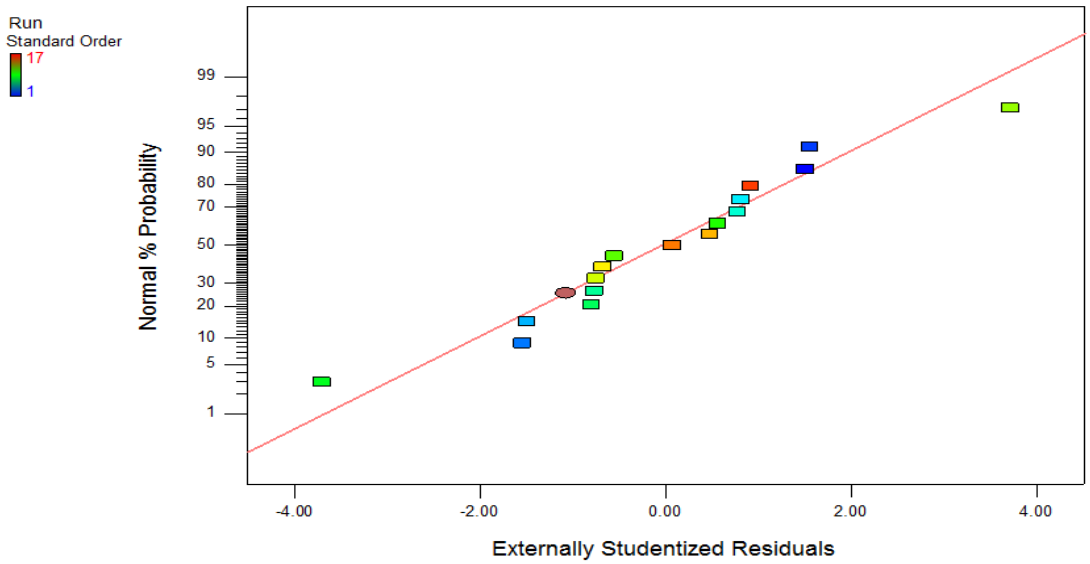

Figure 5.11: COD - Normal plot of residuals.

The data points in Fig. 5.11 are slightly deviating from the normally distribution given. The deviation is not very critical and can be corrected by using the Box-Cox transformation (Appendix B).

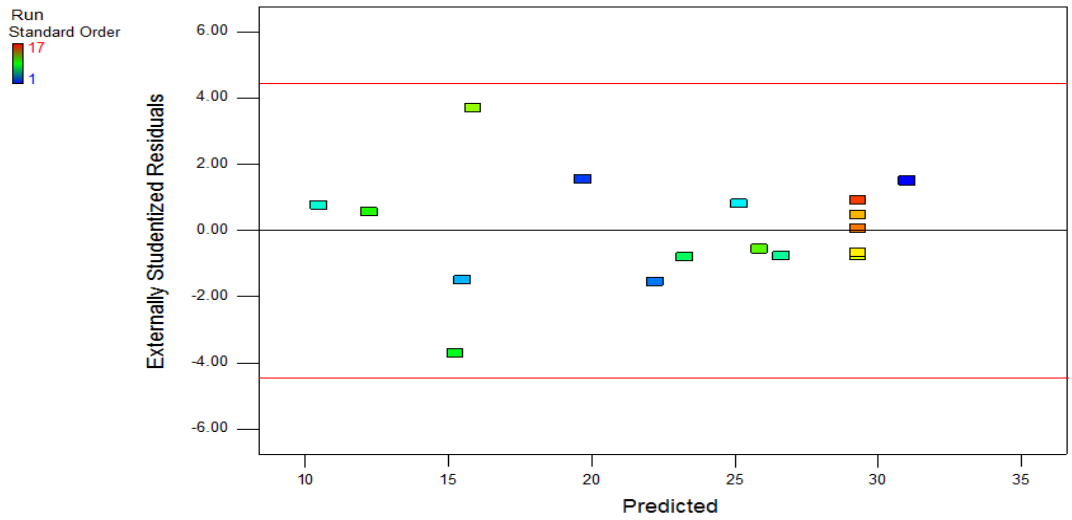

Figure 5.12: COD - Residuals vs. predicted values.

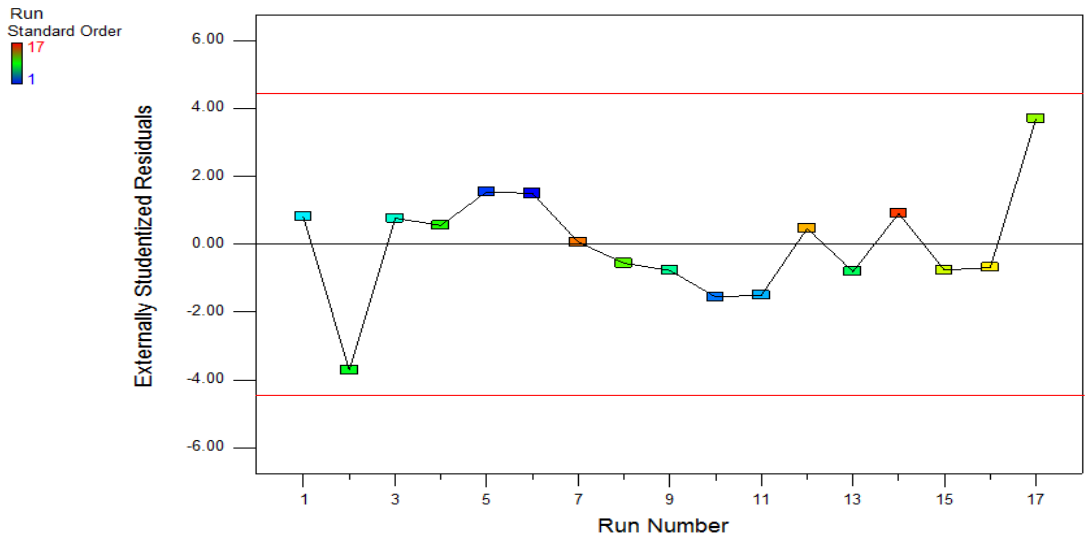

Figure 5.13: COD - Residuals vs. run number.

The data points in Fig. 5.12 are scattered randomly and Fig. 5.13 does not form a trend. All the data points in both plots are within the boundaries marked by the red line. Therefore, there are no outlier data.

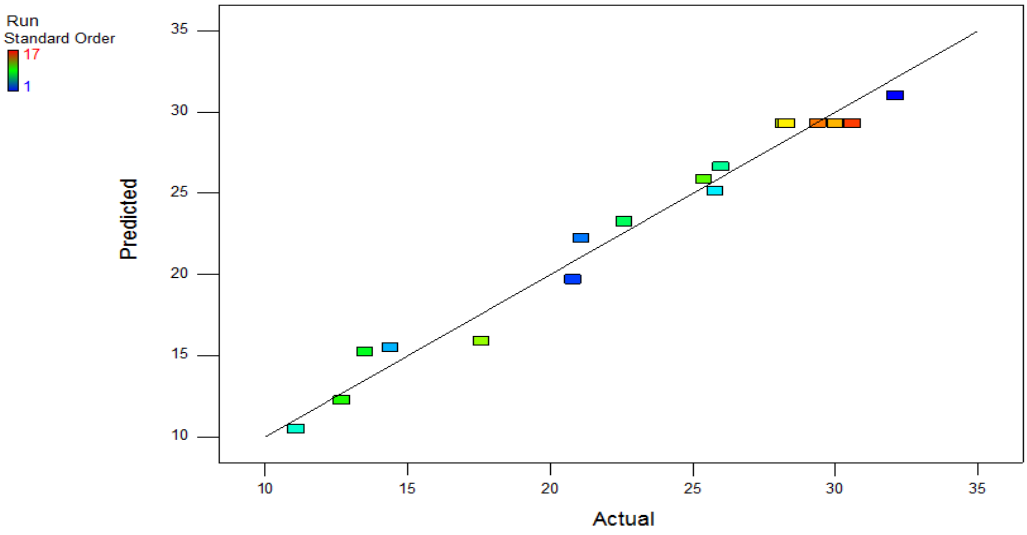

Figure 5.14: COD - Predicted vs. actual.

The data points in Fig. 5.14 are distributed randomly on the 45 degree line, indicating that the model provides an acceptable fit for the experimental data.

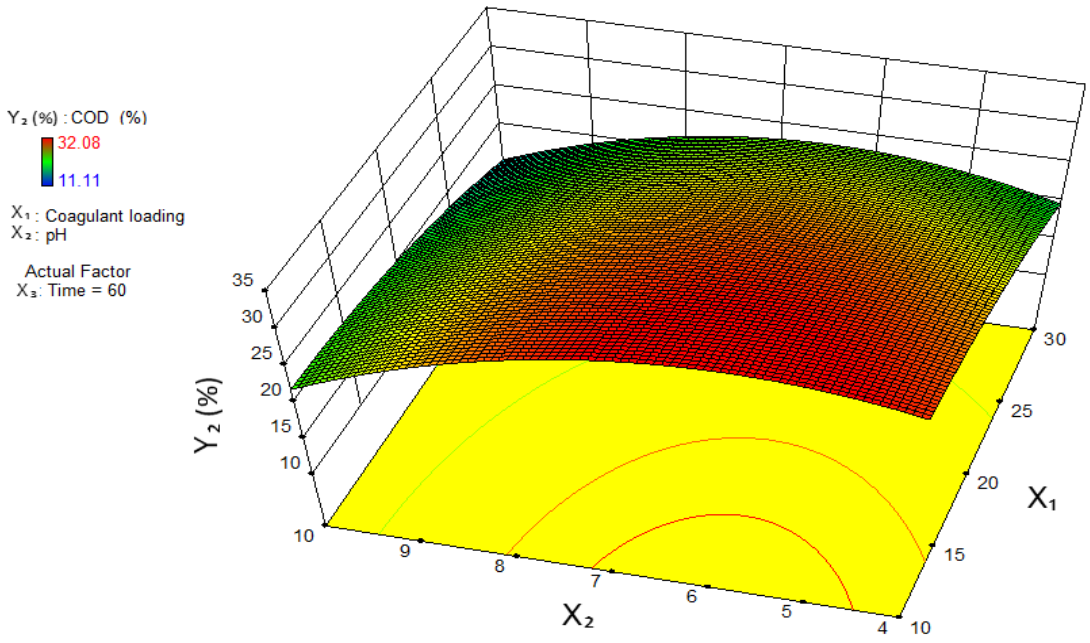

Figure 5.15: COD - RSM plot for coagulant loading and pH.

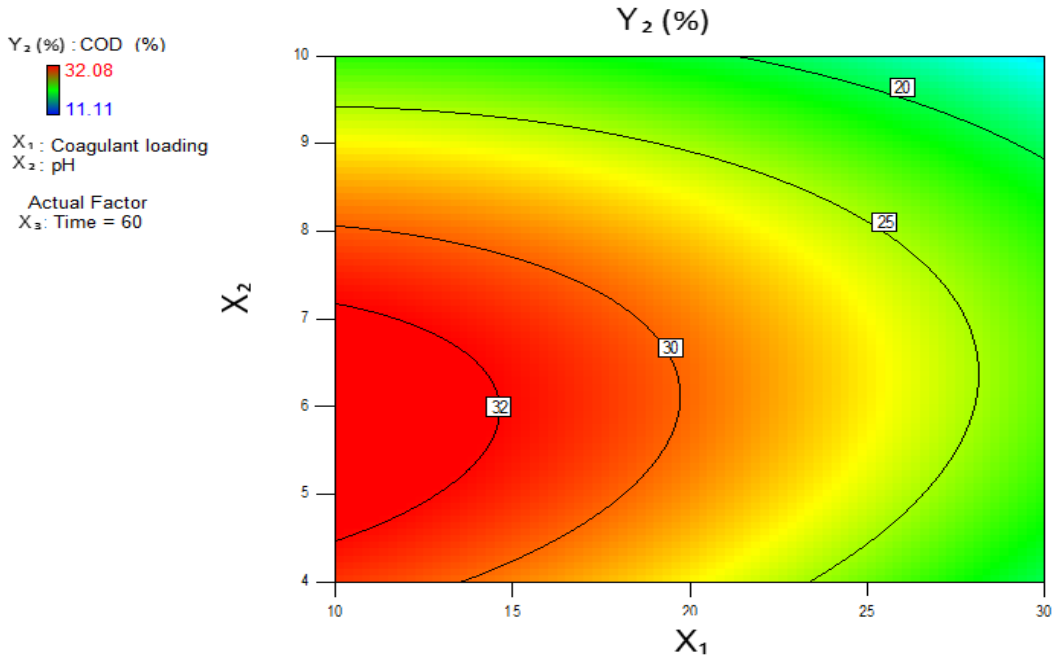

Figure 5.16: COD - Contour plot for coagulant loading and pH.

The removal of COD was high from pH 4 to 8 and coagulant loading of 10 to 20 ml (3.85 mg/l and 7.41 mg/l) beyond which the efficiency decreased (Fig. 5.15 and Fig. 5.16). This phenomenon was explained in Chapter 4: At high pH the chitosan

precipitates and adds to the organic content of the water. The coagulant dosage reaches a limit when there are no more particles for the chitosan cations to form bonds with, the excess either precipitates or forms a layer of gelled chitosan on the surface of the effluent and increases the COD of the water.

The plots in Fig. 5.17 and Fig. 5.18 show that the COD removal requires low CCo dosage. The optimum range for the settling time lies between 55 and 68 minutes.

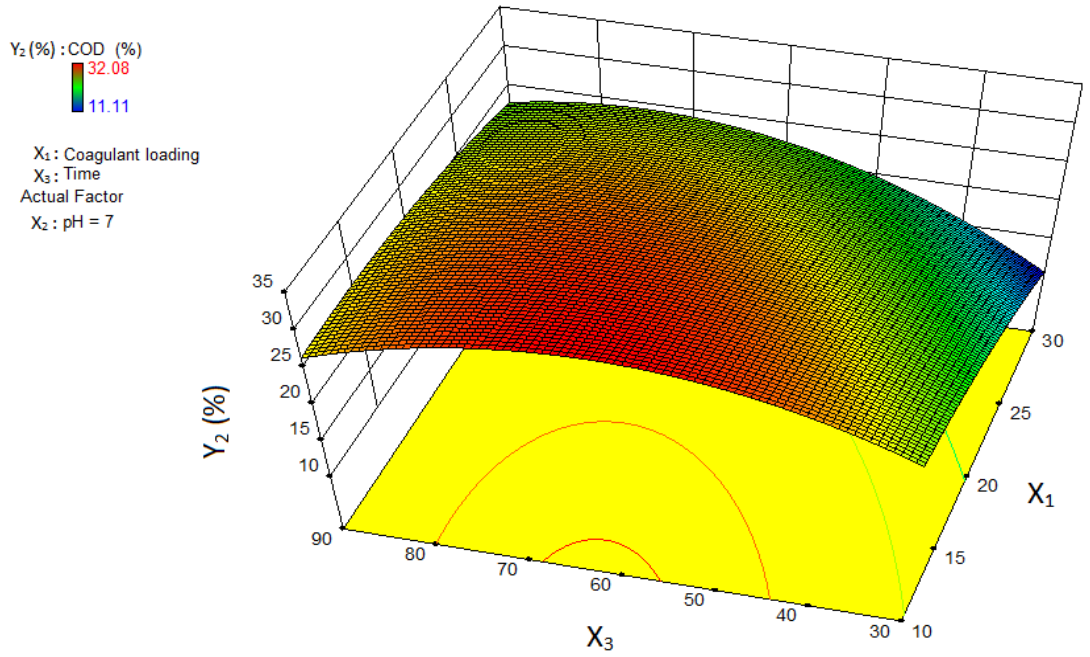

Figure 5.17: COD - RSM plot for coagulant loading and time.

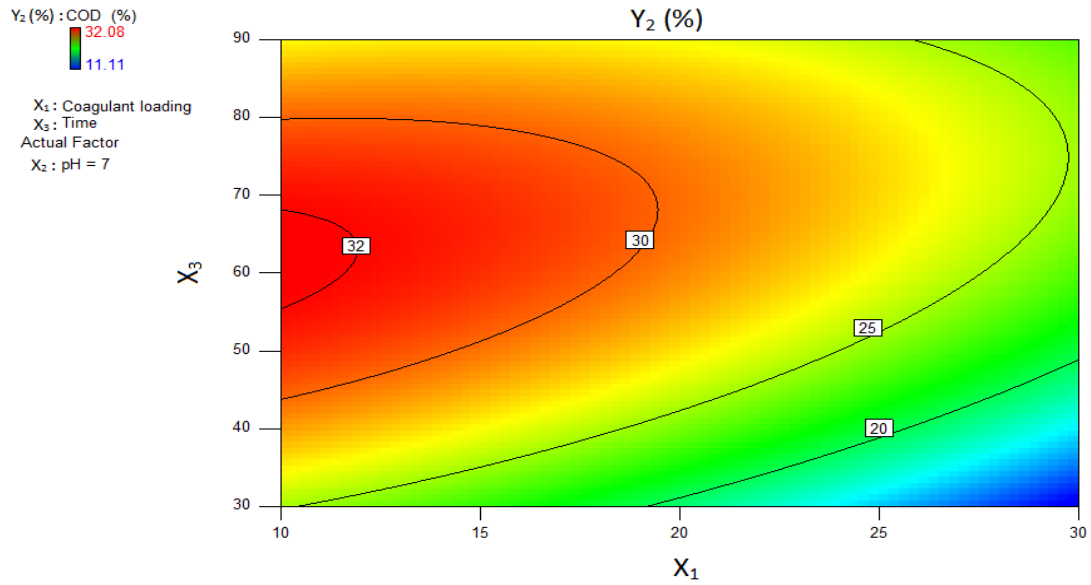

Figure 5.18: COD - Contour plot for coagulant loading and time.

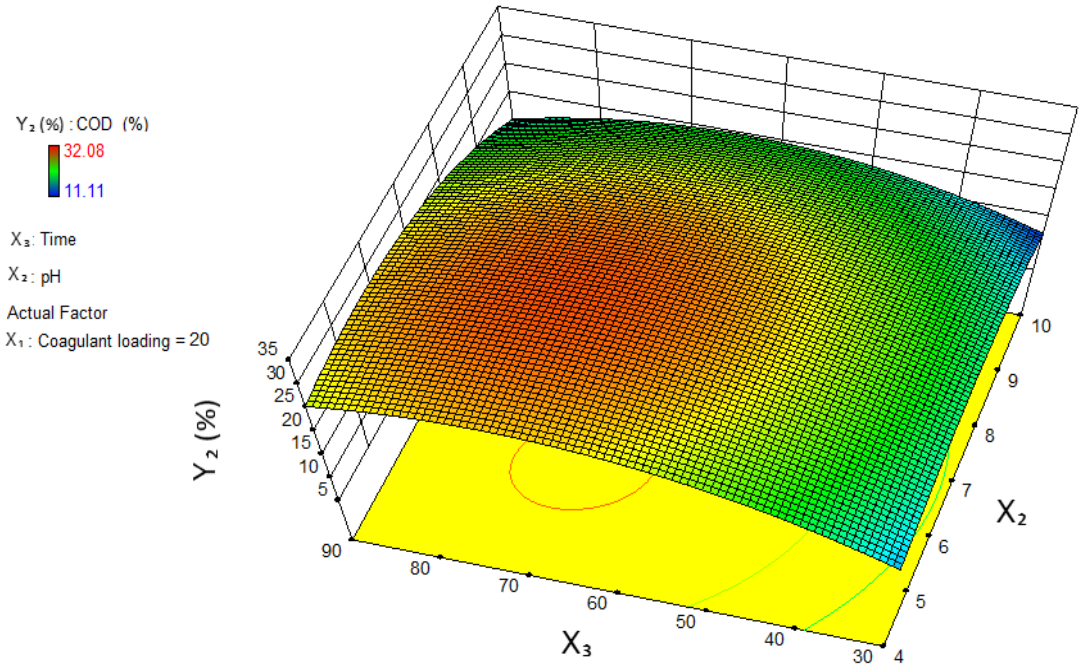

Figure 5.19: COD - RSM plot for time and pH.

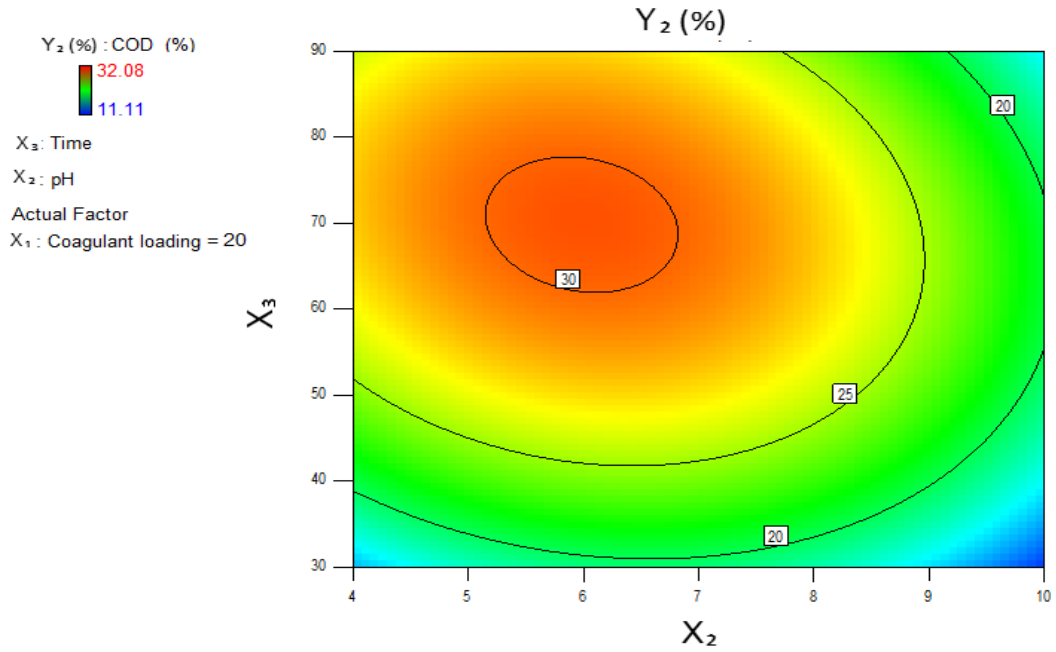

Figure 5.20: COD - Contour plot for time and pH.

At lower pH values the COD removal efficiency is high between 60 to 85 minutes (Fig. 5.19 and Fig. 5.20). This range is higher than in Fig 5.18 due to the pH-dependent nature of chitosan. At low pH, most of the dissolved chitosan formed microflocs with the impurities in the effluent, and those microfllocs continue to agglomerate, grow and settle with longer settling times. When the pH is high, the chitosan recombines and precipitates without neutralizing and absorbing the particles in the water. Furthermore, some of the chitosan remains in suspension in the wastewater in the form of thin gels at pH beyond 6.5 and adds to the total COD of the sample.

From all the graphs above, it can be concluded that the optimum COD removal was achieved at a pH of 7, CCo loading of 10 ml (3.85 mg/l) and a settling time of 60 minutes.

5.5. ANALYSIS FOR COLOUR

The statistical analysis in Table 5.8 shows that the removal of the colour in the effluent is mainly dependent on the pH and the settling time. The ANOVA indicates that the regression is significant due to the F-value of 11.26 and a p>F value of 0.0021. There is 19.45 % chance that the LOF is due to noise which is insignificant; meaning that the model can fit any data.

From Table 5.8 and Eq. 5.3 it can be noticed that X_2 is the most significant linear term, followed by X_3. Whereas the p-value of X_1 indicates that it is an insignificant term in the model equation. This means that the removal of colour using chitosan is more affected by pH of the sample and the settling time than it is affected by the chitosan dosage. The positive signs of the linear coefficients indicates that the colour removal increases with an increase in pH, settling time and coagulant dosage.

The p-value of X_2X_3 shows that it is the most significant interaction term. Therefore, the colour removal will increase with the simultaneous increase of the pH and the settling time. This behaviour was discussed in Chapter 4. The addition of NaOH led to the precipitation of certain elements dissolved in the sample and impeded the coagulation process by recombining the chitosan.

The colour removal is also increased to a smaller extent by the interaction between the coagulant dosage and the pH of the sample. The negative sign of the term X_1X_3 show that the colour removal efficiency decreases with an increase in CCo dosage and settling time.

The model equation for this response is expressed as:

$$Y_3=84.8-1.36X_1+5.26X_2+4.46X_3+0.58X_1X_2-0.15X_1X_3+2.88X_2X_3-3.25X_1^2-1.62X_2^2-2.8X_3^2 \quad (5.3)$$

Table 5.8: ANOVA (Colour)

Variation	SS	df	MS	F-value	p-value p>F
Regression	642.13	9	71.35	11.26	0.0021
X_1	14.85	1	14.85	2.34	0.1697
X_2	218.40	1	218.40	34.46	0.0006
X_3	159.31	1	159.31	25.14	0.0015
X_1X_2	1.32	1	1.32	0.21	0.6616
X_1X_3	0.090	1	0.090	0.014	0.9085
X_2X_3	33.06	1	33.06	5.22	0.0563
X_1^2	44.47	1	44.47	7.02	0.0330
X_2^2	117.16	1	117.16	18.49	0.0036
X_3^2	33.01	1	33.01	5.21	0.0564
Residual	44.36	7	6.34		
LOF	29.10	3	9.70	2.54	0.1945
Pure Error	15.26	4	3.81		
Total	686.50	16			

The presence of quadratic terms indicates the presence of curvature. The negative signs these terms in the equation above, shows that the curves of X_1^2, X_2^2 and X_3^2 are concave.

Table 5.9: Model coefficients (Colour).

SD	CV (%)	R^2	$\check{R}^2$	$\acute{R}^2$	AP
2.52	3.17	0.9354	0.8523	0.2870	10.449

There is 3.17% of unexplained variations in the model, which is acceptable. The value of the R^2 is close to 1, indicating a good fit. The $\acute{R}^2$ is not close to the $\check{R}^2$ (The difference between the two values is greater than 0.2), which can be corrected by applying Box-Cox transformations (See Appendix B). The value of the AP (10.449) indicate that this

model will give good predictions of colour removal for this particular case of experiment.

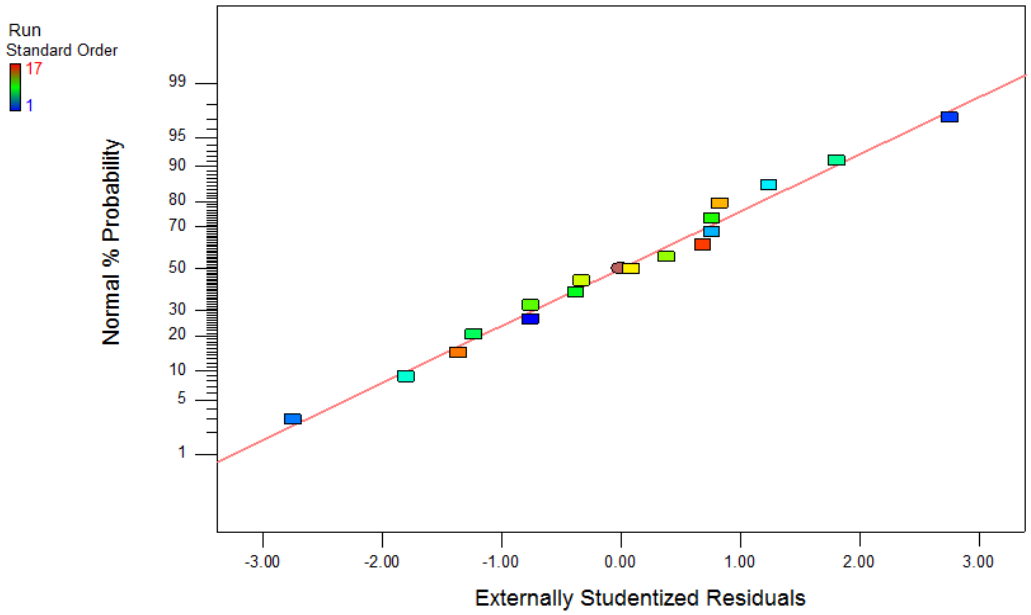

Figure 5.21: Colour - Normal plot of residuals.

The data points in Fig. 5.21 approximates a straight line, which indicates that the data used for this experiment is normally distributed.

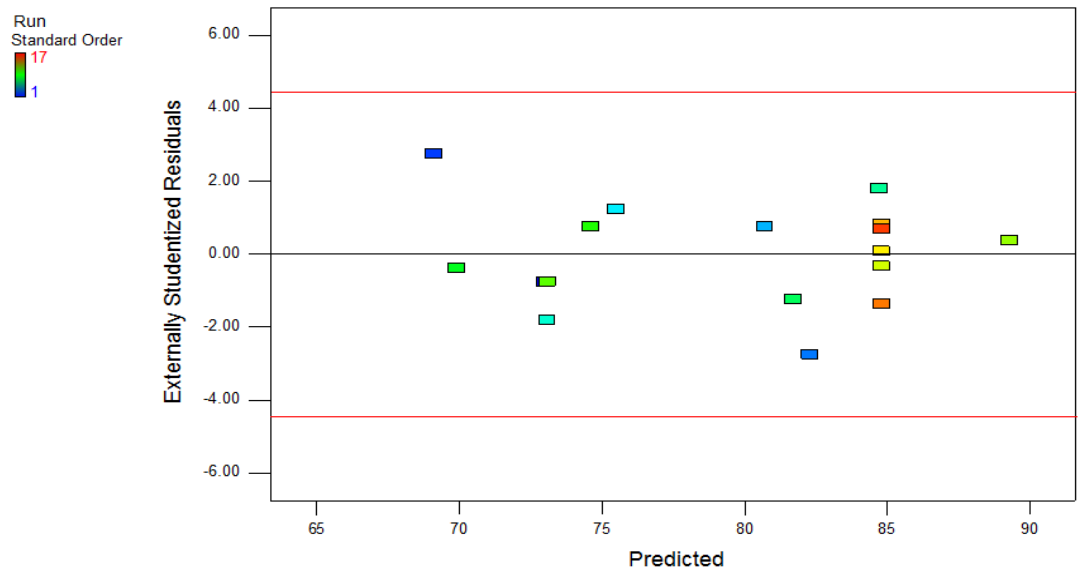

Figure 5.22: Colour - Residuals vs. predicted values.

From Fig. 5.22 it can be seen that the data are scattered randomly and there are no outliers.

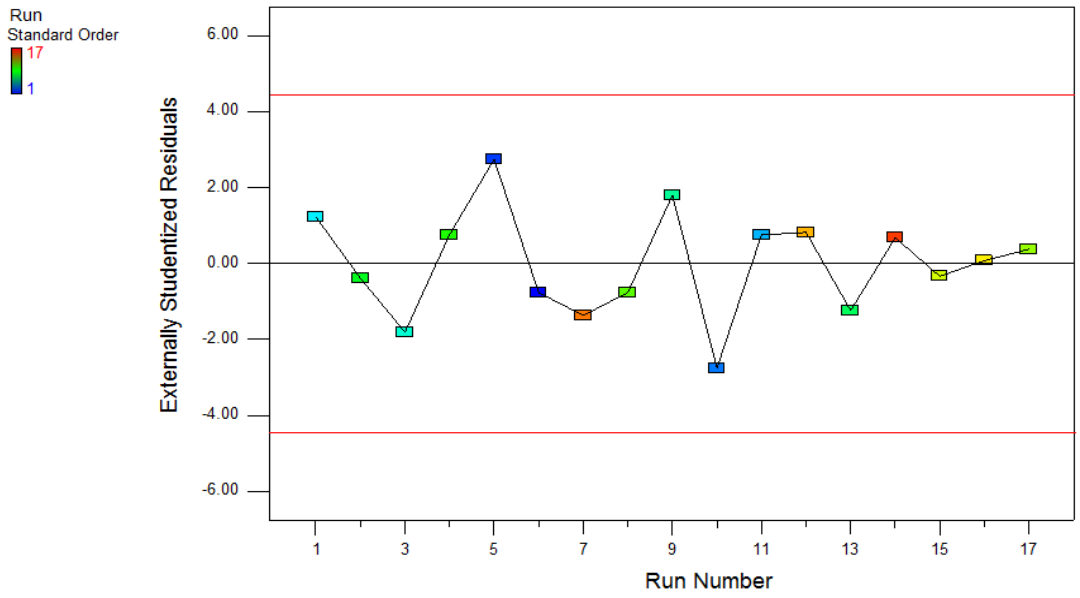

Figure 5.23: Colour - Residuals vs. run number.

The pattern of the data plotted in Fig. 5.23 does not form a set trend (Chapter 2).

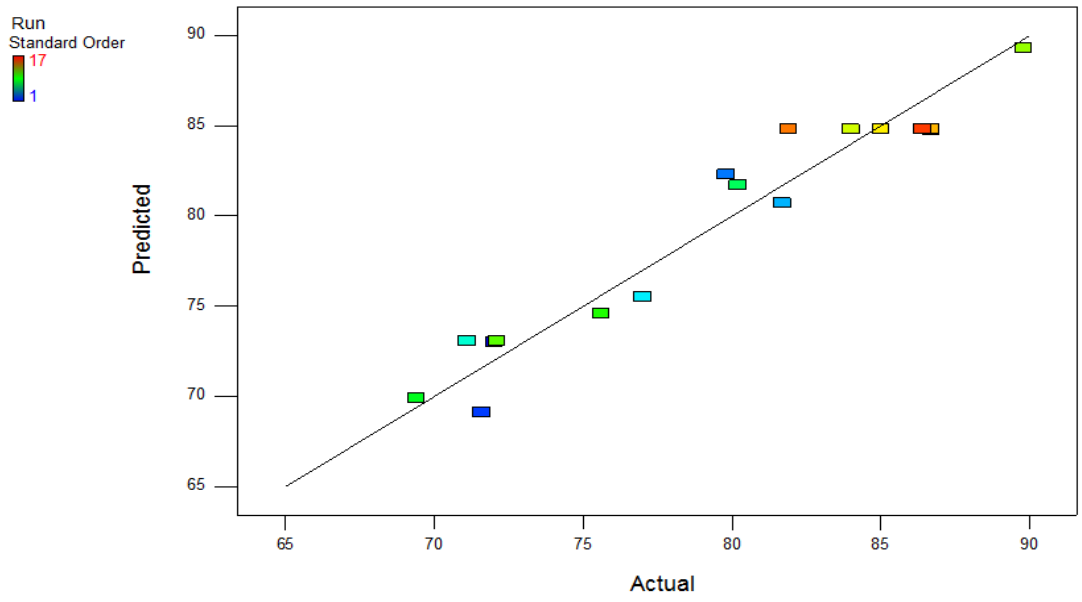

Figure 5.24: Colour - Predicted vs. actual.

Fig. 5.24 shows that the model is a good fit due to the fact that the data points are distributed randomly along the 45 degree line.

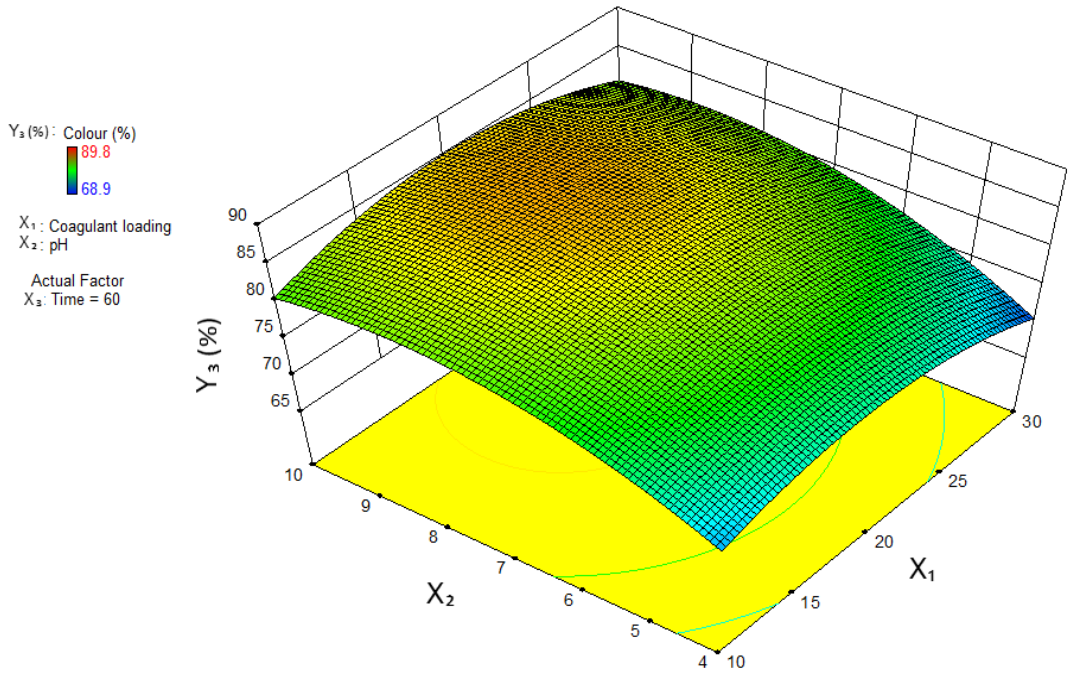

Figure 5.25: Colour - RSM plot for coagulant loading and pH.

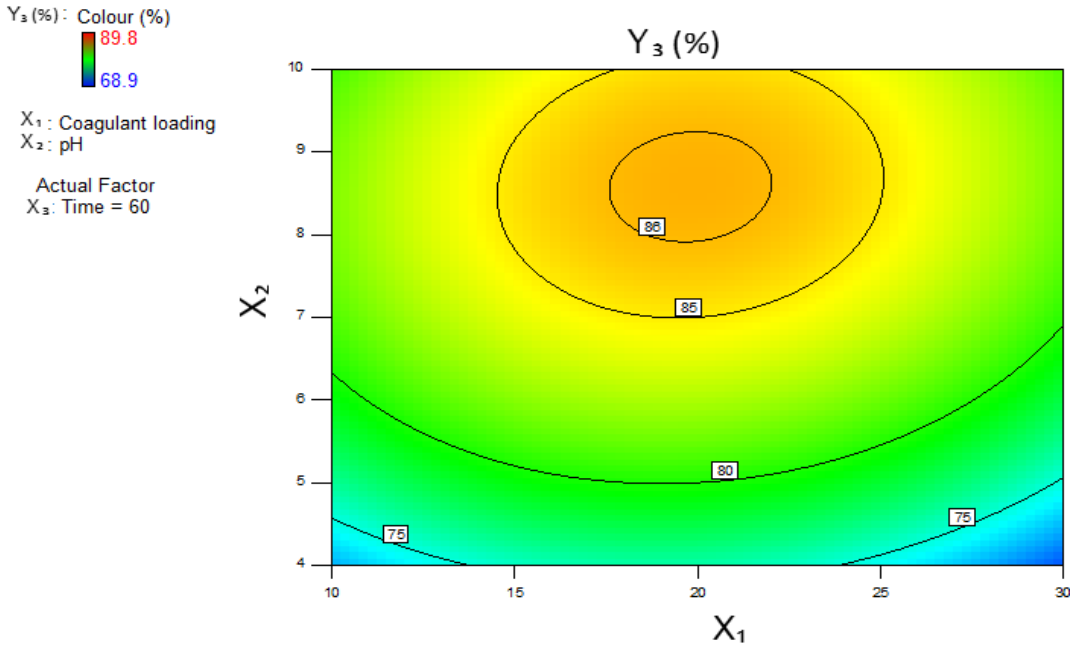

Figure 5.26: Colour - Contour plot for coagulant loading and pH.

The optimum chitosan dosage for removal of colour was found to be 20 ml (7.41 mg/l) and the pH range of 7.5 to 10 provided high colour removals (Fig. 5.25 and Fig. 5.26).

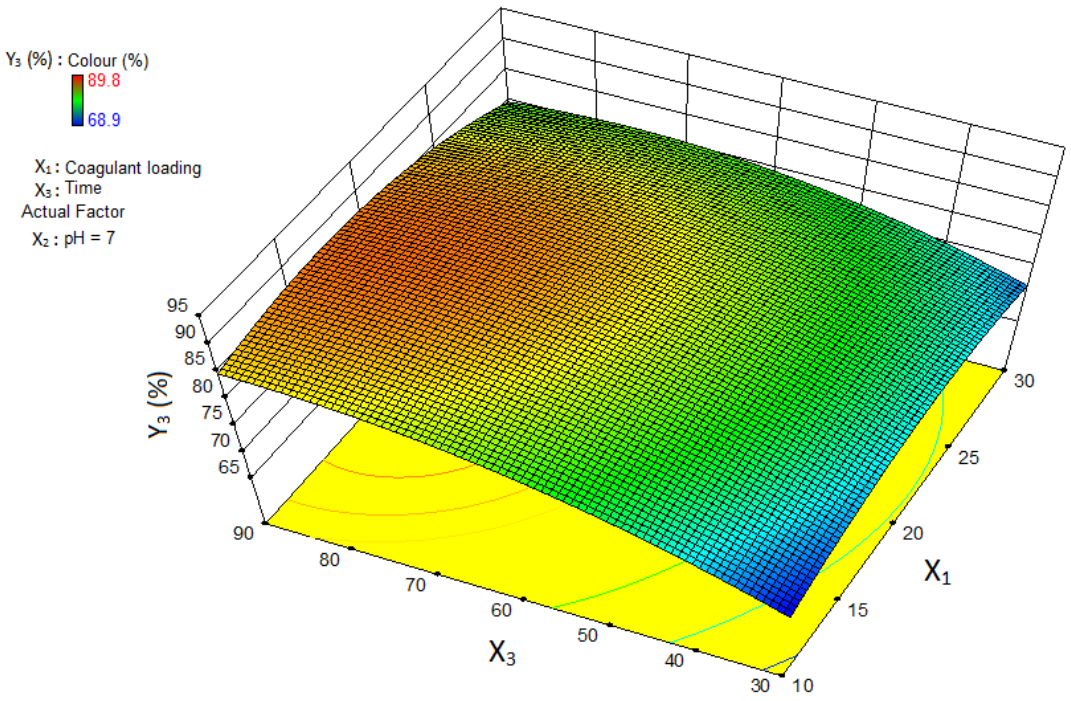

Figure 5.27: Colour - RSM plot for coagulant loading and time.

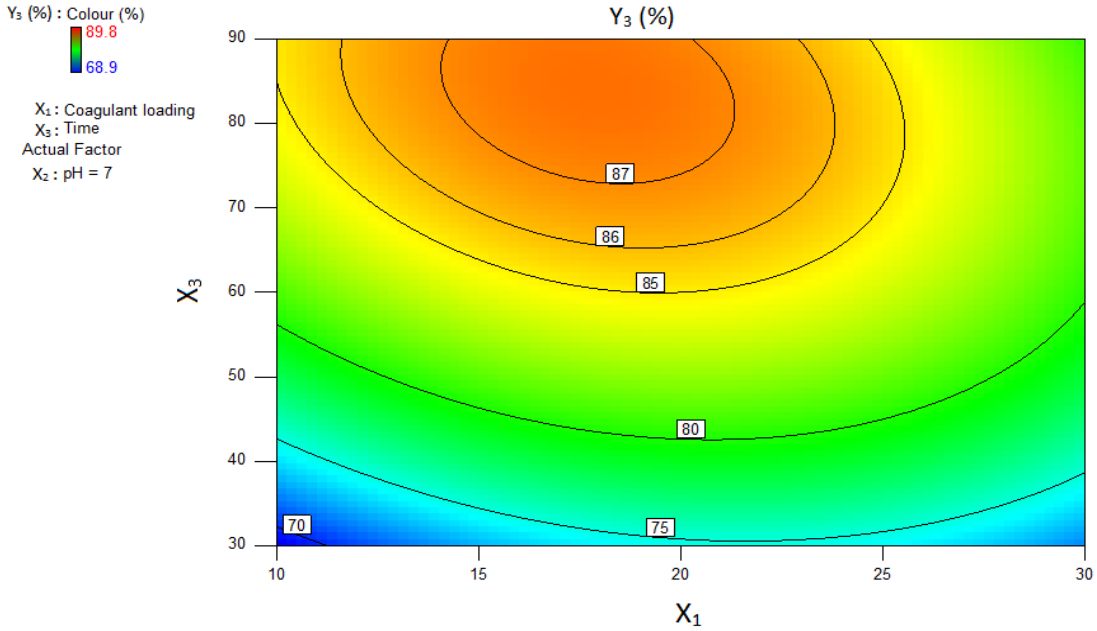

Figure 5.28: Colour - Contour plot for coagulant loading and time.

Fig. 5.27 and Fig. 5.28 show that the settling time has more effect on the colour removal than the coagulant dosage as mentioned earlier.

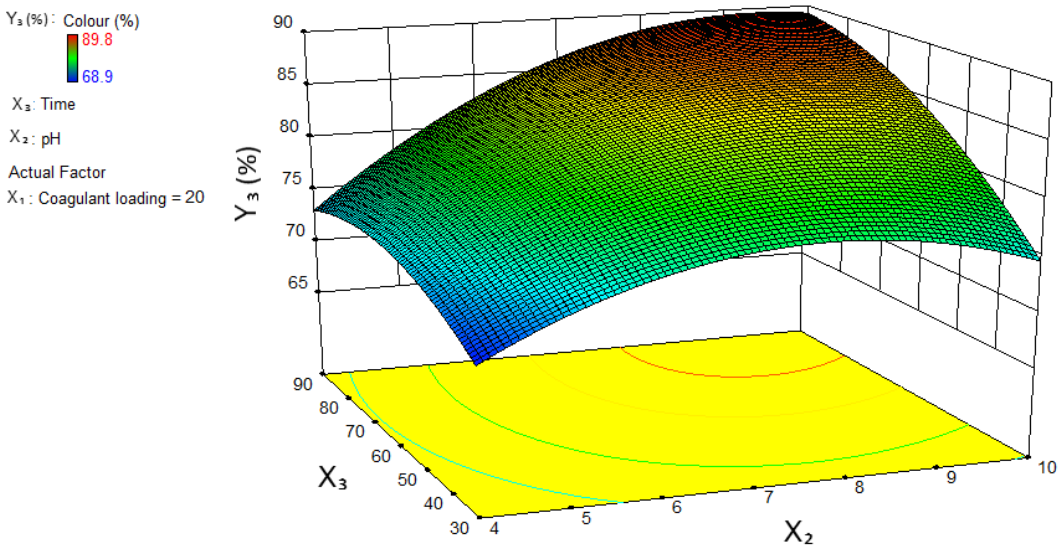

Figure 5.29: Colour - RSM plot for time and pH.

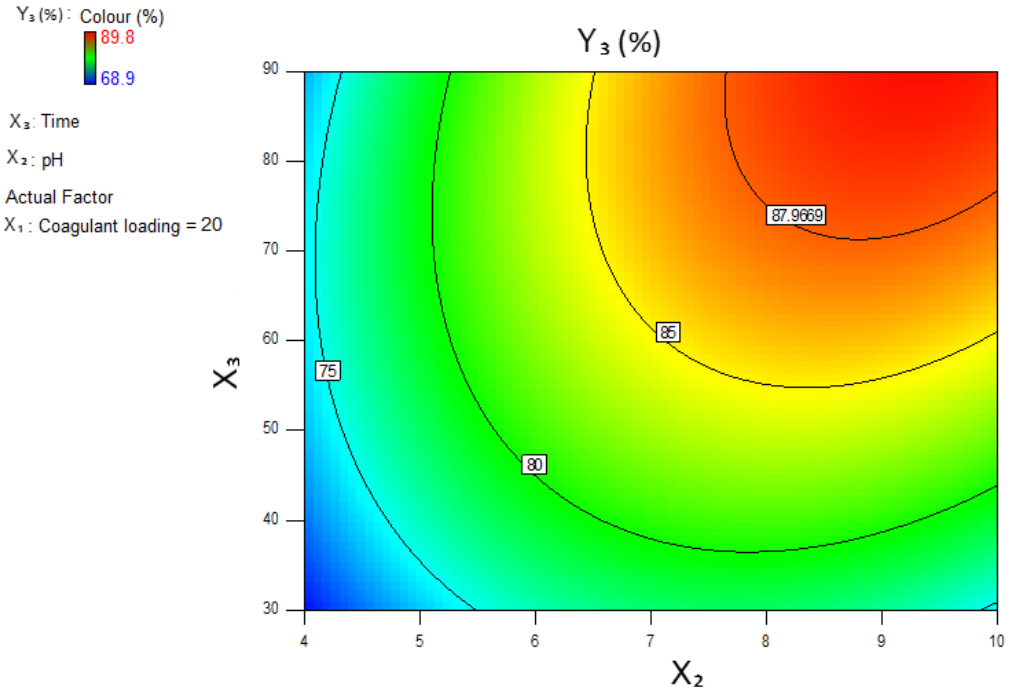

Figure 5.30: Colour - Contour plot for time and pH.

The removal of colour was related to removal of TSS. The effluent became clearer as the solids settled. It can be seen in Fig. 5.29 and Fig. 5.30 that the removal of colour increased with an increase in settling time.
In conclusion, the optimum colour removal was achieved at a pH of 10, CCo loading of 20 ml (7.41 mg/l) and a settling time of 90 minutes.

5.6. OPTIMIZATION

The optimization process was done to find the values of the manipulated variables that would provide high removal efficiency for all three responses while taking into account industrial productivity, by generating an overlay plot. The data on the overlay plot are computed using individual model equations in order to find a common optimum region for all variables.

The constraints below were defined to generate the optimum region using Design expert software:

(1) The target for the coagulant loading was 20 ml (7.41 mg/l)
(2) The pH was set in range from 6 to 8. Very acidic or basic solutions will cause damages to equipment. Furthermore the pH-dependent behaviour of the chitosan and the natural pH of the FE needed to be considered.
(3) In industry, time is an important factor. The aim was to achieve maximum removal of impurities in a short period of time. Therefore, 60 minutes was the selected settling time for the optimization.

When computing the overlay plot, the software extends these constraints in order to find and suggest optimum values.
The plot in Fig. 5.31 identifies the optimum region for the three response simultaneously in the yellow shade. It can be seen that the optimum region for chitosan loading is between 10.2 ml and 21 ml (3.92 mg/l and 7.75 mg/l); the pH lies between 6.4 and 8.3. The minimum values of the responses in the plot are indicated as 92% for TSS, 83% for colour and 29% for COD.

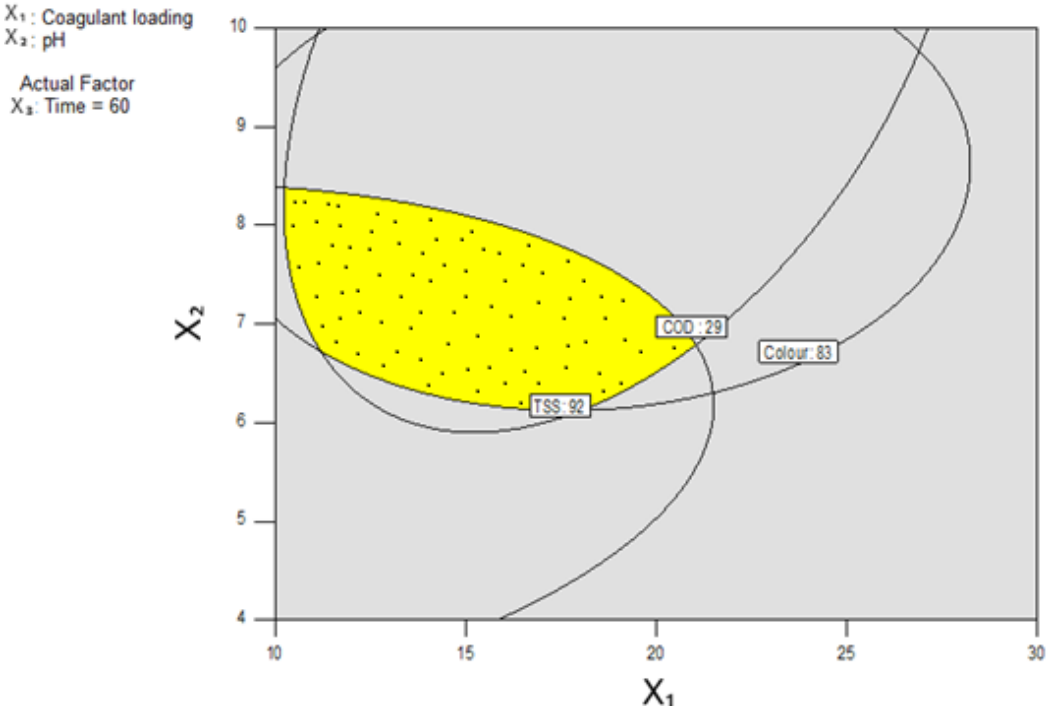

Figure 5.31: Overlay plot.

Table 5.10 shows the values of the responses when the neutral pH is selected as the optimum. These values are deduced from the overlay plot above.

Table 5.10: Optimization.

	X_1 (mg/l)	X_2 (pH)	X_3 (min)	Y_1 (TSS)	Y_2 (COD)	Y_3 (Colour)
Optimized values	7.41	7	60	92.6	29.3	84.8

The values in Table 5.10 provided high removal efficiencies under the selected constraints. The neutral pH was safe for the equipment and machinery within the refinery, under the low dosage of 7.41 mg/l.

5.7. SUMMARY

In this chapter the Box-Behnken method was used to design the order of the experimental runs and to statistically analyse the data obtained. This was done to find optimum conditions for the removal of the impurities from the FE.

The model evaluation indicated that the terms were orthogonal from each other. Model equations and RSM graphs for all the responses were generated using experimental data. These models passed most of the evaluation tests showing that they fit the experimental data and are significant. The settling time was found to have a great impact on all the responses investigated. For each variable, the performance of the chitosan increased until a maximum point beyond which the efficiency decreased.

The optimum dosage, pH and settling time varied with each response. However, during the optimization stage, an overlay plot was generated by considering the optimum for all three responses simultaneously.

CHAPTER 6: COMPARISON BETWEEN OFAT AND RSM

6.1. INTRODUCTION

The coagulation of the FE from the sugar refinery was investigated using two different experimental designs. This chapter compares the findings from both methods in terms of efficiency and reliability.

6.2. OPTIMUM RANGES

The traditional jar test experiments conducted using OFAT is discussed in detail in the Chapters 4. The settling time was constant for all OFAT experiments (2 hours) as suggested from the literature.

Table 6.1: Optimum regions for OFAT.

Sample pH	TSS	Colour	COD	Dosage	TSS	Colour	COD
4	97	88	11	3.7 mg/l	79.31	41.85	38.08
5	98	86	11	7.41 mg/l	96.72	61.35	34.78
6	98	85	10	14.81 mg/l	90.62	57.11	18.51
7	97	86	9	29.63 mg/l	85.52	55.12	13.50
8	95	85	5	44.44 mg/l	79.81	41.20	5.56
9	87	76	-7	59.26 mg/l	67.77	26.41	3.42
10	84	74	-12	74.1 mg/l	64.83	14.19	0.11

In Table 6.1, the values within the red dashed box represent the optimum regions for the pH of the sample and coagulant dosage. The data from this table indicate that the highest removal of all three responses was obtained between the pH of 4 and 7; while the optimum range for chitosan dosage was found to be between 3.7 mg/l and 14.81 mg/l.

Using Box-Behnken design, the optimum range for chitosan loading was found to be between 3.92 mg/l and 7.75 mg/l; and the optimum range for the pH is between 6.4 and 8.3 for the pH, as generated in the overlay plot (Fig. 5.31) which is reproduced below.

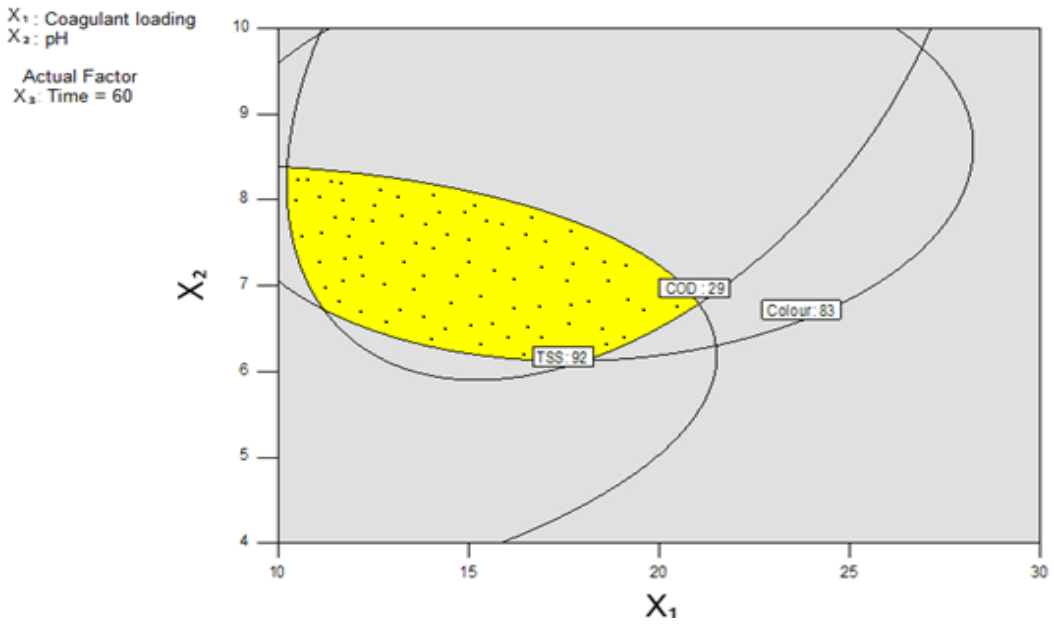

Figure 5.31: Overlay plot.

The optimum conditions selected from Chapter 4 were compared to the optimized conditions found in Chapter 5 (Table 6.2)

Table 6.2: Optimum conditions.

	Optimum					
	Dosage (mg/l)	pH	Settling time (minutes)	TSS (%)	COD (%)	Colour (%)
OFAT	7.41	Natural: 7	120	63	5	16
		Adjusted: 5		98	11	86
BBD	7.41	7	60	92.6	29.3	84.8

Table 6.2 shows similarities in the optimum conditions for both methods. It can also be seen that the COD removal under the OFAT did not exceed 11%. This is due to the difference in the settling time between the two sets of experiments. The interaction between the pH-dependent behaviour of the chitosan and the settling time affects the COD removal in two ways:

(1) At low pH, there is a high amount of chitosan dissolved in the effluent. As the settling time increase, more chitosan gels continue to dissolve in the acid and add to the total COD of the water sample.

(2) At high pH, the chitosan recombines and a lower amount of the impurities in the water is absorbed and neutralized. Therefore, a smaller portion of the COD is removed.

The influence of the interaction between the settling time and the pH of the effluent can also be seen in the comparative table below.

Table 6.3: Traditional jar tests results vs. Box-Behnken tests.

Optimum dosage (mg/l): 7.41						
	OFAT Maximum settling time (Minutes)			BBD Maximum settling time (Minutes)		
	120			90		
Sample pH	TSS	Colour	COD	TSS	Colour	COD
4	97	88	11	92	73	26
5	98	86	11	94	79	27
6	98	85	10	96	83	28
7	97	86	9	97	86	27
8	95	85	5	98	89	24
9	87	76	-7	99	90	21
10	84	74	-12	99	89	16

The OFAT values in Table 6.3 indicate that at low pH ($\leq$ 6) the removal of TSS and colour continued to increase beyond the 90 minutes settling time set for the BBD. It can be seen that at 120 minutes the TSS and colour removal reached an equilibrium before decreasing. The behaviour of the COD removal was discussed earlier. The difference between the COD removal at 90 minutes and at 120 minutes is quite considerable.

In terms of identifying the optimum conditions, RSM method using BBD had the following advantages:

- The optimum conditions could be spotted from the experimental matrix without requiring special statistical training (see Table 5.2).
- The statistical analyses generated model equations that helped with further optimization of the process.
- It allowed the experimenter to analyse all factors and responses simultaneously.

- The ANOVA and the RSM graphs (3D plots and contours) allowed the quick identification of main effects and interactions.

The OFAT method is familiar and simple to understand. In the case of this study, it provided a good identification of important variables. Parameters such as the concentration of the impurities and the use of CCo on RE were eliminated due to their poor performances.

The use of OFAT as a screening experimental design prior to RSM also allows the experimenter to take notice of parameters that are easily overlooked. For example, the settling time was overlooked in the preliminary experiments. After screening with OFAT only pH and CCo dosage remained as important variables, thus a third variable was required. Thus, the settling time was identified as an important parameter.

6.3. RELIABILITY OF THE EXPIMENTAL DESIGN METHODS MODELS EQUATIONS

The OFAT does not require statistical analysis in order to deduce the behaviour of a system or to generate graphical analysis. However, it is possible to deduct equations predicting the response based on the manipulated factor from data in Chapter 4 using Design expert 9.0 for one factor analysis.

Considering the two important variables under OFAT, the pH (*A*) and the coagulant dosage (*B*), the model equations for the three responses variables are as follows:

$$Y_1 = 96.6667 - 6.85714A - 6.64286A^2 \tag{6.1}$$

$$Y_1 = \frac{1}{\sqrt[3]{\left(1.86 + 1.16B + 0.848B^2\right) \times 10^{-6}}} \tag{6.2}$$

$$Y_2 = 7.9524 - 11.7857A - 9.2143A^2 \tag{6.3}$$

$$Y_2 = 7.3565 - 17.3883B + 11.6904B^2 \tag{6.4}$$

$$Y_3 = \sqrt[3]{\left(6.13 - 1.31A - 0.852A^2\right) \times 10^5} \tag{6.5}$$

$$Y_3 = e^{(3.8731 - 0.6354B - 0.6127B^2)} \quad (6.6)$$

Y_1, Y_2 and Y_3 represent the TSS, COD and colour removal respectively. The manipulated variables are coded according to equation 3.1 (See Table 6.4).

Table 6.4: Coding of OFAT variables.

	-1	1
A: pH	4	10
B: CCo dosage	3.7	74.1

The model equations for the RSM studies were discussed in chapter 5. Three model equations were generated for the prediction of TSS, COD and colour. Comparing Eq. 5.1, 5.2 and 5.3 with the OFAT equations (Eq. 6.1 to 6.6) it can be noted that the OFAT requires six equations for two manipulated variables, whereas the RSM uses three equations for 3 manipulated variables.

In Table 6.5, the equations 5.1 and 6.1 are used to predict the TSS removal of FE over time. The actual values were obtained from a preliminary experiment that investigated the removal of TSS over time for various coagulant concentration.

Table 6.5: Actual TSS removal at natural pH vs. predicted TSS removal.

Settling time (Minutes)	%TSS removal (actual)	% TSS removal (RSM)	% TSS removal (OFAT)
30	91	87	N/A
60	96	93	N/A
70	99	95	N/A
90	99	98	N/A
120	99	100	95

The other variables were not considered in this particular run due to the fact that the TSS removal was the most significant response, and it was noticed that when a high amount of suspended particles was removed, the colour content of the water decreased. Furthermore, it was established that the COD removal for this study was minimal. The

experiment took place at natural pH (7.83). The values in Table 6.5 are for the coagulant dosage of 7.41 mg/l (Appendix C).

In terms of reliability, the R^2 of each of these equations (for OFAT and RSM) was satisfactory within their experimental constraints (See Table 6.6).

Table 6.6: R-squared for OFAT models

	Eq.6.1	Eq.6.2	Eq.6.3	Eq.6.4	Eq.6.5	Eq.6.6
R^2	0.894	0.963	0.959	0.969	0.965	0.881

The OFAT equations were found to be very limited due to the following reasons:

- It was impossible to predict responses for any other settling time than the traditional 2 hours (See Table 6.5).
- In order to deduct equations for different factors (such as different settling times), more experimental runs are required. Therefore, one response may end with many predictive equations.
- The response is predicted based on the variation of a single factor, failing to account for interactions.

The RSM prediction equations have the following advantages:

- Flexibility: The model equations can predict the responses based on the variation of ay factor individually or in combination with other factors.
- From Table 6.5, it can be noted that the RSM model equation (Eq. 5.1) provided a better prediction of the TSS removal at 120 minutes than the OFAT model equation (Eq. 6.1).
- Less number of model equations required compared to the OFAT.

6.4. SUMMARY

Based on the results in chapter 4 and chapter 5, it can be seen that the OFAT and the RSM produced similar results for the responses investigated. The RSM plots on their own are similar the OFAT plots and can be used for screening significant parameters, identifying optimum ranges and optimum values of the variables in an experiment.

The biggest difference between the two experimental designs is the use of statistical analysis in the RSM, which generate model equations that predict the responses by considering all the variables while OFAT equations only considers one factor to generate a regression. These model equations are used to optimize the responses numerically and produce overlay plots.

The RSM model equations were found to be more accurate in predicting the responses than the OFAT regressions. Furthermore, the RSM model equations covered for a wider range of constraints and allowed more flexibility than the OFAT model equations.

CHAPTER 7: CONCLUSION AND RECOMMENDATIONS

Industries such as sugar processing plants consume large amounts of fresh water daily and approximately 40 % of that water is released as effluents. These effluents are either treated by the local municipality or disposed of in authorized landfills by waste management companies. Due to the cost of wastewater treatment and the new regulations from the South African department of water affairs, most companies have invested in research activities to find cost efficient and sustainable methods of reducing the pollution load in their effluents before disposal or for reuse within the plant.

Coagulation has been widely used in wastewater treatment mostly as a pre-treatment process for effluent purification prior to filtration (Membrane filtration, microfiltration, nanofiltration), or as a sludge recovery method. However, the use of inorganic coagulants has been associated with neurological diseases such as Alzheimer disease. Research on the performance of organic and natural coagulant is still being perfected as new findings emerge.

Chitosan is a polymer produced from the de-acetylation of chitin, a naturally occurring polymer found in the exoskeleton of most crustaceans, insects and fungi. The treatment of sugar industry resin effluent (RE) and the final effluent (FE) using chitosan was investigated under various conditions. The RE, a dark brown effluent produced from the regeneration of the resin used to bleach the brown sugar syrup, is disposed of in landfills due to its high pollution load. The FE which includes all the wastewaters generated by the processes in the refinery, is sent to the local municipality for treatment.

The main objective of this work was to investigate the possibility of using chitosan as a coagulant for the treatment of ESR for colour, chemical oxygen demand (COD) and TSS reductions. The specific objectives of this work were: (1) To evaluate the performance of the coagulant in terms of the concentration of chitosan, the initial pH of the wastewater and the influence of the concentration of the impurities using the traditional jar-test method. (2) To identify the factors that influence the performance of chitosan and the variables that can be optimized to enhance the performance of

chitosan. (3) Compare results obtained from the ESR with those obtained from similar industries using chitosan as a coagulant. (4) To evaluate the efficiency using statistical design of experiment and compare the outcomes of the RSM method with the results from the traditional jar-test method (OFAT).

Preliminary experiments were done using the OFAT design in order to screen the parameters and identify the optimum ranges for the optimization studies. The coagulant was prepared by dissolving chitosan flakes in aqueous acidic solutions.
From the preliminary studies it was found that HCl was a better solvent than acetic acid (AA), especially due to the fact that the organic nature of AA increased the final COD of the effluent.

Results indicated that the optimum chitosan dosage was found to be 138 mg/l and 7.41 mg/l for RE and FE respectively, beyond which, the efficiency of the coagulant decreased. The treatment of FE yielded 97% total suspended solids (TSS), 61% colour and 35% chemical oxygen demand (COD). The coagulation of RE resulted in 68% TSS, 30% colour and 15% COD. The performance of the chitosan was found to be pH-dependent and high removal efficiencies were achieved under acidic conditions. The addition of NaOH considerably reduced the coagulation efficiency, possibly gelling the polymer.

The influence of the impurity content in the effluent was investigated. The performance of chitosan for RE increased with a decrease of impurity load, while the FE demonstrated poor results at lower impurity concentrations. The important variables selected based on the results from the OFAT experiments were the pH and coagulant loading. Due to the fact that all experiments were done at HC, the settling time was used

It was identified that the COD in the effluents from the food processing industry is related to the TDS, which is difficult to remove because most of the dissolved particles are stable in the wastewater. A model developed for the removal of TSS in relationship with the TDS and the COD in water, provided a good fit when applied to the effluents from two other food and beverage industries.

The Box-Behnken design (BBD) was used to analyse the data and generate model equations for the response variables. The overlay plot provided the optimum region for all three responses based on the results computed from the model equations. A comparison between the RSM and the OFAT showed that the model equations from the RSM analysis were more reliable and allowed for more flexibility than the OFAT regressions. Although the optimum ranges from both DOE were similar, the OFAT could not readily identify nor quantify the interaction between the factors.

Overall it can be concluded that chitosan can remove impurities from the ESR. The efficiency of the chitosan depends on the impurity load in the wastewater. The performance of the chitosan was found to be limited by the level of TDS in the effluents. Chitosan yielded good TSS and colour removal for the FE but failed to decrease the COD in the water, which is the major concern in the sugar industry. The implementation of the chitosan coagulant for large scale application was found to be costly and unsustainable for this highly polluted wastewater.

Further, work need to be conducted on the performance of the chitosan and on the destabilization of dissolved solids from wastewater. Technologies such as electrocoagulation are good alternatives that can be optimized to provide TDS removal at low cost. The TSS model developed in chapter 4 may provide grounds for further studies on modelling the behaviour of the coagulation process.

REFERENCES

American Public Health Association (APHA), American Water Works Association (AWWA) and Water Environment Federation (WEF). 1999. *Standard methods for the examination of water and wastewater*. 20th ed. Washington, DC.

Amuda, O. S., Amoo, I. A. and Ajayi, O. O. 2006. Performance optimization of coagulant/flocculant in the treatment of wastewater from a beverage industry. *Journal of hazardous materials B,* 129: 69-72.

Anderson, M. J. and Whitcomb, P. J. 2000. *DOE Simplified: Practical tools for effective experimentation*. Ortland, Oregon: Productivity, Inc.

Annadurai, G., Sung, S. S. and Lee, D. J. 2004. Simultaneous removal of turbidity and humic acid from high turbidity stormwater. *Advances in environmental research*, 8 (3–4): 713-725.

Aranaz, I., Mengibar, M., Harris, R., Panos, I., Miralles, B., Acosta, N., Galed, G. and Heras, A. 2009. Functional characterization of chitin and chitosan. *Current chemical biology,* 3(2): 203-230.

Archer, M., Watson, R. and Denton, J. W. 2001. *Fish waste production in the United Kingdom. The quantities produced and opportunities for better utilisation*. The Sea Fish Industry Authority.

Asthon, P. 2000. Southern African water conflicts: are they inevitable or preventable? *Water for peace in the Middle East and southern Africa.* Green Cross International, Geneva; .94-98.

Asthon, P.J. 2007. Disputes and Conflicts over Water in Africa. *Violent conflicts, fragile peace: Perspectives on Africa's security*. London: Adonis and Abbey.

Ayyasamy, P. M., Yasodha, R., Rajakumar, S., Lakshmanaperumalsamy, P., Rahman, P. K. S. M. and Lee, S. 2008. Impact of sugar factory effluent on the growth and biochemical characteristics of terrestrial and aquatic plants. *Bulletin of environmental contamination and toxicology*, 81 (5): 449–454.

Azlan, K., Wan Saime, W. N. and Lai ken, L. 2009. Chitosan and chemically modified chitosan beads or acid dyes sorption. *Journal of environmental sciences*, 21 (3): 296-302.

Barreiro-Iglesias, R., Coronilla, R., Concheiro, A. and Alvarez-Lorenzo, C. 2005. Preparation of chitosan beads by simultaneous cross-linking/insolubilisation in basic pH: Rheological optimization and drug loading/release behaviour. *European journal of pharmaceutical sciences*, 24 (1): 77-84.

Baş, D. and Boyaci, İ. H. 2007. Modeling and optimization I: Usability of response surface methodology. *Journal of food engineering*, 78 (3): 836-845.

Bauer, R., Waldner, G., Fallmann, H., Hager, S., Klare, M., Krutzler, T., Malato, S. and Maletzky, P. 1999. The photo-fenton and the TiO_2/UV process for waste water treatment- novel developments. *Catalyst today*, 53 (1): 131-144.

Bezerra, M. A., Santelli, R. E., Oliveira, E. P., Villar, L. S. and Escaleira, L. A. 2008. Response surface methodology (RSM) as a tool for optimization in analytical chemistry. *Talanta*, 76 (5): 965-977.

Bina, B., Mehdinejad, M. H., Nikaeen, M. and Attar, H. M. 2009. Effectiveness of chitosan as natural coagulant aid in treating turbid waters. *Iranian journal of environmental health science & engineering editorial*, 6 (4): 247-252.

Cao, C., Xiao, L., Liu, L., Zhu, H., Chen, C. and Gao, L. 2013. Visible-light photocatalytic decolorization of reactive brilliant red X-3B on Cu_2O/crosslinked-

chitosan nanocomposites prepared via one step process. *Applied surface science*, 271: 105-112.

Cestari, A. R., Vieira, E. F. S., Tavares, A. M. G. and Bruns, R. E. 2008. The removal of the indigo carmine dye from aqueous solutions using cross-linked chitosan—Evaluation of adsorption thermodynamics using a full factorial design. *Journal of Hazardous materials*, 153 (1–2): 566-574.

Chambers, J. M., Cleveland, W. S., Kleiner, B. and Tukey, P. A. 1983. *Graphical methods for data analysis*. New York: Chapman and Hall.

Cheng, W. P., Chi, F. H., Yu, R. F. and Lee, Y. C. 2005. Using chitosan as a coagulant in recovery of organic matters from the mash and lauter wastewater of brewery. *Journal of polymers and the environment*, 13 (4): 383-388.

Cheng, Y. L., Wong, R. J., Chun-Te Lin, J., Huang, C., Lee, D. J. and Mujumdar, A. S. 2010. Water coagulation using electrostatic patch coagulation (EPC) mechanism. *Drying technology: an international journal*, 28 (7): 850-857.

Chi, F. H. and Cheng, W. P. 2006. Use of Chitosan as Coagulant to Treat Wastewater from Milk Processing Plant. *Journal of polymer and environment*, 14 (4): 411-417.

Chiou, M. S., Ho, P. Y. and Li, H. Y. 2004. Adsorption of anionic dyes in acid solutions using chemically cross-linked chitosan beads. *Dyes and pigments*, 60 (1): 69-84.

Crini, G. and Badot, P.-M. 2008. Application of chitosan, a natural aminopolysaccharide, for dye removal from aqueous solutions by adsorption processes using batch studies: A review of recent literature. *Progress in polymer science*, 33 (4): 399-447.

Czitrom, V. 1999. One-factor-at-a-time versus designed experiments. *The American statistician*, 53 (2): 126-131.

Dash, M., Chiellini, F., Ottenbrite, R. M. and Chiellini, E. 2011. Chitosan-A versatile semi-synthetic polymer in biomedical applications. *Progress in polymer science*, 36 (8): 981-1014.

Divakaran, R. and Sivasankara Pillai, V. N. 2001. Flocculation of kaolinite suspensions in water by chitosan. *Water research*, 35 (16): 3904-3908.

Doke, K. M., Khan, E. M., Rapolu, J. and Shaikh, A. 2011. Physico-chemical analysis of sugar industry effluent and its effect on seed germination of vigna angularis, vigna cylindrical and sorghum cernum. *Annals of environmental science*, 5:7-11.

DPW (South African Department of Public works). 2012. *Small waste water treatment works DPW design guidelines*. (Notice PW 2011/1). (Accessed 13-January-2013).

DWA (South African Department of Water Affairs). 2012. *Chemical spill into Ngagane River Newcastle – Kwa Zulu Natal*. Available:www.dwaf.gov.za/Communications/PresESRleases/2012/ChemicalSpill.pdf (Accessed 17-February-2012).

Dwyer, J., Griffiths, P. and Lant, P. 2009. Simultaneous colour and DON removal from sewage treatment plant effluent: Alum coagulation of melanoidin. *Water Research*, 43 (2): 553-561.

EPA (United States Environmental protection agency). 2000. *The history of drinking water treatment*. (Notice EPA-816-F-00-006). Available: www.epa.gov/safewater/sdwa25/sdwa.html (Accessed 12-May-2013).

Ferreira, S. L. C., Bruns, R. E., Ferreira, H. S., Matos, G. D., David, J. M., Brandão, G. C., da Silva, E. G. P., Portugal, L. A., dos Reis, P. S., Souza, A. S. and dos Santos, W. N. L. 2007. Box-Behnken design: An alternative for the optimization of analytical methods. *Analytica chimica acta*, 597 (2): 179-186.

Filloux, E., Gallard, H. and Croue, J. P. 2012. Identification of effluent organic matter fractions responsible for low-pressure membrane fouling. *Water research*, 46 (17): 5531-5540.

Freese, S. D., Trollip, D. L. and Nozaic, D. J. 2003. *Manual for testing of water and wastewater treatment chemicals*. Water Research Commission (WRC). Report No K5/1184.

Friedman, M. and Savage, L. J. 1947. *Planning experiments seeking maxima*. New York and London: McGraw-Hill.

Gao, B. Y., Hahn, H. H. and E., H. 2002. Evaluation of aluminum-silicate polymer composite as a coagulant for water treatment. *Water research*, 36 (14): 3573–3581.

Gleick, P. H. 1998. *The World's Water 1998-1999: The biennial report on freshwater resources*. Washington, D.C.: Island Press.

Guibal, E., Van Vooren, M., Dempsey, B. A. and Roussy, J. 2006. A review of the use of chitosan for the removal of particulate and dissolved contaminants. *Separation science and technology*, 41 (11): 2487-2514.

Gunkel, G., Kosmol, J., Sobral, M., Rohn, H., Montenegro, S. and Aureliano, J. 2007. Sugar cane industry as a source of water pollution - Case study on the situation in Ipojuca River, pernambuco, Brazil. *Water air soil pollution*, 180 (1-4): 261–269.

Gyananath, G. and Balhal, D. K. 2012. Removal of Lead (II) from aqueous solutions by adsorption onto chitosan beads. *Cellulose chemistry and technology,* 46 (1-2): 121-124.

Hattingh, H., Turton, A., Colvin, C. and Claa, M. 2015. *Water: Sustainable development and awareness* (online). Available:

www.enviropedia.com/topic/default.php?topic_id=240 (Accessed 04-February-2015).

Heinecken, C. and Smith, M. 2007. Overview of the South African oceans, coastal areas and fisheries. *Course:-Environmental engineering – sustainable development in coastal areas (MEV040).* Available: http://www.dlist.org/sites/default/filesdoclib/.../...PQ (Accessed 3-June-2013).

Integrated Regional Information Networks. 2013. *South Africa: The quiet water crisis*. Available: http://www.irinnews.org/Report/82750/SOUTH-AFRICA-The-quiet-water-crisis. (Accessed 23-May-2013).

International Organization for Standardization, ISO 9001:2008. *Quality management systems- Requirements.* Available: http://www.iso.org/catalogue_detail%...(Accessed 7-Mars-2014).

Islam, A. and Guha, A. K. 2013. Removal of pH, TDS and color from textile effluent by using coagulants and aquatic/non aquatic plants as adsorbents. *Resources and Environment* 3(5): 101-114.

Jadhav, M. V. and Mahajan, Y. S. 2013. Investigation of the performance of chitosan as a coagulant for flocculation of local clay suspensions of different turbidities. *KSCE Journal of civil engineering*, 17 (2): 328-334.

Jambrak AR (2011) Experimental Design and Optimization of Ultrasound Treatment of Food Products. *Journal of food processing technology*, 2(3): 1-3.

Karaan, M. and Rossouw, S. 2004. *A baseline assessment of the fishing and aquaculture industry in the Western Cape*. Department of Agricultural Economics. Stellenbosch University. Available: http://www.westerncape.gov.za/other/2005/10/final_first_paper_fishing.pdf... (Accessed 10-April-2013).

Khan, T., Peh, K. and Seng Ching, H. 2002. Reporting the degree of deacetylation values of Chitosan: The influence of analytical methods. *Journal of pharmacy and pharmaceutical sciences,* 5 (3):205-212.

Kowsalya, R., Noorjahan, C. M., M.Karrunakaran, C. M., Deecaraman, M. and Vijayalakshmi, M. 2010. Physico-chemical characterisation of brewery effluent and its degradation using native fungus aspergillus Niger. *Journal of industrial pollution control*, 26 (2): 171-176.

Li, S. Q., Zhou, P. J., Yao, P. J., Wei, Y. A., Zhang, Y. H. and Yue, W. 2010. Preparation of O-Carboxymethyl-N-Trimethyl chitosan chloride and flocculation of the wastewater in sugar refinery. *Journal of applied polymer science*, 116 (5): 2742-2748.

Liang, Z., Wang, Y., Zhou, Y. and Liu, H. 2009. Coagulation removal of melanoidins from biologically treated molasses wastewater using ferric chloride. *Chemical engineering journal*, 152 (1): 88-94.

Lopus, S. E., Bachand, P. A. M., Heyvaert, A. C., Werner, I., Teh, S. J. and Reuter, J. E. 2009. Potential toxicity concerns from chemical coagulation treatment of stormwater in the Tahoe basin, California, USA. *Ecotoxicology and environmental safety*, 72 (7): 1933-1941.

Lukum, A. and Djafar, F. 2012. Application of chitosan from peneaus monodon as coagulant of Pb(II) in waste water from tolangohula sugar factory kabupaten gorontalo. *Indonesian journal of chemistry*, 3 (12): 297-301.

Masondo, S. 2011. Water crisis by 2020. *Times Live,* 14-February-2011. Available: http://www.timeslive.co.za/local/article913892.ece/Water-crisis-by-2020 (Accessed 17-April-2013).

Matilainen, A., Vepsäläinen, C. and Sillanpää, M. 2010. Natural organic matter removal by coagulation during drinking water treatment: A review. *Advances in Colloid and Interface Science*, 159 (2): 189–197.

McDaniel, W. R. and Ankenman, B. E. 2000. Comparing experimental design strategies for quality improvement with minimal changes to factor levels. *Quality and Reliability Engineering International*, 16: 355-362.

Miller, M. 2013. *Coagulation and flocculation in water and wastewater treatment*. Available: http://www.iwawaterwiki.org/xwiki/bin/view/Articles/CoagulationandFlocculationinWaterandWastewaterTreatment (Accessed 08-June-2013).

Montgomery, D. C. 1997. *Design and analysis of experiments*. 4th ed. Hoboken: NJ: John Wiley & Sons, Inc.

Montgomery, D. C. 2005. *Design and analysis of experiments*. 6th ed. Hoboken: NJ: John Wiley & Sons, Inc.

Montgomery, D. C. 2009. *Design and analysis of experiments*. 7th ed. Hoboken: NJ: John Wiley & sons (Asia) Pte Ltd.

Mutambanengwe, C., Oyekola, O., Togo, C. and Whiteley, C. G. 2008. *Production of enzymes for industrial wastewater treatment: Proof of concept and application to the textile dye industry*. Water Research Commission of South Africa (WRC). Report No 1541/1/08.

Myers, R. H., Mongomery, D. C. and Anderson-Cook, C. M. 2009. *Response surface methodology. Process and product optimization using designed experiments*. 3rd edition ed. Hoboken, New Jersey: John Wiley and Sons, Inc.

NIST/SEMATECH. 2012. *e-Handbook of statistical methods.* Available: http://www.itl.nist.gov/div898/handbook/pri/section3/pri3363.htm. (Accessed 7-February-2015)

Nozaic, D. J., Freese, S. D. and Thompson, P. 2001. Long term experience in the use of polymeric coagulants at Umgeni Water. *Water science and technology: Water supply*, 1 (1): 43–50.

Oelofse, S. 2014. *Food waste in SA - The magnitude, cost and impacts.* (Online). 2014. Available: www.saafost.org.za (Accessed 2-February-2015).

Osifo, P. O., Webster, A., van der Merwe, H., Neomagus, H. W. J. P., van der Gun, M. A. and Grant, D. M. 2008. The influence of the degree of cross-linking on the adsorption properties of chitosan beads. *Bioresource technology*, 99 (15): 7377-7382.

Pambi, R. L. L. and Musonge, P. 2014. Influence of effluent type on the performance of chitosan as a coagulant. *International journal of futuristic trends in engineering and technology*, 2(1):1-6.

Pambi R.L.L. and Musonge P. 2015. The efficiency of chitosan as a coagulant in the treatment of the effluents from the sugar industry. *Journal of polymers and materials*, 32(1):59-65.

Pan, J. R. S., Huang, C. P., Chen, S. C. and Chung, Y. C. 1999. Evaluation of a modified chitosan biopolymer for coagulation of colloidal particles. *Colloids surface A: Physicochemical and engineering aspects* 143 (3): 359-364.

Pant, D. and Adholeya, A. 2007. Biological approaches for treatment of distillery wastewater: A review. *Bioresource technology*, 98 (12): 2321-2334.

Purchase, B. S. 1996. *Disposal of liquid effluents from cane sugar factories*. Available: www.sasta.co.za/.../Factory/1996%20Purchase,%20Effluent%20disposal (Accessed 13-May-2013).

Qu, X. and Wu, C. F. J. 2005. One-factor-at-a-time designs of resolution V. *Journal of statistical planning and inference*, 131 (2): 407-416.

Ramjeawon, T. 2000. Cleaner production in Mauritian cane-sugar factories. *Journal of cleaner production*, 8(6): 503-510.

Rizzo, L., Lofrano, G. and Belgiorno, V. 2010. Olive mill and winery wastewaters pre-treatment by coagulation with chitosan. *Separation science and technology*, 45 (16): 2447-2452.

Robles-González, V., Galíndez-Mayer, J., Rinderknecht-Seijas, N. and Poggi-Varaldo, H. M. 2012. Treatment of mezcal vinasses: A review. *Journal of biotechnology*, 157 (4): 524-546.

Roussy, J., Van Vooren, M., Dempsey, B. A. and Guibal, E. 2005. Influence of chitosan characteristics on the coagulation and the flocculation of bentonite suspensions. *Water Research*, 39 (14): 3247-3258.

Sadighi, A. and Faramarzi, M. A. 2013. Congo red decolorization by immobilized laccase through chitosan nanoparticles on the glass beads. *Journal of the Taiwan institute of chemical engineers*, 44 (2): 156-162.

Safferman, S. I. 2010. *Fundamentals of coagulation and flocculation*. Available: http://www.waterworldce.com/courses/46/PDF/Fund%20of%20Coagulation.pdf (Accessed 23-November-2013).

Samuel, S. and Muthukkaruppan, S. M. 2011. Physico-Chemical Analysis of Sugar Mill Effluent, Contaminated Soil and its Effect on Seed Germination of Paddy (Oryza sativa L.). *International journal of pharmaceutical and biological archives,* 2 (5).

Sansalone, J. J. and Kim, J. Y. 2008. Suspended particle destabilization in retained urban stormwater as a function of coagulant dosage and redox conditions. *Water research*, 42 (4–5): 909-922.

SANS (South African National standards) 241-1: 2011. *Drinking Water (Online).* Available: www.ewisa.co.za/.../Session4.1.1_SANS241_Part1.pdf (Accessed 10-October-2014).

SASA (South African Sugar Association). 2014. Available: http://www.sasa.org.za/HomePage1.aspx (Accessed 16-February-2014).

Satyawali, Y. and Balakrishnan, M. 2008. Wastewater treatment in molasses-based alcohol distilleries for COD and color removal: A review. *Journal of Environmental Management,* 86 (3):481–497.

Sautour, M., Rouget, A., Dantigny, P., Divies, C. and Bensoussan, M. 2001. Application of Doehlert design to determine the combined effects of temperature, water activity and pH on conidial germination of Penicillium chrysogenum. *Journal of applied microbiology,* 91 (2001): 900-906.

Setthamongkol, P. and Salaenoi, J. 2012. Adsorption Capacity of Chitosan Beads in Toxic Solutions. *World academy of science, engineering and technology*, 6 (9): 161-166.

Siew-Teng Ong, Pei-Sin Keng, Wan-Tung Liw, Sheer- Leen Wan and Hung, Y.T. 2010. Photodegradation of Congo Red and Reactive Yellow 2 Using Immobilized TiO2 under sunlight Irradiation. *World applied sciences journal*, 9(3): 303-370.

Statease Inc. *Stat-ease handbook for experimenters* (Online). 2014. Available: www.statease.com (Accessed 15-July-2014).

Szugula, A., Guilbal, E., Palacin, M. A., Ruiz, M. and Sastre, A. M. 2009. Removal of an anionic dye (Acid Blue 92) by coagulation–flocculation using chitosan. *Journal of environmental management*, 90 (10): 2979–2986.

Szygula, A., Guilbal, E., Palacin, M. A., Ruiz, M. and Sastre, A. M. 2009. Removal of an anionic dye (Acid Blue 92) by coagulation–flocculation using chitosan. *Journal of environmental management*, 90 (10): 2979–2986.

Tokumura, M., Znad, H. T. and Kawase, Y. 2008. Decolorization of dark brown colored coffee effluent by solar photo-Fenton reaction: Effect of solar light dose on decolorization kinetics. *Water research*, 42 (18): 4665-4673.

Trinh, T. K. and Kang, L. S. 2011. Response surface methodological approach to optimize the coagulation–flocculation process in drinking water treatment. *Chemical engineering research and design*, 89 (7): 1126-1135.

Tzoupanos, N. D. and Zouboulis, A. I. 2008. Coagulation-flocculation processes in water/wastewater treatment: The application of new generation of chemical reagents. Paper presented at the *6th IASME/WSEAS International conference on heat transfer, thermal engineering and environment (hte'08)*. Rhodes, Greece, August 20-22, 2008.

Vijayaraghavan, G., Sivakumar, T. and Vimal Kumar, A. 2011. Application of plant based coagulants for waste water treatment. *International journal of advanced engineering research and studies*, 1 (1): 88-92.

Wadley, S. and Buckley, C. A. 1991. *Recovery of sugar refinery ion-exchange regeneration effluent by nanofiltration*. Available: www.ewisa.co.za/literature/files/1991%20-%2045.pdf (Accessed 27-October-2013).

Wahid, Z. and Nadir, N. 2013. Improvement of one factor at a time through design of experiments. *World applied sciences journal (Mathematical applications in engineering)*, 21: 56-61.

Wan Ngah, W. S., Hanafiah, M. A. K. M. and Yong, S. S. 2008. Adsorption of humic acid from aqueous solutions on crosslinked chitosan–epichlorohydrin beads: Kinetics and isotherm studies. *Colloids and surfaces B: Biointerfaces*, 65 (1): 18-24.

Zainal, Z., Hui, L. K., Hussein, M. Z., Abdullah, A. H. and Hamadneh, I. R. 2009. Characterization of TiO2–Chitosan/Glass photocatalyst for the removal of a monoazo dye via photodegradation–adsorption process. *Journal of hazardous materials*, 164 (1): 138-145.

Zemmouri, H., Kadouche, S., Lounici, H., Hadioui, M. and Mameri, N. 2011. Use of chitosan in coagulation flocculation of raw water of Keddara and Beni Amrane dams. *Water science and technology: Water supply* 11 (2): 202–210.

Zhang, J., Zhang, F., Luo, Y. and Yang, H. 2006. A preliminary study on cactus as coagulant in water treatment. *Process biochemistry* 41 (2006): 730-733.

Zhao, Y., Song, L. and Ong, S. L. 2010. Fouling of RO membranes by effluent organic matter (EfOM): Relating major components of EfOM to their characteristic fouling behaviors. *Journal of membrane science*, 349 (1–2): 75-82.

APPENDIX A: PRELIMINARY EXPERIMENTS

S.V. = solvent volume

I= initial

F= Final

AVRG= average

%C= Percentage change between the initial and the final value.

$$\%C = \left[{}^{(I-F)}\!/_{I} \right] \times 100 \quad \text{(A-1)}$$

Ctrl= control runs (Without coagulant)

%CC= Percentage change between the initial and the control run.

$$\%CC = \left[{}^{(I-CtrL)}\!/_{I} \right] \times 100 \quad \text{(A-2)}$$

Conc. = Concentration.

D.F.= Dilution fraction.

R1, R2, R3= Replicates

A-1. EXPERIMENTAL DATA FOR SOLVENT SELECTION

A-1.1. Control tests without chitosan coagulant

Table A-1: Resin effluent without coagulant.

	I	Ctrl	%CC	I	Ctrl	%CC	I	Ctrl	%CC	AVRG(%CC)
COD	12750	12750	0	12300	12270	0.24	11640	11640	0	0.08
TSS	1200	1179	1.75	789	782	0.89	479	4.76	99.01	33.88
Colour	2.816	2.801	0.53	2.551	2.522	1.14	2.337	2.332	0.21	0.63

Table A-2: Final effluent without coagulant.

	I	Ctrl	%CC	I	Ctrl	%CC	I	Ctrl	%CC	AVRG(%CC)
COD	1360	1340	1.47	7250	7250	0.00	5640	5660	-0.35	0.37
TSS	213	199	6.57	359	311	13.37	248	233	6.05	8.66
Colour	0.372	0.37	0.54	0.344	0.335	2.62	0.199	0.195	2.01	1.72

A-1.2. Raw data for resin effluent

Table A-3: Effect of Acetic acid (RE).

S.V.		Run 1 (R1)			Run 1 (R2)			Run 1 (R3)			AVRG (%C)
		I	F	%C	I	F	%C	I	F	%C	
1 ml	COD	12750	12270	3.76	12300	11610	5.61	11640	10770	7.47	5.62
	TSS	1200	870	27.50	789	569	27.88	479	387	19.21	24.86
	Colour	2.816	2.698	4.19	2.551	2.432	4.66	2.337	2.276	2.61	3.82
		Run 2 (R1)			Run 2 (R2)			Run 2 (R3)			AVRG (%C)
		I	F	%C	I	F	%C	I	F	%C	
5 ml	COD	12750	12060	5.41	12300	11220	8.78	11640	11370	2.32	5.50
	TSS	1200	688	42.67	789	457	42.08	479	284	40.71	41.82
	Colour	2.816	2.665	5.36	2.551	2.388	6.39	2.337	2.239	4.19	5.32
		Run 3 (R1)			Run 3 (R2)			Run 3 (R3)			AVRG (%C)
		I	F	%C	I	F	%C	I	F	%C	
10 ml	COD	12750	12480	2.12	12300	11880	3.41	11640	11670	-0.26	1.76
	TSS	1200	577	51.92	789	389	50.70	479	286	40.29	47.64
	Colour	2.816	2.588	8.10	2.551	2.354	7.72	2.337	2.201	5.82	7.21
		Run 4 (R1)			Run 4 (R2)			Run 4 (R3)			AVRG (%C)
		I	F	%C	I	F	%C	I	F	%C	
15 ml	COD	12750	12720	0.24	12300	12300	0.00	11640	11700	-0.52	-0.09
	TSS	1200	562	53.17	789	381	51.71	479	265	44.68	49.85
	Colour	2.816	2.559	9.13	2.551	2.322	8.98	2.337	2.17	7.15	8.42
		Run 5 (R1)			Run 5 (R2)			Run 5 (R3)			AVRG (%C)
		I	F	%C	I	F	%C	I	F	%C	
20 ml	COD	12750	12840	-0.71	12300	12360	-0.49	11640	11790	-1.29	-0.83
	TSS	1200	511	57.42	789	354	55.13	479	239	50.10	54.22
	Colour	2.816	2.519	10.55	2.551	2.301	9.80	2.337	2.158	7.66	9.34

Table A-4: Effect of Hydrochloric acid (RE).

S.V.		Run 1 (R1)			Run 1 (R2)			Run 1 (R3)			AVRG (%C)
		I	F	%C	I	F	%C	I	F	%C	
1 ml	COD	12750	11070	13.18	12300	10530	14.39	11640	10740	7.73	11.77
	TSS	1200	876	27.00	789	599	24.08	479	401	16.28	22.46
	Colour	2.816	2.683	4.72	2.551	2.465	3.37	2.337	2.286	2.18	3.43
		Run 2 (R1)			Run 2 (R2)			Run 2 (R3)			AVRG (%C)
		I	F	%C	I	F	% C	I	F	% C	
5 ml	COD	12750	11670	8.47	12300	11130	9.51	11640	11130	4.38	7.45
	TSS	1200	683	43.08	789	487	38.28	479	271	43.42	41.59
	Colour	2.816	2.655	5.72	2.551	2.428	4.82	2.337	2.261	3.25	4.60
		Run 3 (R1)			Run 3 (R2)			Run 3 (R3)			AVRG (%C)
		I	F	%C	I	F	%C	I	F	%C	
10 ml	COD	12750	11910	6.59	12300	11730	4.63	11640	11370	2.32	4.51
	TSS	1200	569	52.58	789	388	50.82	479	264	44.89	49.43
	Colour	2.816	2.557	9.20	2.551	2.341	8.23	2.337	2.203	5.73	7.72
		Run 4 (R1)			Run 4 (R2)			Run 4 (R3)			AVRG (%C)
		I	F	%C	I	F	%C	I	F	%C	
15 ml	COD	12750	12210	4.24	12300	11910	3.17	11640	11700	-0.52	2.30
	TSS	1200	549	54.25	789	375	52.47	479	245	48.85	51.86
	Colour	2.816	2.531	10.12	2.551	2.321	9.02	2.337	2.15	8.00	9.05
		Run 5 (R1)			Run 5 (R2)			Run 5 (R3)			AVRG (%C)
		I	F	%C	I	F	%C	I	F	%C	
20 ml	COD	12750	12300	3.53	12300	11670	5.12	11640	11400	2.06	3.57
	TSS	1200	480	60.00	789	296	62.48	479	219	54.28	58.92
	Colour	2.816	2.445	13.17	2.551	2.143	15.99	2.337	2.091	10.53	13.23

A-1.3. Raw data for final effluent

Table A-5: Effect of Acetic acid (FE).

S.V.		Run 1 (R1)			Run 1 (R2)			Run 1 (R3)			AVRG (%C)
		I	F	%C	I	F	%C	I	F	%C	
1 ml	COD	1360	1350	0.74	7250	7220	0.41	5640	5650	-0.18	0.32
	TSS	213	191	10.33	359	307	14.48	248	229	7.66	10.82
	Colour	0.372	0.355	4.57	0.344	0.329	4.36	0.199	0.191	4.02	4.32
		Run 1 (R1)			Run 1 (R2)			Run 1 (R3)			AVRG (%C)
		I	F	%C	I	F	%C	I	F	%C	
5 ml	COD	1360	1350	0.74	7250	7230	0.28	5640	5620	0.35	0.46
	TSS	213	128	39.91	359	184	48.75	248	125	49.60	46.08
	Colour	0.372	0.347	6.72	0.344	0.316	8.14	0.199	0.182	8.54	7.80
		Run 1 (R1)			Run 1 (R2)			Run 1 (R3)			AVRG (%C)
		I	F	%C	I	F	%C	I	F	%C	
10 ml	COD	1360	1380	-1.47	7250	7270	-0.28	5640	5660	-0.35	-0.70
	TSS	213	116	45.54	359	170	52.65	248	119	52.02	50.07
	Colour	0.372	0.334	10.22	0.344	0.296	13.95	0.199	0.163	18.09	14.09
		Run 1 (R1)			Run 1 (R2)			Run 1 (R3)			AVRG (%C)
		I	F	%C	I	F	%C	I	F	%C	
15 ml	COD	1360	1410	-3.68	7250	8220	-13.38	5640	6230	-10.46	-9.17
	TSS	213	110	48.36	359	169	52.92	248	118	52.42	51.23
	Colour	0.372	0.341	8.33	0.344	0.312	9.30	0.199	0.177	11.06	9.56
		Run 1 (R1)			Run 1 (R2)			Run 1 (R3)			AVRG (%C)
		I	F	%C	I	F	%C	I	F	%C	
20 ml	COD	1360	1580	-16.18	7250	9050	-24.83	5640	6810	-20.74	-20.58
	TSS	213	93	56.34	359	106	70.47	248	83	66.53	64.45
	Colour	0.372	0.336	9.68	0.344	0.302	12.21	0.199	0.169	15.08	12.32

Table A-6: effect of Hydrochloric acid (FE).

S.V.		Run 1 (R1)			Run 1 (R2)			Run 1 (R3)			AVRG (%C)
		I	F	%C	I	F	%C	I	F	%C	
1 ml	COD	1360	1330	2.21	7250	7220	0.41	5640	5630	0.18	0.93
	TSS	213	193	9.39	359	320	10.86	248	213	14.11	11.46
	Colour	0.372	0.36	3.23	0.344	0.326	5.23	0.199	0.188	5.53	4.66
		Run 2 (R1)			Run 2 (R2)			Run 2 (R3)			AVRG (%C)
		I	F	%C	I	F	%C	I	F	%C	
5 ml	COD	1360	1290	5.15	7250	7010	3.31	5640	5470	3.01	3.82
	TSS	213	125	41.31	359	191	46.80	248	123	50.40	46.17
	Colour	0.372	0.343	7.80	0.344	0.309	10.17	0.199	0.181	9.05	9.01
		Run 3 (R1)			Run 3 (R2)			Run 3 (R3)			AVRG (%C)
		I	F	%C	I	F	%C	I	F	%C	
10 ml	COD	1360	1250	8.09	7250	6680	7.86	5640	5250	6.91	7.62
	TSS	213	110	48.36	359	171	52.37	248	115	53.63	51.45
	Colour	0.372	0.331	11.02	0.344	0.301	12.50	0.199	0.173	13.07	12.20
		Run 4 (R1)			Run 4 (R2)			Run 4 (R3)			AVRG (%C)
		I	F	%C	I	F	%C	I	F	%C	
15 ml	COD	1360	1380	-1.47	7250	7590	-4.69	5640	5960	-5.67	-3.94
	TSS	213	100	53.05	359	154	57.10	248	104	58.06	56.07
	Colour	0.372	0.325	12.63	0.344	0.3	12.79	0.199	0.168	15.58	13.67
		Run 5 (R1)			Run 5 (R2)			Run 5 (R3)			AVRG (%C)
		I	F	%C	I	F	%C	I	F	%C	
20 ml	COD	1360	1600	-17.65	7250	8170	-12.69	5640	6510	-15.43	-15.25
	TSS	213	84	60.56	359	111	69.08	248	79	68.15	65.93
	Colour	0.372	0.314	15.59	0.344	0.299	13.08	0.199	0.17	14.57	14.42

A-2. EXPERIMENTAL DATA FOR COAGULANT LOADING

A-2.1. Data for resin effluent

Table A-7: Coagulant loading for RE.

Conc.		Run 1 (R1)			Run 1 (R2)			Run 1 (R3)			AVRG (%C)
		I	F	%C	I	F	%C	I	F	%C	
56.6 mg/l	COD	9000	8980	0.22	9000	8900	1.11	9000	8970	0.33	0.56
	TSS	1024	514	49.80	1024	472	53.91	1024	483	52.83	52.18
	Colour	2.902	2.449	15.61	2.902	2.436	16.06	2.902	2.436	16.06	15.91
138 mg/l		Run 2 (R1)			Run 2 (R2)			Run 2 (R3)			AVRG (%C)
		I	F	%C	I	F	%C	I	F	%C	
	COD	16500	14160	14.18	16500	14670	11.09	16500	13230	19.82	15.03
	TSS	1103	341	69.08	1103	406	63.19	1103	312	71.71	68.00
	Colour	2.713	1.886	30.48	2.713	1.933	28.75	2.713	1.877	30.81	30.02
192.31 mg/l		Run 3 (R1)			Run 3 (R2)			Run 3 (R3)			AVRG (%C)
		I	F	%C	I	F	%C	I	F	%C	
	COD	14120	13110	7.15	14120	13150	6.87	14120	13130	7.01	7.01
	TSS	1067	299.2	71.96	1067	350	67.20	1067	324.6	69.58	69.58
	Colour	2.709	2.271	16.17	2.709	2.3	15.10	2.709	2.2855	15.63	15.63
385 mg/l		Run 4 (R1)			Run 4 (R2)			Run 4 (R3)			AVRG (%C)
		I	F	%C	I	F	%C	I	F	%C	
	COD	12600	11910	5.48	12600	11890	5.63	12600	11870	5.79	5.63
	TSS	1155	602	47.88	1155	589	49.00	1155	601	47.97	48.28
	Colour	3.025	2.7	10.74	3.025	2.806	7.24	3.025	2.799	7.47	8.48

A-2.2. Data for final effluent

Table A-8: Coagulant loading for (FE).

S.V.	Run 1 (R1)				Run 1 (R2)			AVRG (%C)
		I	F	%C	I	F	%C	
3.7 mg/l	COD	4630	3050	34.13	1570	910	42.04	38.08
	TSS	100	22	78.00	129	25	80.62	79.31
	Colour	0.128	0.08	37.50	0.21	0.113	46.19	41.85
	Run 2 (R1)				Run 2 (R2)			AVRG (%C)
		I	F	%C	I	F	%C	
7.41 mg/l	COD	4630	3120	32.61	1570	990	36.94	34.78
	TSS	100	5	95.00	129	2	98.45	96.72
	Colour	0.128	0.052	59.38	0.21	0.077	63.33	61.35
	Run 3 (R1)				Run 3 (R2)			AVRG (%C)
		I	F	%C	I	F	%C	
14.81 mg/l	COD	4630	3860	16.63	1570	1250	20.38	18.51
	TSS	100	11	89.00	129	10	92.25	90.62
	Colour	0.128	0.058	54.69	0.21	0.085	59.52	57.11
	Run 4 (R1)				Run 4 (R2)			AVRG (%C)
		I	F	%C	I	F	%C	
29.63 mg/l	COD	4630	3940	14.90	1570	1380	12.10	13.50
	TSS	100	15	85.00	129	18	86.05	85.52
	Colour	0.128	0.057	55.47	0.21	0.095	54.76	55.12
	Run 5 (R1)				Run 5 (R2)			AVRG (%C)
		I	F	%C	I	F	%C	
44.44 mg/l	COD	4630	4410	4.75	1570	1470	6.37	5.56
	TSS	100	21	79.00	129	25	80.62	79.81
	Colour	0.128	0.078	39.06	0.21	0.119	43.33	41.20
	Run 5 (R1)				Run 5 (R2)			AVRG (%C)
		I	F	%C	I	F	%C	
59.26 mg/l	COD	4630	4520	2.38	1570	1500	4.46	3.42
	TSS	100	35	65.00	129	38	70.54	67.77
	Colour	0.128	0.1	21.88	0.21	0.145	30.95	26.41
	Run 5 (R1)				Run 5 (R2)			AVRG (%C)
		I	F	%C	I	F	%C	
74.1 mg/l	COD	4630	4590	0.86	1570	1580	-0.64	0.11
	TSS	100	37	63.00	129	43	66.67	64.83
	Colour	0.128	0.113	11.72	0.21	0.175	16.67	14.19

A-3. EXPERIMENTAL DATA FOR pH

A-3.1. Experiments with Resin effluent

Table A-9: Raw data for adjusted pH (RE).

pH		Run 1 (R1)			Run 1 (R2)			Run 1 (R3)			AVRG (%C)
		I	F	%C	I	F	%C	I	F	%C	
4	COD	9840	8440	14.23	9840	8500	13.62	9840	8470	13.92	13.92
	TSS	1007	226	77.56	1007	230	77.16	1007	228	77.36	77.36
	Colour	2.859	2.308	19.27	2.859	2.312	19.13	2.859	2.31	19.20	19.20
		Run 2 (R1)			Run 2 (R2)			Run 2 (R3)			AVRG (%C)
		I	F	%C	I	F	%C	I	F	%C	
	COD	10850	9300	14.29	10850	9310	14.19	10850	9305	14.24	14.24
	TSS	914	289	68.38	914	302	66.96	914	295.5	67.67	67.67
5	Colour	2.748	2.473	10.01	2.748	2.5	9.02	2.75	2.487	9.52	9.52
		Run 3 (R1)			Run 3 (R2)			Run 3 (R3)			AVRG (%C)
		I	F	%C	I	F	% C	I	F	%C	
	COD	10500	9670	7.90	10500	9660	8.00	5640	5250	6.91	7.61
	TSS	1067	545	48.92	1067	566	46.95	248	115	53.63	49.84
6	Colour	2.746	2.573	6.30	2.746	2.574	6.26	0.199	0.173	13.07	8.54
		Run 4 (R1)			Run 4 (R2)			Run 4 (R3)			AVRG (%C)
		I	F	%C	I	F	%C	I	F	%C	
	COD	10450	10410	0.38	10450	10400	0.48	10450	10405	0.43	0.43
	TSS	1067	675	36.74	1067	677	36.55	1067	676	36.64	36.64
7	Colour	2.777	2.601	6.34	2.777	2.635	5.11	2.777	2.618	5.73	5.73
		Run 5 (R1)			Run 5 (R2)			Run 5 (R3)			AVRG (%C)
		I	F	%C	I	F	%C	I	F	%C	
8	COD	10500	10470	0.29	10500	10510	-0.10	10500	10490	0.10	0.10
	TSS	1067	1064	0.28	1067	1067	0.00	1067	1066	0.14	0.14
	Colour	2.782	2.779	0.11	2.782	2.781	0.04	2.782	2.78	0.07	0.07
		Run 5 (R1)			Run 5 (R2)			Run 5 (R3)			AVRG (%C)
		I	F	%C	I	F	%C	I	F	%C	
9	COD	10500	10490	0.10	10500	10500	0.00	10500	10490	0.10	0.06
	TSS	1067	1067	0.00	1067	1067	0.00	1067	1067	0.00	0.00
	Colour	2.779	2.777	0.07	2.779	2.782	-0.11	2.779	2.78	-0.02	-0.02

Table A-9 (continuous).

pH		Run 1 (R1)			Run 1 (R2)			Run 1 (R3)			AVRG (%C)
		I	F	%C	I	F	%C	I	F	%C	
10	COD	10490	10510	-0.19	10490	10480	0.10	10490	10495	-0.05	-0.05
	TSS	1067	1067	0.00	1067	1067	0.00	1067	1067	0.00	0.00
	Colour	2.801	2.799	0.07	2.801	2.8	0.04	2.801	2.798	0.11	0.07

Table A-10: Raw data for natural pH (RE).

pH		Run 1 (R1)			Run 1 (R2)			Run 1 (R3)			AVRG (%C)
		I	F	%C	I	F	%C	I	F	%C	
7	COD	11510	10910	5.21	11510	10890	5.39	11510	10900	5.30	5.30
	TSS	946	323	65.86	946	411	56.55	946	315	66.70	63.04
	Colour	1.998	1.685	15.67	1.998	1.702	14.81	1.998	1.701	14.86	15.12
		Run 2 (R1)			Run 2 (R2)			Run 2 (R3)			AVRG (%C)
		I	F	%C	I	F	%C	I	F	%C	
	COD	12300	11820	3.90	12300	11690	4.96	12300	11800	4.07	4.31
	TSS	1154	431	62.65	1154	471	59.19	1154	470	59.27	60.37
8	Colour	3.187	2.711	14.94	3.187	2.831	11.17	3.19	2.773	12.99	13.03
		Run 3 (R1)			Run 3 (R2)			Run 3 (R3)			AVRG (%C)
		I	F	%C	I	F	% C	I	F	%C	
	COD	17640	17200	2.49	17640	17400	1.36	17640	17200	2.49	2.12
	TSS	1470	667	54.63	1470	637	56.67	1470	601	59.12	56.80
9	Colour	2.896	2.573	11.15	2.896	2.534	12.50	2.896	2.533	12.53	12.06
		Run 4 (R1)			Run 4 (R2)			Run 4 (R3)			AVRG (%C)
		I	F	%C	I	F	%C	I	F	%C	
	COD	9870	9670	2.03	9870	9710	1.62	9870	9660	2.13	1.93
	TSS	1440	675	53.13	1440	677	52.99	1440	677	52.99	53.03
10	Colour	3.009	2.702	10.20	3.009	2.635	12.43	3.009	2.667	11.37	11.33

A-3.2. Experiments with final effluent

Table A-11: Raw data for adjusted pH (FE).

pH	Run 1 (R1)				Run 1 (R2)			Run 1 (R3)			AVRG (%C)
		I	F	%C	I	F	%C	I	F	%C	
4	COD	4700	4170	11.28	4700	4160	11.49	4700	4165	11.38	11.38
	TSS	107	3	97.20	107	4	96.26	107	3.5	96.73	96.73
	Colour	0.277	0.031	88.81	0.277	0.033	88.09	0.277	0.032	88.45	88.45
	Run 2 (R1)				Run 2 (R2)			Run 2 (R3)			AVRG (%C)
		I	F	%C	I	F	%C	I	F	%C	
	COD	4640	4140	10.78	4640	4110	11.42	4640	4125	11.10	11.10
	TSS	107	2	98.13	107	2	98.13	107	2	98.13	98.13
5	Colour	0.281	0.038	86.48	0.281	0.04	85.77	0.28	0.039	86.12	86.12
	Run 3 (R1)				Run 3 (R2)			Run 3 (R3)			AVRG (%C)
		I	F	%C	I	F	%C	I	F	%C	
	COD	4690	4220	10.02	4690	4250	9.38	4690	4235	9.70	9.70
	TSS	107	2	98.13	107	2	98.13	107	2	98.13	98.13
6	Colour	0.295	0.044	85.08	0.295	0.042	85.76	0.295	0.043	85.42	85.42
	Run 4 (R1)				Run 4 (R2)			Run 4 (R3)			AVRG (%C)
		I	F	%C	I	F	%C	I	F	%C	
	COD	4670	4230	9.42	4670	4230	9.42	4670	4230	9.42	9.42
	TSS	107	3	97.20	107	4	96.26	107	3.5	96.73	96.73
7	Colour	0.318	0.041	87.11	0.318	0.046	85.53	0.318	0.044	86.32	86.32
	Run 5 (R1)				Run 5 (R2)			Run 5 (R3)			AVRG (%C)
8		I	F	%C	I	F	%C	I	F	%C	
	COD	4670	4410	5.57	4670	4420	5.35	4670	4480	4.07	5.00
	TSS	107	5	95.33	107	3	97.20	107	8	92.52	95.02
	Colour	0.318	0.055	82.70	0.318	0.043	86.48	0.318	0.042	86.79	85.32
	Run 5 (R1)				Run 5 (R2)			Run 5 (R3)			AVRG (%C)
9		I	F	%C	I	F	%C	I	F	%C	
	COD	4690	5090	-8.53	4690	5020	-7.04	4690	4970	-5.97	-7.18
	TSS	107	13	87.85	107	15	85.98	107	13	87.85	87.23
	Colour	0.351	0.088	74.93	0.351	0.081	76.92	0.351	0.08	77.21	76.35

Table A-11 (continuous).

pH		Run 1 (R1)			Run 1 (R2)			Run 1 (R3)			AVRG (%C)
		I	F	%C	I	F	%C	I	F	%C	
10	COD	4690	5250	-11.94	4690	5270	-12.37	4690	5260	-12.15	-12.15
	TSS	107	16	85.05	107	18	83.18	107	17	84.11	84.11
	Colour	0.351	0.095	72.93	0.351	0.091	74.07	0.351	0.093	73.50	73.50

Table A-12: Raw data for natural pH (FE).

pH		Run 1 (R1)			Run 1 (R2)			Run 1 (R3)			AVRG (%C)
		I	F	%C	I	F	%C	I	F	%C	
7	COD	3590	3270	8.91	3590	3260	9.19	3590	3240	9.75	9.29
	TSS	100	3	97.00	100	3	97.00	100	2	98.00	97.33
	Colour	0.412	0.053	87.14	0.412	0.051	87.62	0.412	0.051	87.62	87.46
		Run 2 (R1)			Run 2 (R2)			Run 2 (R3)			AVRG (%C)
		I	F	%C	I	F	%C	I	F	%C	
	COD	5190	4610	11.18	5190	4780	7.90	5190	4780	7.90	8.99
	TSS	120	4	96.67	120	5	95.83	120	3	97.50	96.67
8	Colour	0.522	0.071	86.40	0.522	0.084	83.91	0.52	0.075	85.63	85.31
		Run 3 (R1)			Run 3 (R2)			Run 3 (R3)			AVRG (%C)
		I	F	%C	I	F	% C	I	F	%C	
	COD	4650	4350	6.45	4650	4410	5.16	4650	4380	5.81	5.81
	TSS	107	6	94.39	107	5	95.33	107	5.5	94.86	94.86
8.5	Colour	0.32	0.051	84.06	0.32	0.049	84.69	0.32	0.05	84.38	84.38

A-4. EXPERIMENTAL DATA FOR CONCENTRATION OF IMPURITIES

A-4.1. Data for resin effluent

Table A-13: Experimental data for impurities concentration (RE).

D.F.		Run 1 (R1)			Run 1 (R2)			Run 1 (R3)			AVRG (%C)
		I	F	%C	I	F	%C	I	F	%C	
1	COD	9000	9060	-0.67	9000	8980	0.22	9000	8900	1.11	0.22
	TSS	1024	489	52.25	1024	514	49.80	1024	472	53.91	51.99
	Colour	2.902	2.515	13.34	2.902	2.449	15.61	2.902	2.436	16.06	15.00
		Run 2 (R1)			Run 2 (R2)			Run 2 (R3)			AVRG (%C)
		I	F	%C	I	F	%C	I	F	%C	
	COD	4980	4050	18.67	4980	4260	14.46	4980	4200	15.66	16.27
	TSS	572	160	72.03	572	163	71.50	572	155	72.90	72.14
1/2	Colour	2.465	1.286	47.83	2.465	1.407	42.92	2.47	1.335	45.84	45.53
		Run 3 (R1)			Run 3 (R2)			Run 3 (R3)			AVRG (%C)
		I	F	%C	I	F	% C	I	F	%C	
	COD	2970	2820	5.05	2970	2790	6.06	2970	2820	5.05	5.39
	TSS	348	71	79.60	348	73	79.02	348	71	79.60	79.41
1/4	Colour	2.26	0.886	60.80	2.26	0.854	62.21	2.26	0.833	63.14	62.05
		Run 4 (R1)			Run 4 (R2)			Run 4 (R3)			AVRG (%C)
		I	F	%C	I	F	%C	I	F	%C	
	COD	1230	1410	-14.63	1230	1350	-9.76	1230	1320	-7.32	-10.57
	TSS	167	210	-25.75	167	186	-11.38	167	191	-14.37	-17.17
1/8	Colour	1.327	1.213	8.59	1.327	1.155	12.96	1.327	1.174	11.53	11.03

A-4.2. Data for final effluent

Table A-14: Experimental data for impurities concentration (FE).

D.F.		Run 1 (R1)			Run 1 (R2)			Run 1 (R3)			AVRG (%C)
		I	F	%C	I	F	%C	I	F	%C	
1	COD	8530	10240	-20.05	8530	10210	-19.70	8530	10240	-20.05	-19.93
	TSS	591	219	62.94	591	221	62.61	591	223	62.27	62.61
	Colour	0.903	0.804	10.96	0.903	0.801	11.30	0.903	0.811	10.19	10.82
1/2		Run 2 (R1)			Run 2 (R2)			Run 2 (R3)			AVRG (%C)
		I	F	%C	I	F	%C	I	F	%C	
	COD	4310	5250	-21.81	4310	5200	-20.65	4310	5270	-22.27	-21.58
	TSS	300	237	21.00	300	242	19.33	300	232	22.67	21.00
	Colour	0.644	0.605	6.06	0.644	0.593	7.92	0.64	0.602	6.52	6.83
1/4		Run 3 (R1)			Run 3 (R2)			Run 3 (R3)			AVRG (%C)
		I	F	%C	I	F	% C	I	F	%C	
	COD	2140	3010	-40.65	2140	3050	-42.52	2140	3000	-40.19	-41.12
	TSS	165	187	-13.33	165	185	-12.12	165	185	-12.12	-12.53
	Colour	0.405	0.408	-0.74	0.405	0.405	0.00	0.405	0.407	-0.49	-0.41
1/8		Run 4 (R1)			Run 4 (R2)			Run 4 (R3)			AVRG (%C)
		I	F	%C	I	F	%C	I	F	%C	
	COD	1070	1600	-49.53	1070	1590	-48.60	1070	1600	-49.53	-49.22
	TSS	93	120	-29.03	93	125	-34.41	93	122	-31.18	-31.54
	Colour	0.224	0.233	-4.02	0.224	0.229	-2.23	0.224	0.231	-3.13	-3.13

A-4.2.4 Data for RE experiments at MC

When RE was diluted to MC, the optimum range for the coagulant loading in terms of TSS, and colour removal was found to be between 0.06 to 0.07g/l; while the COD removal was at its best between 0.04 to 0.06g/l. High of coagulant decreased the sample final pH and increases the COD due to high organic content of chitosan.

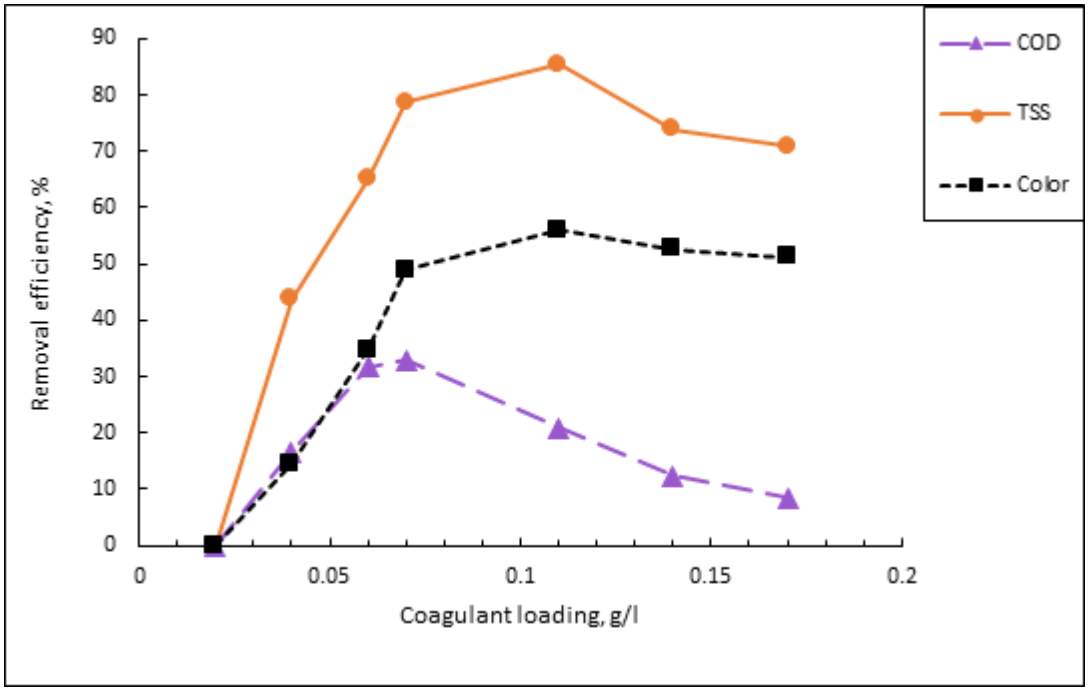

Figure A-1: Effect of the coagulant dosage on TSS, COD and colour removal for RE at medium concentration.

At 0.07 g/l, the CCo removed 85% TSS removal, 56% colour and 21% COD.

Table A-15: Raw data for the effect of coagulant for RE at medium concentration.

Runs	Coagulant loading (R1)											
Variables	Initial (0 mg/l)	4 mg/l	8 mg/l	12 mg/l	16 mg/l	20 mg/l	38 mg/l	57 mg/l	74 mg/l	107 mg/l	138 mg/l	167 mg/l
pH	6.72	6.46	6.38	6.31	6.15	6.05	5.38	5.24	5	4.46	4.36	4.25
COD	5420	5390	5340	5200	4750	4410	3560	3660	4360	4930	5010	5300
TSS	441	360	351	331	273	250	155	106	74	125	134	135
Color	2.29	2.289	2.276	2.191	2.031	1.896	1.464	1.217	1.033	1.133	1.152	1.183
	% change R 1											
	Initial (0 mg/l)	4 mg/l	8 mg/l	12 mg/l	16 mg/l	20 mg/l	38 mg/l	57 mg/l	74 mg/l	107 mg/l	138 mg/l	167 mg/l
pH	0	3.87	5.06	6.10	8.48	9.97	19.94	22.02	25.60	33.63	35.12	36.76
COD	0	0.55	1.48	4.06	12.36	18.63	34.32	32.47	19.56	9.04	7.56	2.21
TSS	0	18.37	20.41	24.94	38.10	43.31	64.85	75.96	83.22	71.66	69.61	69.39
Color	0	0.04	0.61	4.32	11.31	17.21	36.07	46.86	54.89	50.52	49.69	48.34
Runs	Coagulant loading (R2)											
Variables	Initial (0 mg/l)	4 mg/l	8 mg/l	12 mg/l	16 mg/l	20 mg/l	38 mg/l	57 mg/l	74 mg/l	107 mg/l	138 mg/l	167 mg/l
pH	8.01	7.69	7.54	7.53	7.5	7.31	6.95	6.44	6.18	5.77	5.43	5.31
COD	4750	4710	4620	4510	4370	4060	3370	3160	3700	4000	4300	4550
TSS	655	512	499	472	402	366	228	122	81	155	183	187
Color	2.578	2.571	2.554	2.475	2.357	2.272	1.713	1.268	1.103	1.171	1.221	1.255
	% change R 2											
	Initial (0 mg/l)	4 mg/l	8 mg/l	12 mg/l	16 mg/l	20 mg/l	38 mg/l	57 mg/l	74 mg/l	107 mg/l	138 mg/l	167 mg/l
pH	0	4.00	5.87	5.99	6.37	8.74	13.23	19.60	22.85	27.97	32.21	33.71
COD	0	0.84	2.74	5.05	8.00	14.53	29.05	33.47	22.11	15.79	9.47	4.21
TSS	0	21.83	23.82	27.94	38.63	44.12	65.19	81.37	87.63	76.34	72.06	71.45
Color	0	0.27	0.93	4.00	8.57	11.87	33.55	50.81	57.21	54.58	52.64	51.32

A-5. ADDITIONAL EXPERIMENTS

A-5.1. Effect of heat on coagulant efficiency

The dissolution of the chitosan in HCl at room temperature had two inconveniences: It took longer to dissolve compared to AA and the dissolution was not complete. A similar observation was made by Divakaran and Sivasankara Pillai (2001) who also reported the presence of thin gels after dissolving the chitosan in HCl for an hour, which indicates inadequate dissolution of the chitosan. The effect of temperature was investigated during the coagulation preparation stage. 1g of chitosan was dissolved in 20ml HCl and stirred for an hour to make the cold CCo in HCl (CCH). A portion of the chitosan-acid mixture was heated to 50℃ using a magnetic stirrer with a hot-plate. Once the solution reached 50℃. The experiments proceeded as mentioned in chapter 4.

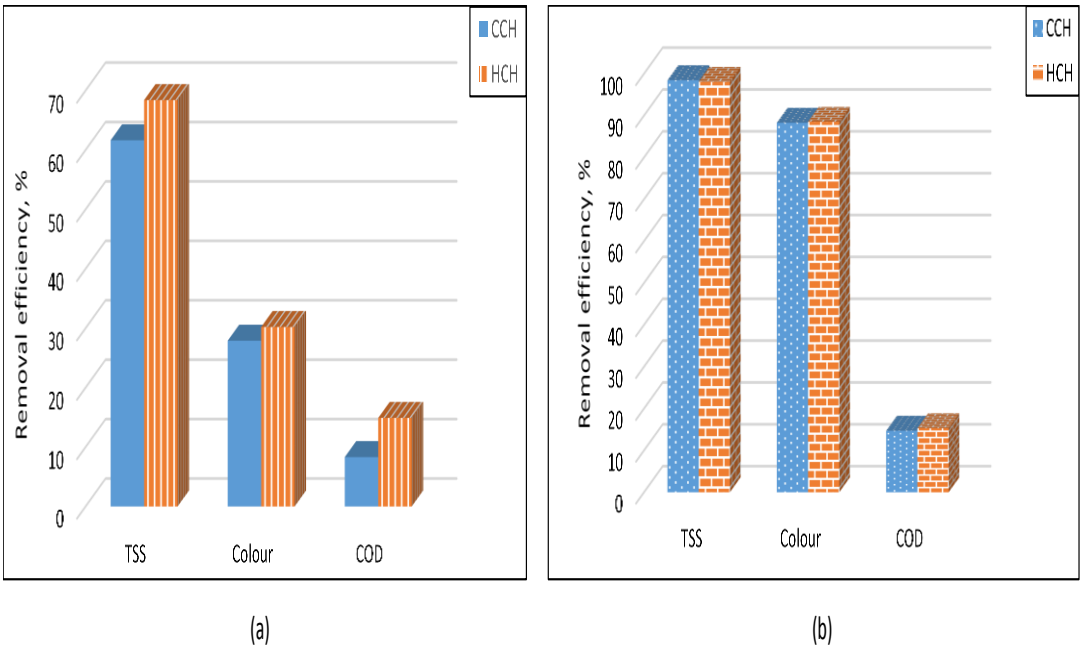

Figure A-2: Influence of preparation temperature on the impurities removal on (a) RE and (b) FE.

In the case of the RE (Fig. A-2a), the addition of heat improved the dissolution of chitosan in acid by shortening the dissolution time. It also improve the efficiency of the coagulant as seen in Figure A-2a. The TSS removal increase by 6.77%, the colour

and the COD removal efficiency improved by an additional 2.31% and 6.6% respectively. The influence of temperature on the FE was negligible.

The main advantage of adding heat in the preparation stage was the fact that chitosan dissolved faster.

Table A-16: Raw data for the effect of temperature for RE.

Factor	R 1					Average	
	Initial	CCH	% decrease	HCH	% decrease	CCH	HCH
TSS	864	345	60.07	279	67.71	61.63	68.40
Colour	2.255	1.67	25.94	1.58	29.93	27.90	30.21
COD	14840	13740	7.41	12520	15.63	8.31	14.91
Factor	R 2						
	Initial	CCH	% decrease	HCH	% decrease		
TSS	1103	406	63.19	341	69.08		
Colour	2.713	1.903	29.86	1.886	30.48		
COD	16500	14980	9.21	14160	14.18		

Table A-17: Raw data for the effect of temperature for FE.

Factor	R 1						
	Initial	CCH	% decrease	HCH	% decrease	CCH	HCH
TSS	129	2	98.45	2	98.45	98.45	98.06
Colour	0.209	0.027	87.08	0.024	88.52	88.28	88.52
COD	1700	1440	15.29	1440	15.29	14.71	15.29
Factor	R 2						
	Initial	CCH	% decrease	HCH	% decrease		
TSS	129	2	98.45	3	97.67		
Colour	0.209	0.022	89.47	0.024	88.52		
COD	1700	1460	14.12	1440	15.29		

A-5.2. Investigation of the coagulant shelf-life

The coagulant shelf-life was investigated using 136 mg/l of HCH for RE and 7.41 mg/l for FE. For the treatment of RE, the coagulant was used for up to 5 days without a major decrease on its efficiency (less than 5% decrease in efficiency). The efficiency begin to decrease considerably after using CCo conserved for 7 days, reaching the lowest percentage removal at 14 days shelf-life (Fig. A-3).

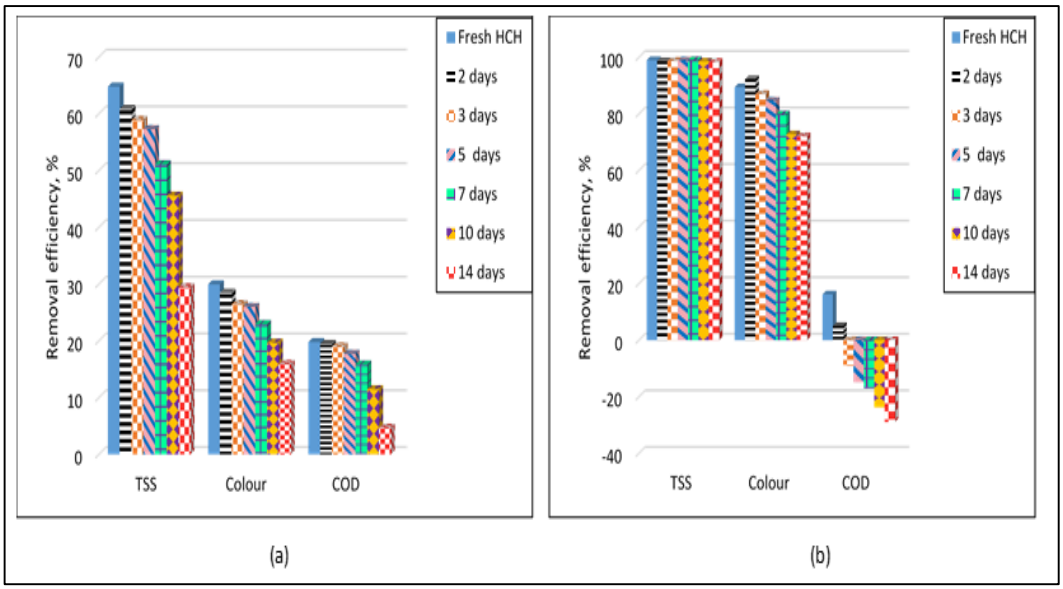

Figure A-3: Investigation of coagulant shelf-life.

The efficiency of the chitosan for the removal of TSS from FE was relatively constant regardless of the coagulant shelf-life. The colour removal efficiency began to decrease considerably from the 5th day of the CCo shelf-life and continued to decline until the 14th day. Poor results were observed for COD removal when the old CCo was used. Fig. A-3b shows that the efficiency drastically declines after second day of coagulant conservation.

From Fig. A-3, it can be concluded that the performance of the CCo decreases with time. It is possible that the chitosan begins to slowly decay in the aqueous acidic mixture, thus adding to the final COD of the water and hindering its adsorbing capacity. The difference between the performance of RE and FE can be attributed to the nature of the impurities in each effluent.

Table A-18: Raw data for coagulant shelf-time for RE.

Day 0	R 1			R 2		
	Initial	HCH	% decrease	Initial	HCH	% decrease
TSS	663	213	67.87	464	178	61.64
Colour	2.255	1.58	29.93	2.255	1.58	29.93
COD	11020	8520	22.69	12840	10680	16.82
Day 2	R 1			R 1		
	Initial	HCH	% decrease	Initial	HCH	% decrease
TSS	663	244	63.20	464	193	58.41
Colour	2.255	1.583	29.80	2.255	1.645	27.05
COD	11020	8580	22.14	12840	10700	16.67
Day 3	R 1			R 1		
	Initial	HCH	% decrease	Initial	HCH	% decrease
TSS	663	265	60.03	464	196	57.76
Colour	2.255	1.653	26.70	2.255	1.664	26.21
COD	11020	8620	21.78	12840	10760	16.20
Day 5	R 1			R 1		
	Initial	HCH	% decrease	Initial	HCH	% decrease
TSS	663	281	57.62	464	200	56.90
Colour	2.255	1.671	25.90	2.255	1.669	25.99
COD	11020	8700	21.05	12840	11000	14.33
Day 7	R 1			R 1		
	Initial	HCH	% decrease	Initial	HCH	% decrease
TSS	663	320	51.73	464	230	50.43
TDS	10279.41	9680.16	5.83	10233.31	9822.96	4.01
COD	11020	8980	18.51	12840	11160	13.08
Day 10	R 1			R 1		
	Initial	HCH	% decrease	Initial	HCH	% decrease
TSS	663	352	46.91	464	259	44.18
Colour	2.255	1.832	18.76	2.255	1.791	20.57
COD	11020	9320	15.43	12840	11880	7.48
Day 14	R 1			R 1		
	Initial	HCH	% decrease	Initial	HCH	% decrease
TSS	663	463	30.17	464	331	28.66
Colour	2.255	1.885	16.41	2.255	1.908	15.39
COD	11020	10420	5.44	12840	12340	3.89

Average							
	Fresh HCH	2 days	3 days	5 days	7 days	10 days	14 days
TSS	64.76	60.80	58.89	57.26	51.08	45.54	29.41
Colour	29.93	28.43	26.45	25.94	22.91	19.66	15.90
COD	19.75	19.40	18.99	17.69	15.80	11.45	4.67

Table A-19: Raw data for coagulant shelf-time for FE.

Day 0	R 1			R 2		
	Initial	HCH	% decrease	Initial	HCH	% decrease
TSS	130	2	98.46	211	1	99.53
Colour	0.211	0.027	87.20	0.372	0.031	91.67
COD	2100	1750	16.67	1530	1290	15.69
Day 2	R 1			R 1		
	Initial	HCH	% decrease	Initial	HCH	% decrease
TSS	130	3	97.69	211	1	99.53
Colour	0.211	0.022	89.57	0.372	0.019	94.89
COD	2100	2000	4.76	1530	1450	5.23
Day 3	R 1			R 1		
	Initial	HCH	% decrease	Initial	HCH	% decrease
TSS	130	2	98.46	211	2	99.05
Colour	0.211	0.036	82.94	0.372	0.033	91.13
COD	2100	2290	-9.05	1530	1670	-9.15
Day 5	R 1			R 1		
	Initial	HCH	% decrease	Initial	HCH	% decrease
TSS	130	1	99.23	211	3	98.58
Colour	0.211	0.042	80.09	0.372	0.04	89.25
COD	2100	2410	-14.76	1530	1760	-15.03
Day 7	R 1			R 1		
	Initial	HCH	% decrease	Initial	HCH	% decrease
TSS	130	2	98.46	211	1	99.53
Colour	0.211	0.051	75.83	0.372	0.060	83.87
COD	2100	2460	-17.14	1530	1790	-16.99
Day 10	R 1			R 1		
	Initial	HCH	% decrease	Initial	HCH	% decrease
TSS	130	2	98.46	211	3	98.58
Colour	0.211	0.066	68.72	0.372	0.086	76.88
COD	2100	2630	-25.24	1530	1870	-22.22
Day 14	R 1			R 1		
	Initial	HCH	% decrease	Initial	HCH	% decrease
TSS	130	3	97.69	211	2	99.05
Colour	0.211	0.066	68.72	0.372	0.091	75.54
COD	2100	2710	-29.05	1530	1970	-28.76

Average							
	Fresh HCH	2 days	3 days	5 days	7 days	10 days	14 days
TSS	98.99	98.61	98.76	98.90	98.99	98.52	98.37
Colour	89.44	92.23	87.03	84.67	79.85	72.80	72.13
COD	16.18	5.00	-9.10	-14.90	-17.07	-23.73	-28.90

APPENDIX B: STATISTICAL AND OPTIMIZATION STUDIES

B-1. RAW DATA FOR BOX-BEHNKEN DESIGN

Table B-1: Experimental data from the BBD

Standard runs	Randomized runs	X_1	X_2	X_3	Repeat 1			Repeat 2			Repeat 3			Average		
					% Y_1 (TSS)	% Y_2 (COD)	% Y_3 (Colour)	% Y_1 (TSS)	% Y_2 (COD)	% Y_3 (Colour)	% Y_1 (TSS)	% Y_2 (COD)	% Y_3 (Colour)	% Y_1 (TSS)	% Y_2 (COD)	% Y_3 (Colour)
1	6	-1	-1	0	88.06	28.75	72.67	88.06	37.50	71.43	88.06	30	72.05	88	32	72
2	5	+1	-1	0	80.60	24.38	71.43	80.60	19.38	70.19	79.10	18.75	73.29	80	21	72
3	10	-1	+1	0	88.97	21.33	79.50	88.97	18.67	83.50	88.97	23.33	76.50	89	21	80
4	11	+1	+1	0	88.97	12	85	92.65	17.33	77.50	90.44	14	82.50	91	14	82
5	1	-1	0	-1	86.84	24.28	70.37	86.84	27.17	68.89	86.84	26.01	67.41	87	26	69
6	3	+1	0	-1	78.95	11.11	72.59	77.63	12.87	71.11	80.26	9.36	69.63	79	11	71
7	9	-1	0	+1	94.74	23.50	88.28	97.37	26.78	86.90	97.37	27.87	84.83	96	26	87
8	13	+1	0	+1	88.75	22.04	83.17	88.75	22.04	81.71	90	23.66	92.93	89	23	80
9	2	0	-1	-1	81.43	14.45	68.15	80	12.14	70.37	80	13.87	69.63	80	13	69
10	4	0	+1	-1	88.30	11.11	73.74	88.30	14.58	76.54	87.23	12.50	76.54	88	13	76
11	8	0	-1	+1	91.67	27.01	74.49	93.33	25.29	72.45	91.67	23.85	69.39	92	25	72
12	17	0	+1	+1	99.13	17.22	88.86	99.13	16.67	89.77	100	18.89	90.68	99	18	90
13	15	0	0	0	92.31	30.34	86.17	92.31	28.03	82.32	93.16	26.12	83.60	93	28	84
14	16	0	0	0	94.02	27.70	82.32	96.58	27.58	82.64	94.02	29.49	90.68	92	28	85
15	12	0	0	0	93.75	29.19	86.83	92.50	30.11	86.59	93.75	30.75	86.83	93	30	87
16	7	0	0	0	89.86	28.31	83.18	91.30	29.36	84.11	92.75	30.47	81.31	92	29	83
17	14	0	0	0	92.50	27.42	89.27	92.50	32.74	86.83	95	31.56	83.17	93	31	86

	Initial
TSS (mg/l)	110
COD (mg/l)	1700
Colour (abs)	0.219

B-2. EVALUATION OF THE DESIGN

Standard errors (SE) must be the same for each type of coefficient. The ideal VIF is 1. VIFs values greater than 10 indicate that the coefficients are poorly estimated due to multicollinearity. Ideally, the value of the Ri^2 should be 0. High values of Ri^2 show that terms are correlated with each other, which can lead to poor predictions and erroneous models. Table B-2 shows that the model chosen does not contain correlated terms.

Table B-2: Evaluation of the chosen design.

Term	SE	VIF	Ri^2
X_1	0.35	1.00	0.0000
X_2	0.35	1.00	0.0000
X_3	0.35	1.00	0.0000
X_1X_2	0.50	1.00	0.0000
X_1X_3	0.50	1.00	0.0000
X_2X_3	0.50	1.00	0.0000
X_1^2	0.49	1.01	0.0058
X_2^2	0.49	1.01	0.0058
X_3^2	0.49	1.01	0.0058

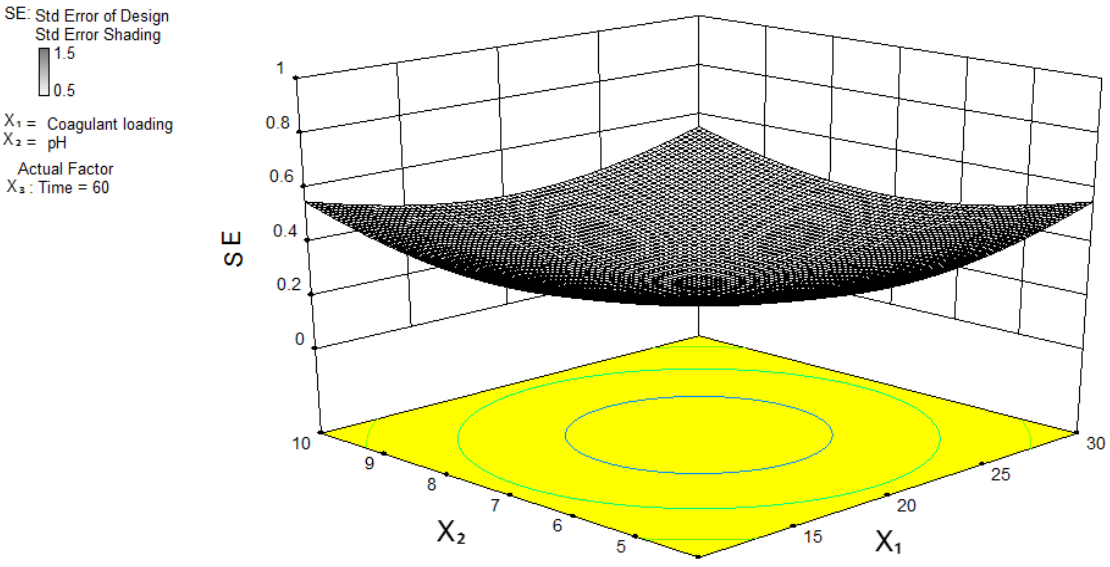

Figure B-1: 3D plot of the standard error.

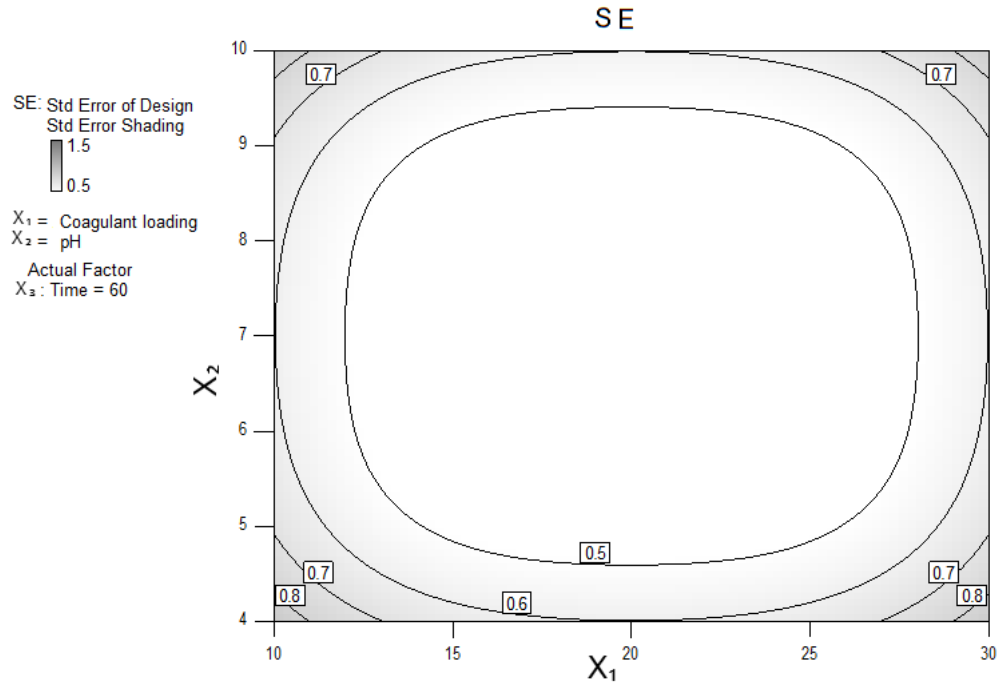

Figure B-2: Contour plot of the standard error.

The profile of the 3D plot is flat centred in the middle of the design space (Fig. B-1) and the contour appears as a square with rounded edges (Fig. B-2).

B-3. TRANSFORMATION ANALYSIS FOR TSS

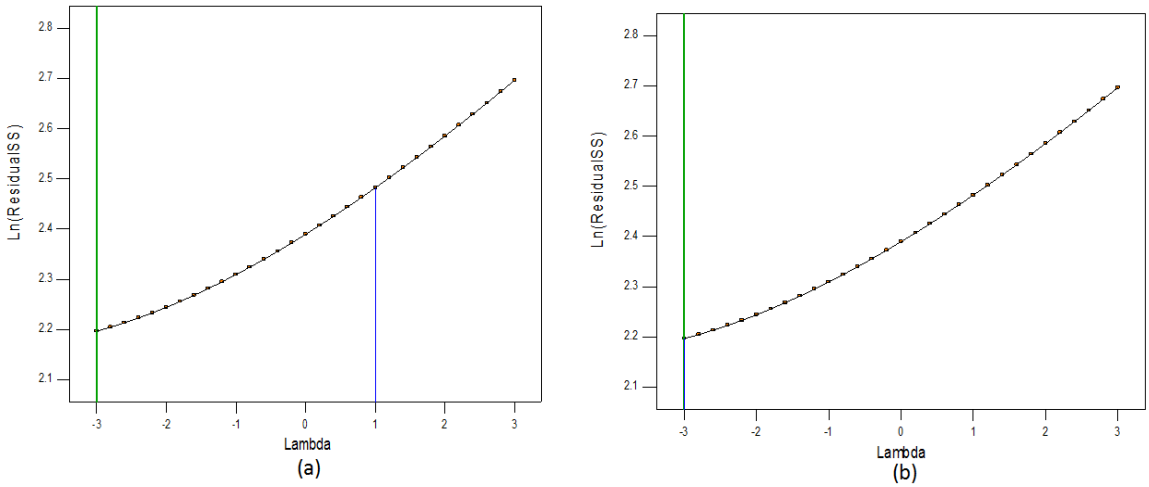

Figure B-3: Box-Cox power transformation plots for (a) No transformation: Lambda=1 (b) Transformed data using the best lambda value: - 3.

The Model F-value of 51.80 implies the model is significant. There is only a 0.01% chance that an F-value this large could occur due to noise. Values of "Prob > F" less coagulation process.

The "Lack of Fit F-value" of 5.52 implies there is a 6.62% chance that a "Lack of Fit F-value" this large could occur due to noise, which is insignificant.

The model equation for this response is expressed as $Y_1^* = Y_1^{-3} \times 10^{-8}$.

$$Y_1^* = 126 + 15.66X_1 - 17.51X_2 - 26.7X_3 - 12.82X_1X_2 - 5.26X_1X_3 + 4.67X_2X_3 + 18.58X_1^2 + 8.49X_2^2 + 7.611X_3^2 \quad \text{(B-1)}$$

Table B-3: ANOVA for transformed TSS.

Variation	SS	df	MS	F-value	P-value p>F
Regression	1.317E-012	9	1.463E-013	51.80	< 0.0001
X_1	1.962E-013	1	1.962E-013	69.46	< 0.0001
X_2	2.452E-013	1	2.452E-013	86.78	< 0.0001
X_3	5.717E-013	1	5.717E-013	202.37	< 0.0001
X_1X_2	6.577E-014	1	6.577E-014	23.28	0.0019
X_1X_3	1.109E-014	1	1.109E-014	3.93	0.0880
X_2X_3	8.731E-015	1	8.731E-015	3.09	0.1222
X_1^2	1.453E-013	1	1.453E-013	51.45	0.0002
X_2^2	3.038E-014	1	3.038E-014	10.75	0.0135
X_3^2	2.439E-014	1	2.439E-014	8.63	0.0218
Residual	1.977E-014	7	2.825E-015		
LOF	1.593E-014	3	5.309E-015	5.52	0.0662
Pure Error	3.847E-015	4	9.618E-016		
Total	1.337E-012	16			

Table B-4: Model coefficients after transformation (TSS)

SD	CV (%)	R^2	$\check{R}^2$	$\acute{R}^2$	AP
5.315E-008	3.74	0.9852	0.9662	0.8049	23.871

The value of the $\acute{R}^2$ (0.8049) is in reasonable agreement with the $\check{R}^2$ (0.9662). An AP of 23.871 indicates an adequate signal. This model can be used to navigate the design space.

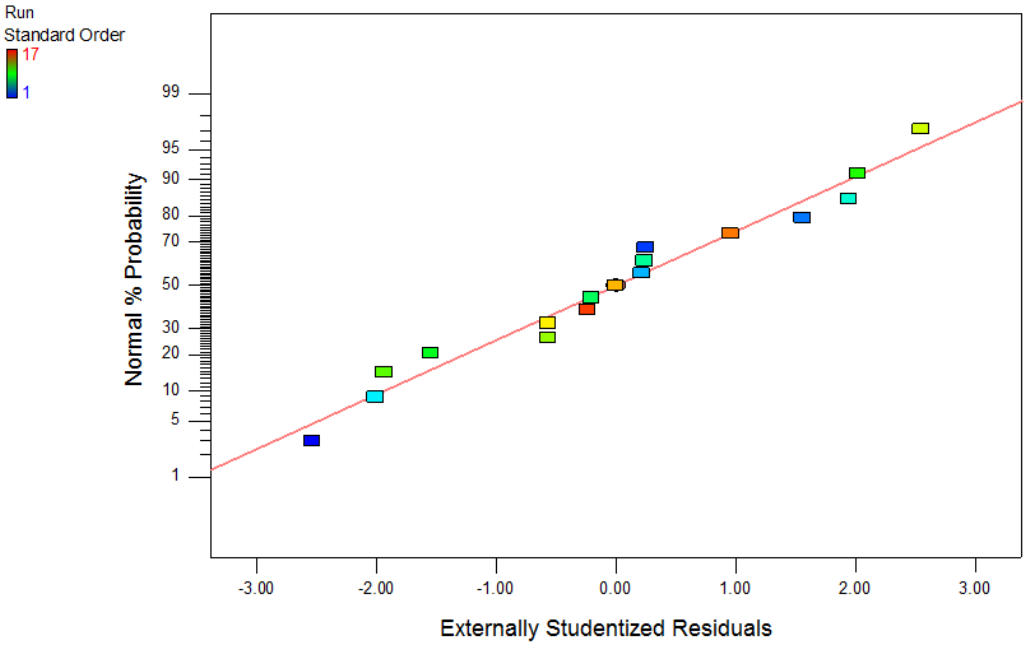

Figure B-4: Normal plot of residuals for transformed TSS.

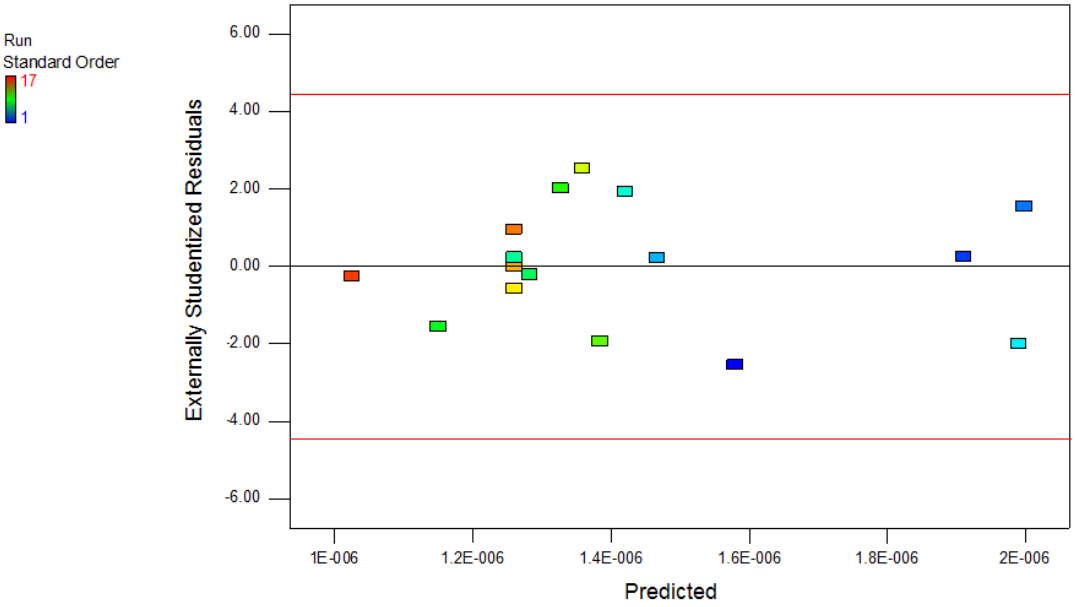

Figure B-5: Residuals vs. predicted values for transformed TSS

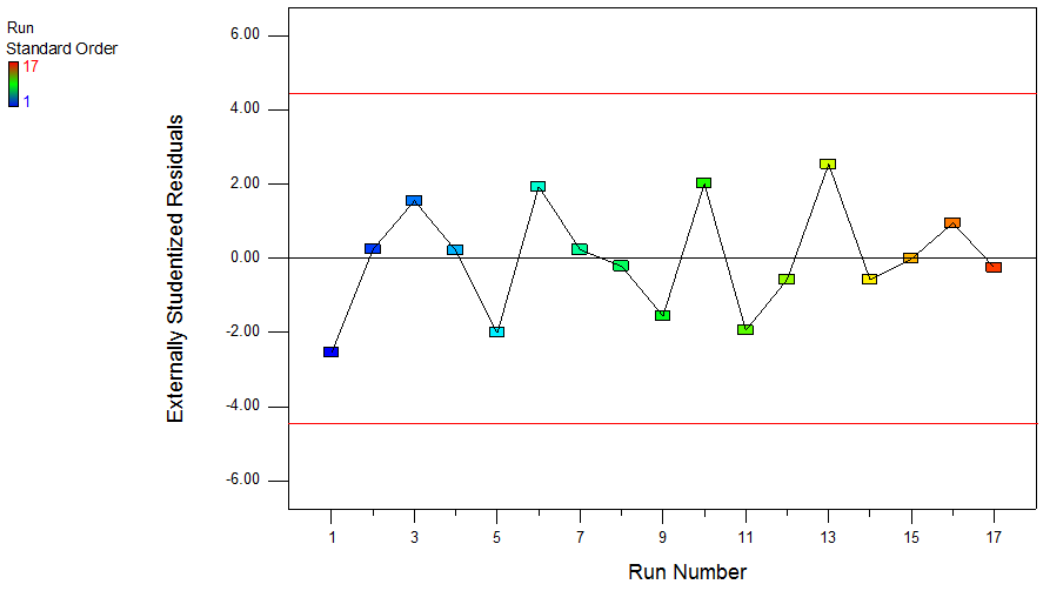

Figure B-6: Residuals vs. run number for transformed TSS.

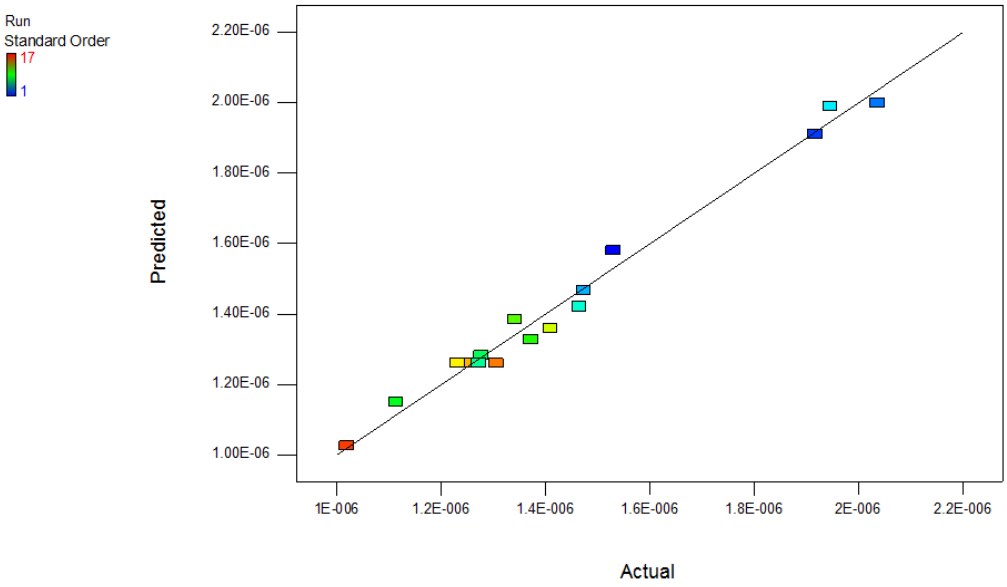

Figure B-7: Predicted vs. actual for transformed TSS.

All the diagnostic plots for the transformed response indicate that the model is a good fit.

B-4. TRANSFORMATION ANALYSIS FOR COD

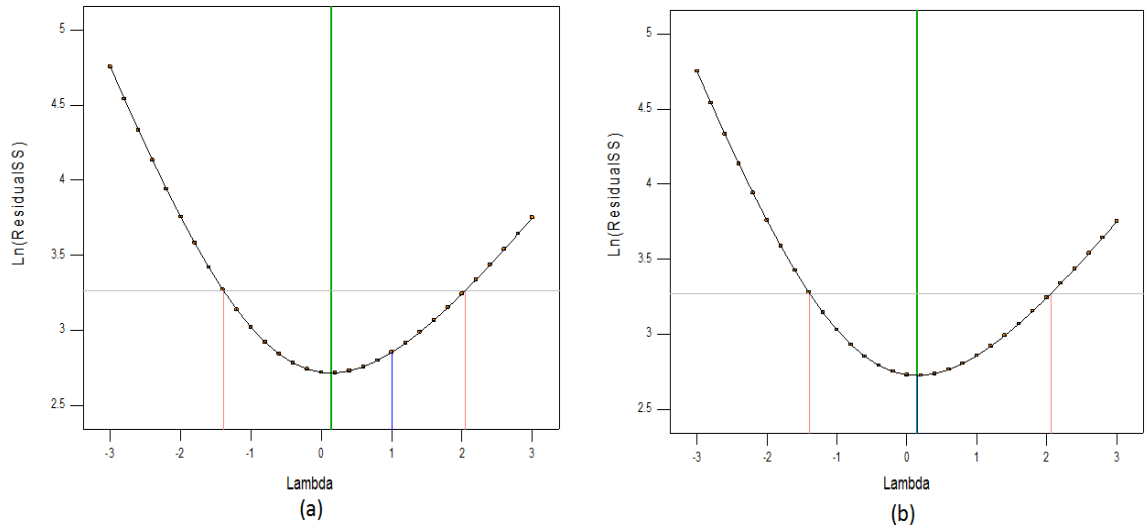

Figure B-8: Box-Cox power transformation plots for (a) No transformation: Lambda=1 (b) Transformed data using the best lambda value: 0.14.

Table B-5: ANOVA for transformed COD.

Variation	SS	df	MS	F-value	P-value p>F
Regression	0.10	9	0.011	43.03	< 0.0001
X_1	0.022	1	0.022	85.38	< 0.0001
X_2	0.010	1	0.010	39.79	0.0004
X_3	0.018	1	0.018	70.80	< 0.0001
X_1X_2	7.584E-005	1	7.584E-005	0.29	0.6060
X_1X_3	6.330E-003	1	6.330E-003	24.33	0.0017
X_2X_3	1.351E-003	1	1.351E-003	5.19	0.0568
X_1^2	9.490E-004	1	9.490E-004	3.65	0.0978
X_2^2	0.016	1	0.016	61.64	0.0001
X_3^2	0.022	1	0.022	83.70	< 0.0001
Residual	1.821E-003	7	2.601E-004		
LOF	1.495E-003	3	4.982E-004	6.11	0.0565
Pure Error	3.262E-004	4	8.156E-005		
Total	0.10	16			

The Model F-value of 43.03 implies the model is significant. There is only 0.01% chance that an F-value this large could occur due to noise. Values of "Prob > F" less than 0.0500 indicate model terms are significant. The LOF greater than 0.05 indicate that the model can fit any other data.

The model equation for this response is expressed as $Y_2^* = Y_2^{0.14}$.

$$Y_2^* = 1.66 - 0.053X_1 - 0.036X_2 + 0.048X_3 - 4.356\times10^{-3}X_1X_2 + 0.04X_1X_3 + 0.018X_2X_3 - 0.015X_1^2 - 0.062X_2^2 - 0.072X_3^2 \quad \text{(B-2)}$$

Table B-6: Model coefficients after transformation (COD).

SD	CV (%)	R^2	$\check{R}^2$	$\acute{R}^2$	AP
0.016	1.01	0.9822	0.9594	0.7619	19.698

The value of the $\acute{R}^2$ (0.7619) is in agreement with the $\check{R}^2$ (0.9594). The value of the AP is greater than 4 which is desirable.

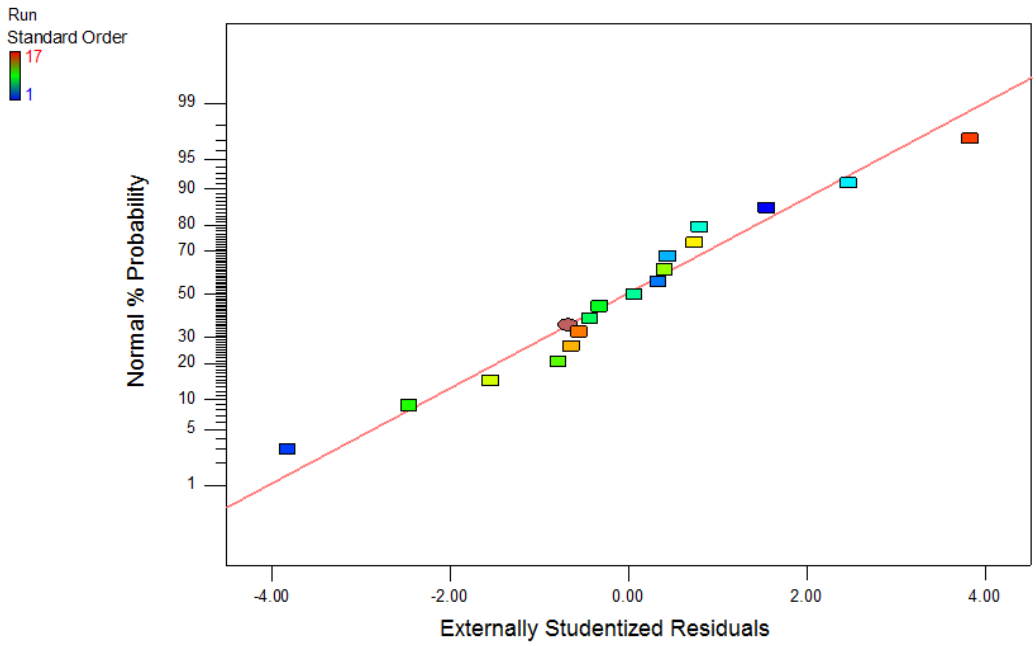

Figure B-9: Normal plot of residuals for transformed COD.

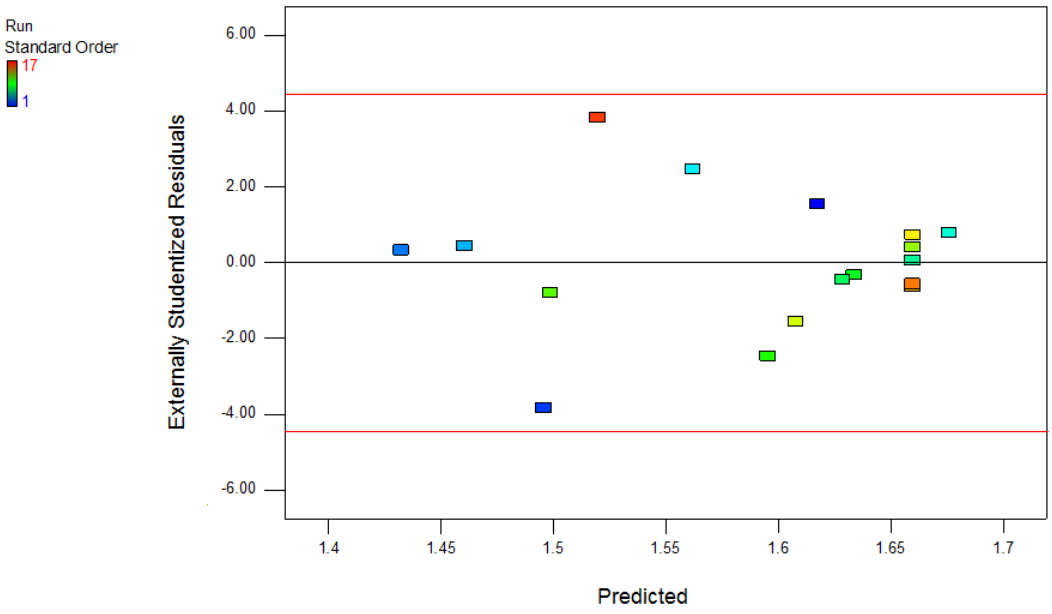

Figure B-10: Residuals vs. predicted values for transformed COD.

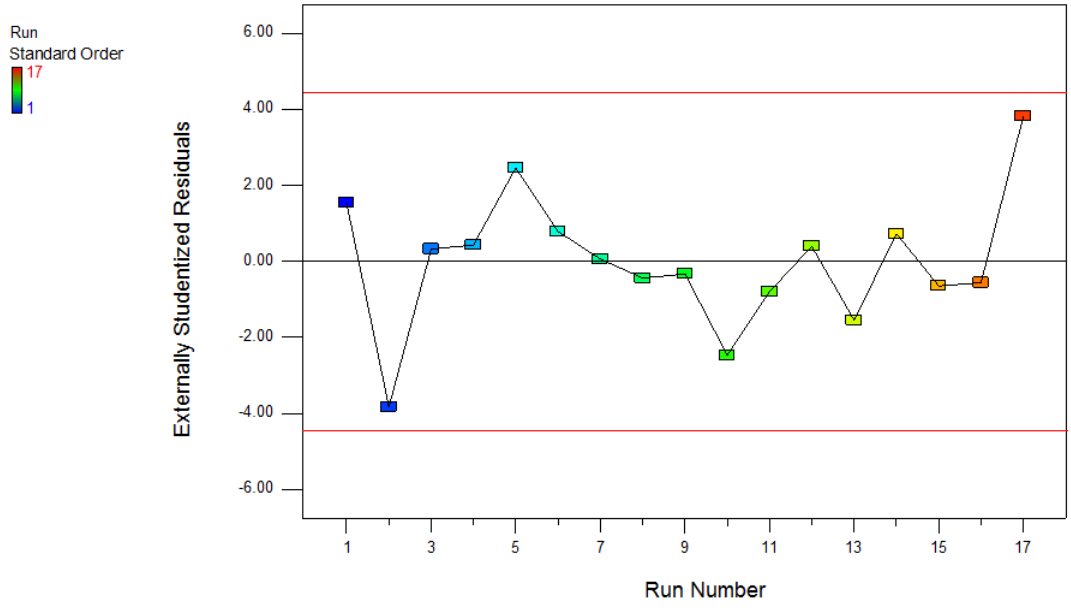

Figure B-11: Residuals vs. run number for transformed COD.

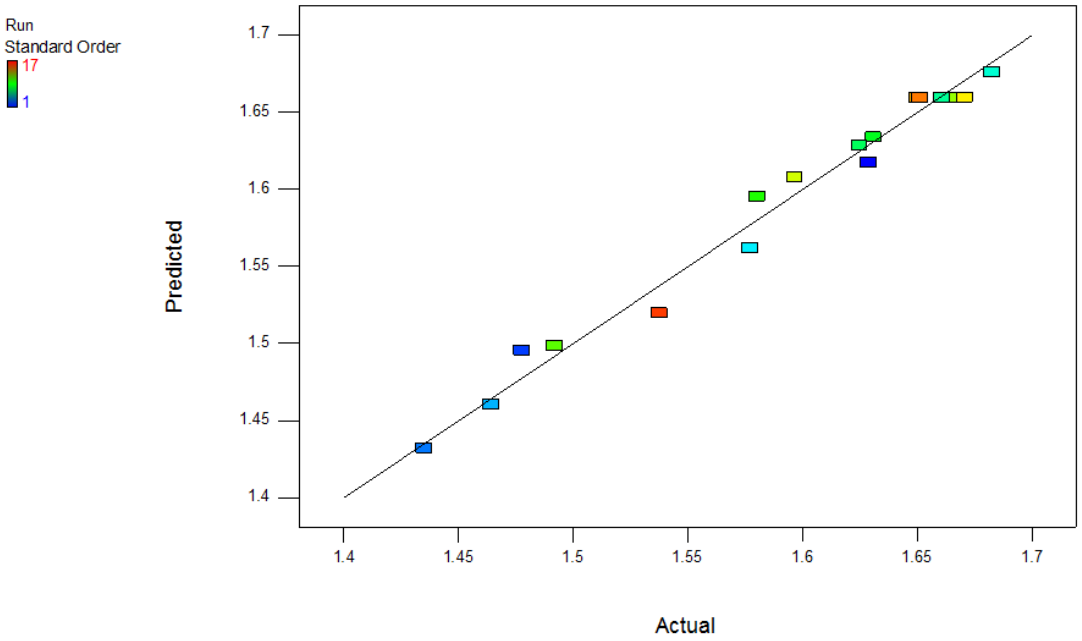

Figure B-12: Predicted vs. actual for transformed COD.

The diagnostic plots show that the model is a good fit.

B-5. TRANSFORMATION ANALYSIS FOR COLOUR

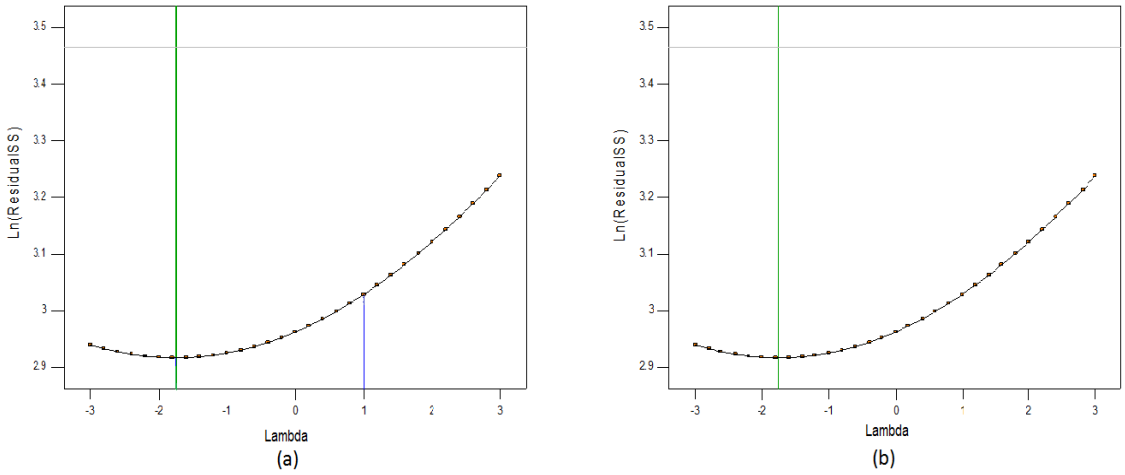

Figure B-13: Box-Cox power transformation plots for (a) No transformation: Lambda=1 (b) Transformed data using the best lambda value: - 1.75.

Table B-7: ANOVA for transformed colour.

Variation	SS	df	MS	F-value	P-value p>F
Regression	9.663E-008	9	1.074E-008	35.39	< 0.0001
X_1	9.675E-011	1	9.675E-011	0.32	0.5899
X_2	2.077E-008	1	2.077E-008	68.46	< 0.0001
X_3	3.941E-008	1	3.941E-008	129.91	< 0.0001
X_1X_2	1.493E-010	1	1.493E-010	0.49	0.5056
X_1X_3	1.497E-009	1	1.497E-009	4.93	0.0618
X_2X_3	2.870E-009	1	2.870E-009	9.46	0.0179
X_1^2	8.749E-009	1	8.749E-009	28.84	0.0010
X_2^2	8.964E-009	1	8.964E-009	29.54	0.0010
X_3^2	1.078E-008	1	1.078E-008	35.53	0.0006
Residual	2.124E-009	7	3.034E-010		
LOF	1.348E-009	3	4.493E-010	2.32	0.2173
Pure Error	7.758E-010	4	1.940E-010		
Total	9.876E-008	16			

The model equation for this response is expressed as $Y_3^* = Y_3^{-1.75} \times 10^{-6}$

$$Y_3^* = 420.5 + 3.48X_1 - 50.95X_2 - 70.19X_3 - 6.11X_1X_2 + 19.34X_1X_3 - 26.79X_2X_3 + 45.59X_1^2 + 46.14X_2^2 + 50.6X_3^2 \quad \text{(B-3)}$$

Table B-8: Model coefficients after transformation (Colour).

SD	CV (%)	R^2	$\check{R}^2$	$\acute{R}^2$	AP
1.742E-005	3.57	0.9785	0.9508	0.7693	18.136

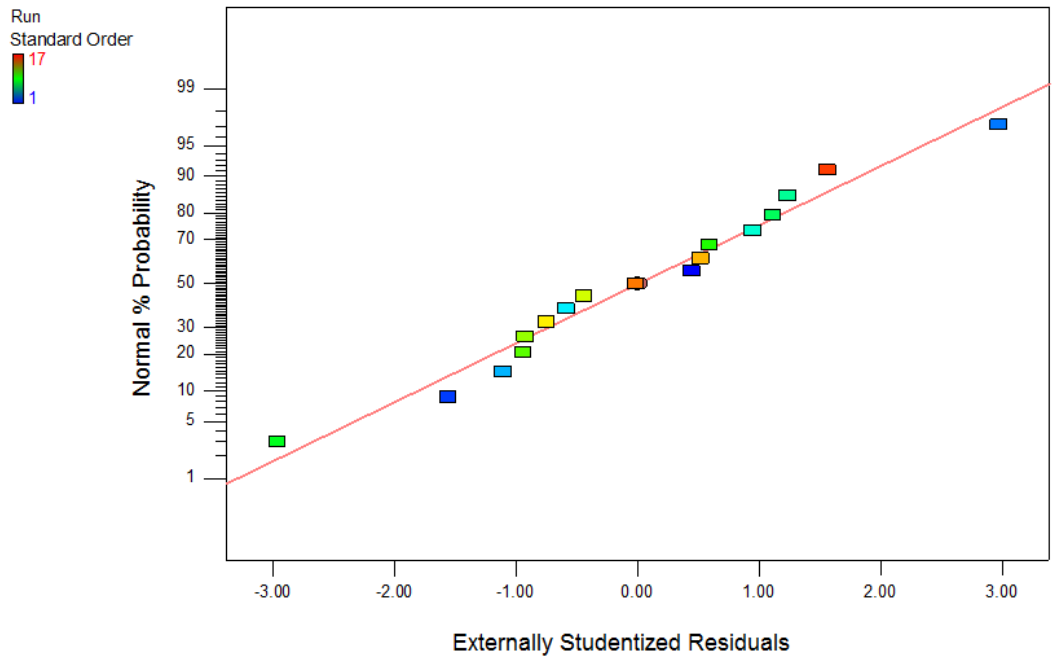

Figure B-14: Normal plot of residuals for transformed colour.

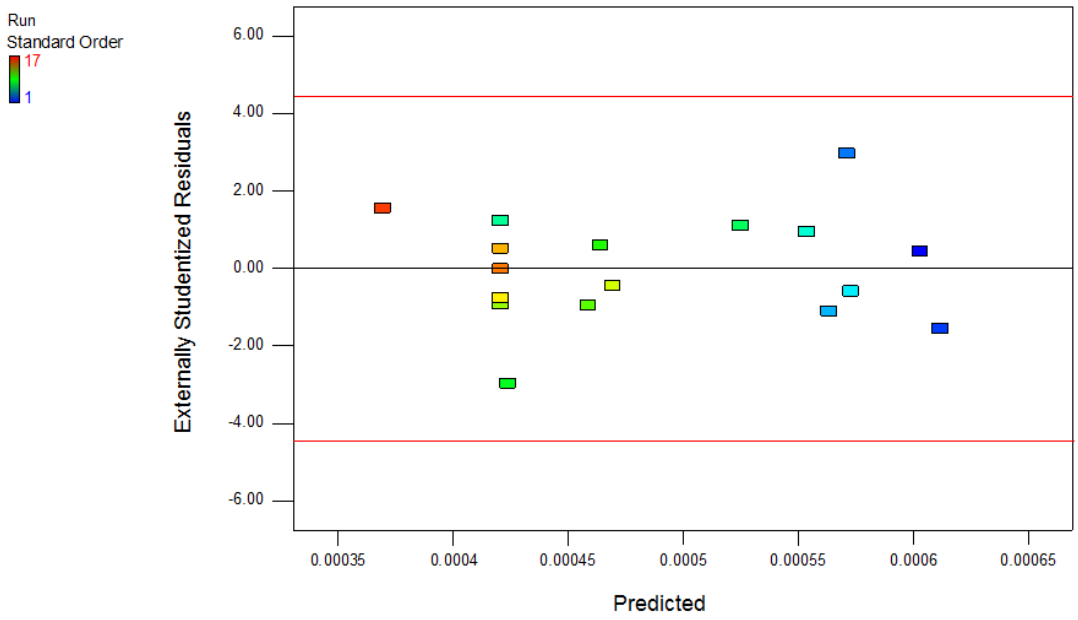

Figure B-15: Residuals vs. predicted values for transformed colour.

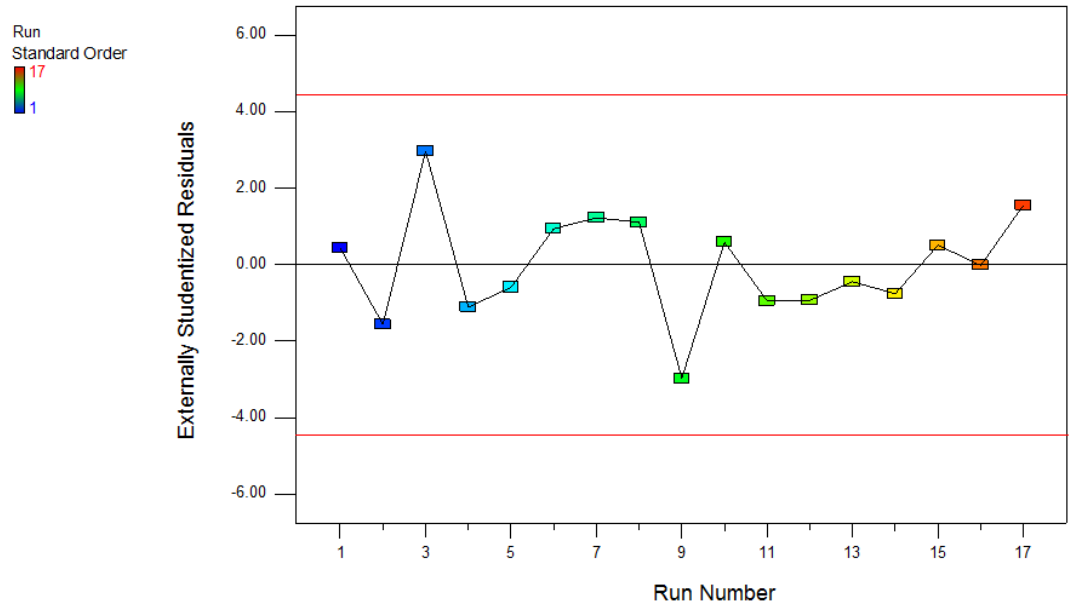

Figure B-16: Residuals vs. run number for transformed colour.

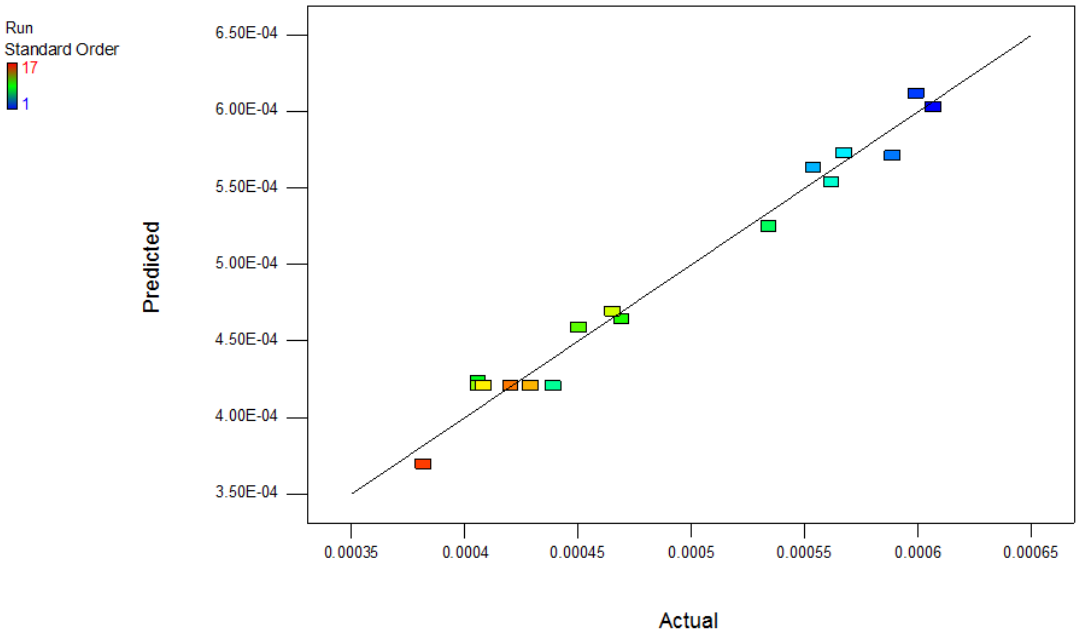

Figure B-17: Predicted vs. actual for transformed colour.

The diagnostic plot above provide a confirmation of the fitness of the model.

The use of Box-Cox transformation stabilized the residuals, in this case using power transformation parameter (lambda). This lead to an improvement of the model fitness, in comparison to the results obtained without transformations. In the case where the

data were transformed, the model passed all the tests of fitness, including the approximate values of the $\check{R}^2$ and the $\acute{R}^2$. However, these parameters ($\check{R}^2$ and $\acute{R}^2$) are not very critical when the R^2 value is close to one and all the other statistical parameters provide a good fit.

B-6. EFFECTS AND INTERACTIONS

Interactions and effects were discussed in the previous chapters. Important variables are referred to as main effects because they have a large influence on the response variables. There are many methods used to identify effects in statistics, one of them is the use of pareto charts.

The pareto charts below are plotted by considering the magnitude of the coefficients in the model equations.

The quadratic terms were not considered here since their magnitude indicates the steepness of the curvatures for a particular term (See Chapter 5 for details).

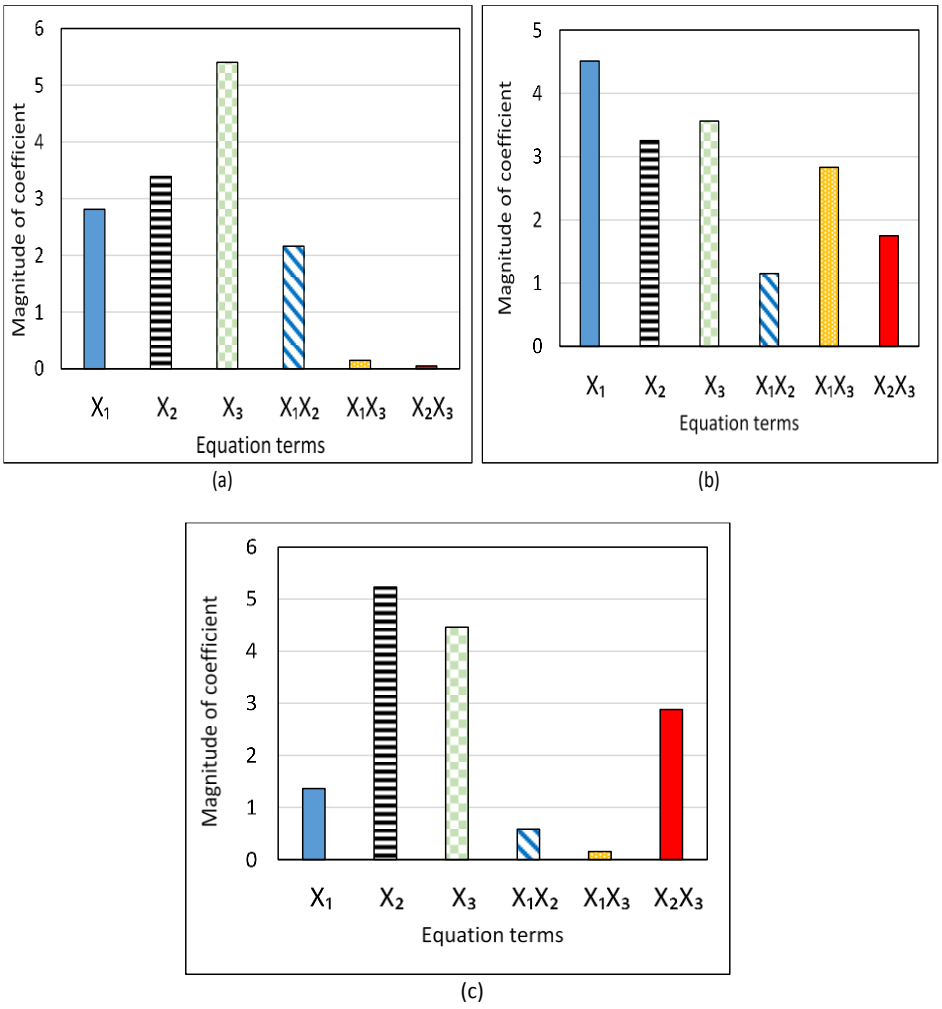

Figure B-18: Pareto chart for analysis of the removal of (a) TSS (b) COD (c) Colour.

APPENDIX C: DATA FOR THE VALIDATION OF THE MODELS

Table C-1: Predictions from OFAT models vs. actual values for pH.

	TSS (%)		COD (%)		Colour (%)	
pH	Actual	Predicted	Actual	Predicted	Actual	Predicted
4	97	97	11	11	88	87
5	98	98	11	12	86	87
6	98	98	10	11	85	87
7	97	97	9	8	86	85
8	95	94	5	3	85	82
9	87	89	-7	-4	76	79
10	84	83	-12	-13	74	73
R^2	0.96		0.97		0.9	

Table C-2: Predictions from OFAT models vs. actual values for CCo dosage.

	TSS (%)		COD (%)		Colour (%)	
Dosage (mg/l)	Actual	Predicted	Actual	Predicted	Actual	Predicted
3.7	79	87	38	36	42	49
7.41	97	87	35	32	61	52
14.81	91	88	19	25	57	56
29.63	86	85	14	13	55	54
44.44	80	79	6	5	41	43
59.26	68	71	3	1	26	27
74.1	65	64	0	2	14	14
R^2	0.8		0.96		0.92	

Table C-3: Removal of TSS at various coagulant loadings over time.

	Coagulant concentration, mg/l (R1)				Coagulant concentration, mg/l (R2)			
	3.7	7.41	37	74.1	3.7	7.41	37	74.1
Time, minutes	TSS, mg/ l				TSS, mg/ l			
0	100	100	100	100	112	112	112	112
10	34	30	52	90	36	29	60	93
20	30	19	44	81	33	16	47	86
30	25	9	32	73	25	11	36	79
40	20	3	27	61	19	6	28	65
50	17	1	20	49	13	3	20	53
60	11	2	19	41	9	2	17	44
70	11	1	17	37	10	1	14	38
80	9	1	15	36	12	2	14	38
90	8	1	17	33	10	2	13	35
100	8	2	14	33	9	1	12	32
110	9	1	17	34	11	1	12	33
120	7	1	16	35	11	1	13	33

	Coagulant concentration, mg/l			
	3.7	7.41	37	74.1
Time minutes	% Average			
0	0	0	0	0
10	67	72	47	13
20	70	83	57	21
30	76	91	68	28
40	82	96	74	40
50	86	98	81	52
60	90	98	83	60
70	90	99	85	65
80	90	99	86	65
90	91	99	86	68
100	92	99	86	68
110	91	99	86	68
120	92	99	86	68

APPENDIX D: RESEARCH OUTPUTS

D-1: PUBLICATIONS PREVIEW

International Journal of Futuristic Trends in Engineering and Technology (Special Issue)
ISSN: 2348-5264 (Print), ISSN: 2348-4071 (Online)
Vol. 2 (1), 2014

Influence of Effluent Type on the Performance of Chitosan as a Coagulant

(Paper ID: 21IC3000801401)

Ritha L. L. Pambi
Department of Chemical Engineering
Institute for Water and Wastewater Technology
Durban University of Technology.
Durban, South Africa.
rluti@hotmail.com

Paul Musonge
Department of Chemical Engineering
Institute for Water and Wastewater Technology
Durban University of Technology.
Durban, South Africa.
paulm@dut.ac.za

Abstract: The use of chitosan as a bio-polymeric coagulant has continued to attract interest in water treatment due to its biodegradability and non-toxicity. Its ability to treat effluents of high organic content has been investigated in some food processing industries. The focus of the present study is to compare results of the use of chitosan in the treatment of effluent from a Sugar Processing Plant (SPP), with those obtained from the treatment of wastewater from a Milk Processing Plant (MPP) and from a Brewery Processing Plant (BPP), in order to determine the influence of effluent type on the impurities removal efficiency.
The treatment of the MPP provided the best removal efficiency (99% suspended solids removal and 70% COD removal) in comparison to the SPP (98% suspended solids removal and 11% COD removal) and BPP (95% suspended solids removal and 50% COD removal). The optimum pH value varied as a function of the type of effluent with BPP= 4.5, SPP = 4.5 and MPP =7. The results indicate that chitosan is not very efficient for the removal of dissolved matter. A relationship between total suspended solids (TSS) and total dissolved solids (TDS) has been developed.
Keywords: Chitosan, coagulation, wastewater, model.

I. INTRODUCTION

There are various methods for the treatment of polluted water, these include among others; evaporation, membrane technology, activated carbon adsorption, biological treatment, chemical and electrochemical treatments (precipitation and coagulation).
Evaporation is an effective and non-toxic way of treating polluted wastewater since there is no need to add chemicals to the process and the condensate is relatively clean water. However, it is inefficient for large scale operations due to the high energy consumption and it poses a problem of solid disposal. Biological treatment involves the action of living microorganisms that utilize the waste material as food and convert it into simpler substances by natural metabolic processes. This process is eco-friendly, but slow. Membrane technology and filtration is also effective but can be costly especially for highly polluted water. Adsorption using activated carbon has been proven efficient for the removal of dissolved particles. However, the cost requirement of the carbon regeneration is a major disadvantage. Electrochemical treatment method is attractive due to its low toxicity, and its efficiency in removing the impurities in the water. But this method is not sustainable for large scale applications [1].
Chemical treatment such as coagulation using inorganic salt and synthetic polymers has been widely used in the treatment of wastewater to remove solids and other impurities. The use of inorganic salts such as alum has become a health concern with reports of illnesses such as Alzheimer disease among others associated with prolonged consumptions of the traces of these chemicals in the water [2]. To remediate with the hazardous effect thereof, inorganic salts are combined with organic or synthetic polymers. Although this combination provides many advantages such as good coagulation efficiency, lower quantity of sludge, ease of dewatering and filtration, their prolonged health impact has not yet been established [3, 4].
There is a growing interest in the use of natural coagulant in wastewater treatment, most of them aiming to plant or animal waste and process them into bioplolymers. Wastes such as crustacean shells from the seafood industry pose a problem due to the fact that they degrade at very slow rates, and in some countries these waste are disposed of on landfills posing a problem of land space [5-7]. Seafood shells however, contain a non-toxic, biodegradable polymer know as chitin. The chitin extracted from the shellfish and crabs is often converted into chitosan by chemical treatment which has more economical value than chitin due to its wider range of application. Chitosan is capturing the attention of scholars mostly as an adsorbent in water treatment for the removal of impurities such as heavy metals and colour among many others [5, 8, 9].
Chitosan is a polymer of β-(1–4) linked 2-acetamido-2-deoxy-β-D-glucopyranose and 2-amino-2-deoxy-β-D-glycopyranose prepared by deacetylation of chitin. Chitosan is protonated by weak acid in aqueous solution under the pH of 6.5. The protonated chitosan forms bonds with the negatively charged impurities in three steps: (1) the cationic charge of the protonated chitosan destabilizes and neutralizes the anionic charge of the impurities, (2) bridging of the polymer with the suspended particles and flocs formation, (3) electrostatic patch [10, 11]. The protonation of chitosan occurs as follow:

The Efficiency of Chitosan as a Coagulant in the Treatment of the Effluents from the Sugar Industry

RITHA L. L. PAMBI* AND PAUL MUSONGE

Institute for Water and Wastewater Technology Department of Chemical Engineering Durban University of Technology, South Africa.

ABSTRACT

Chitosan has been used as a coagulant for industrial wastewater treatment. However, no attention has been given to the coagulation of sugar effluents using this polymer. Two effluent streams from a local sugar refinery, namely the final effluent (FE) and the resin effluent (RE) were treated using chitosan prepared by dissolution in aqueous hydrochloric acid. The optimum chitosan dosage was found to be 138 mg/l and 7.41 mg/l for RE and FE respectively, beyond which, the efficiency of the coagulant decreased. The efficiency of the chitosan was higher under acidic conditions and using sodium hydroxide to adjust the pH negatively affected the performance of the chitosan. The treatment of FE yielded better removal efficiency (97% total suspended solids, 61% colour and 35% chemical oxygen demand) than RE (68% total suspended solids, 30% colour and 15% chemical oxygen demand). This coagulant can be used to pre-treat turbid water for further treatment.

KEYWORDS: *Chitosan, Coagulation, Resin effluent, Sugar wastewater, Polymer.*

1. INTRODUCTION

Coagulation is a process used extensively in the purification of water using inorganic or organic substances known as coagulants. The performance of conventional inorganic and synthetic coagulants such as aluminium sulphate (Alum), polyaluminium chloride (PAC) and acrylamide has been established widely in literature. However, there have been health concerns about the use of these inorganic coagulants. Residues of coagulants containing aluminium and iron have been linked as a possible cause of neurological diseases such as Alzheimer disease, Parkinson disease and clinical neurotoxicity in humans.[1] This has led

J. Polym. Mater. Vol. 32, No. 1, 2015, 59-65

Correspondence author e-mail: rluti@hotmail.com, paulm@dut.ac.za

D-2: PREVIEW OF MANUPSCRIPT UNDER REVIEW

APPLICATION OF RESPONSE SURFACE METHODOLOGY (RSM) IN THE TREATMENT OF THE FINAL EFFLUENT FROM THE SUGAR INDUSTRY USING CHITOSAN

Ritha L. L. Pambi, Paul Musonge and Precious Dlamini
Institute for Water and Wastewater Technology. Department of Chemical Engineering
Durban University of Technology (DUT). Durban, South Africa.

ABSTRACT

The sugar industry contributes significantly to the economic growth of South Africa by creating jobs in the agricultural and industrial sectors. However, this industry discharges large amount of effluent containing high level of suspended and dissolved solids, which impart colour to the wastewater stream and add treatment cost. Chitosan, a natural polymer, has been used in the coagulation of impurities from the sugar refinery using the one-factor-at-a-time (OFAT) method. The results indicated the removal of total suspended solids (TSS) and colour of 87% and 76% respectively at the pH of 9. Response surface methodology (RSM) was used to maximize the efficiency of this coagulant according to the Box-Behnken design (BBD). The use of RSM was found to have several advantages in comparison to the OFAT, such as the identification of interaction, the use of statistical analysis that produce model equations for optimization and prediction of the behavior of a particular system. Furthermore, at the pH of 9, the BBD yielded TSS and colour removals of 99% and 90% respectively. This should be a motivation for industrial researcher to deviate from the traditional OFAT especially in process optimization studies.

Keywords—Chitosan, coagulation, response surface methodology, sugar effluent.

1 INTRODUCTION

Design of experiments (DOE) can be defined as the systematic planning of information gathering with the use of experimental and statistical methods to identify the optimum factors and levels for a particular problem either of industrial scale or for research purposes.

The most commonly used DOE is the one-factor-at-a-time (OFAT) design which vary only one variable at a time while keeping others constant. Pambi and Musonge [1] investigated the removal of impurities from the two effluent streams discharged by a local sugar refinery using the OFAT experimental design. Chi and Cheng [2] also applied the OFAT method in their study of the coagulation of milk processing plant wastewater using chitosan.
The main advantages of the OFAT method is the fact that it allows a rapid identification of the influence of the factors and the experimental outcomes can be readily understood [3, 4].
However, the use of OFAT is being discouraged due to the following reasons [5-8]:

- The OFAT design does not show interactions between the variables.
- The prediction of the response in the factor space is poor.
- The lack of randomization can lead to biased conclusions.

One way of overcoming these short-comings is the use of response surface methodology (RSM). The RSM uses a set of mathematical and statistical procedures to describe the relationship between a set of data. This relationship is described by a polynomial equation that relates to the experimental data, in order to concurrently optimize the responses [8, 9].

The most common types DOE used for the RSM analysis are the three-level full factorial design central composite design (CCD), the Doehlert design (DD) and the Box-Behnken design (BBD) (Baş and Boyaci, 2007; Bezerra et al., 2008).

The main aim of this study was to optimize the removal of total suspended solids (TSS) and colour from final effluent (FE) discharged by the sugar refinery the using RSM. A previous study using OFAT demonstrated that the treatment of FE with the chitosan coagulant (CCo) yielded good results for TSS and colour.

However, using the right combination of variables, the efficiency of the CCo can be improved.

D-3: CONFERENCES

- International Conference on Chemical Thermodynamics (ICCT)/SAIChE. 27 July-1 August 2014.

- 2nd Afro-Asian International Conference of Science, Engineering and Technology. Vadodara, Gujarat, India, 11-12 October 2014.